

7-35
449
CV
[redacted]

QC 320

• M41

• H42

no. 68

AREAS OF CONTACT AND PRESSURE

DISTRIBUTION IN BOLTED JOINTS

Archives

H. H. Gould

B. B. Mikic

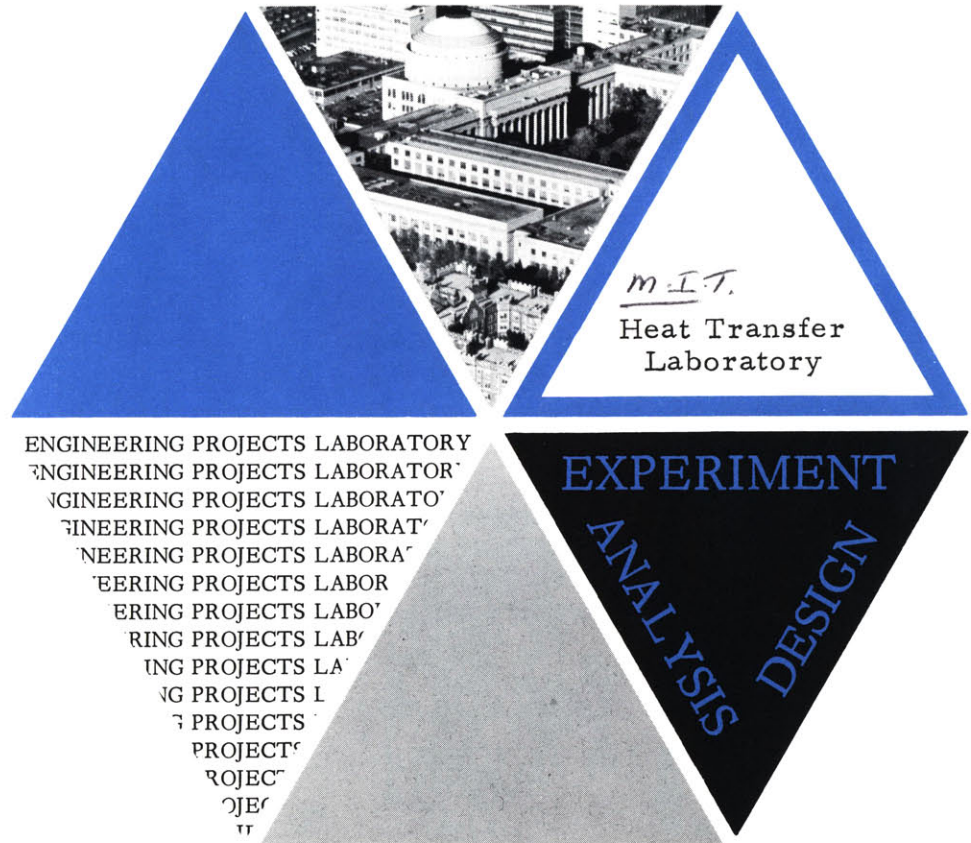


Report No. DSR 71821-68

Contract No. NAS 8-24867

Engineering Projects Laboratory
Department of Mechanical Engineering
Massachusetts Institute of Technology
Cambridge, Massachusetts 02139

June 1970



RECEIVED
SEP 22 1970
M. I. T. LIBRARIES

ABSTRACT

When two plates are bolted (or riveted) together these will be in contact in the immediate vicinity of the bolt heads and separated beyond it. The pressure distribution and size of the contact zone is of considerable interest in the study of heat transfer across bolted joints.

The pressure distributions in the contact zones and the radii at which flat and smooth axisymmetric, linear elastic plates will separate were computed for several thicknesses as a function of the configuration of the bolt load by the finite element method. The radii of separation were also measured by two experimental methods. One method employed autoradiographic techniques. The other method measured the polished area around the bolt hole of the plate's caused by sliding under load in the contact zone. The sliding was produced by rotating one plate of a mated pair relative to the other plate with the bolt force acting.

The computational and experimental results are in agreement and these yield smaller zones of contact than indicated by the literature. It is shown that the discrepancy is due to an assumption made in the previous analyses.

In addition to the above results this report contains the finite element and heat transfer computer programs used in this study. Instructions for the use of these programs are also included.

ACKNOWLEDGMENTS

This report was supported by the NASA Marshall Space Flight Center under contract NAS 8-24867 and sponsored by the Division of Sponsored Research at M.I.T.

TABLE OF CONTENTS

	<u>Page</u>
Title Page	1
Abstract	2
Acknowledgments	3
Table of Contents	4
List of Tables and Figures	6
Nomenclature	8
Chapter I: Introduction	10
Chapter II: Analysis	15
A. Problem Statement	15
B. Method of Analysis	18
Chapter III: Experimental Method	23
Chapter IV: Results	28
A. Pressure Distribution and Radii of Separation from Single Plate and Two Plate Finite Element Models	28
B. Radii of Separation from Experiment and Their Pre- dicted Values from the Two Plate Finite Element Computation	29
Chapter V: Application	32
Chapter VI: Conclusions	35
References	37
Appendices	
A. Finite Element Analysis of Axisymmetric Solids	39

	<u>Page</u>
B. Finite Element Program for the Analysis of Isotropic Elastic Axisymmetric Plates	44
C. Finite Element Program for the Analysis of Isotropic Elastic Axisymmetric Plates — Thermal Strains Included	68
D. Steady State Heat Transfer Program for Bolted Joint	94

LIST OF TABLES AND FIGURES

<u>Table</u>		<u>Page</u>
1	Separation Radius Comparison - Single and Two Plate Models	100
2	Test and Analytical Results for Radii of Separation of Bolted Plates	101
 <u>Figure</u>		
1	Bolted Joint	102
2	Roetscher's Rule of Thumb for Pressure Distribution in a Bolted Joint	102
3	Furnlund's Sequence of Superposition	103
4	Finite Element Idealization of Two Plates in Contact	107
5	Finite Element Models	108
6	Examples of Unacceptable Solutions	109
7	Plate Specimen, Bolt and Nuts, Fixture and Tools	110
8	Footprints on the Mating Surface of 1/16 - 1/16, 1/8 - 1/8, 3/16 - 3/16, 1/4 - 1/4, and 1/8 - 1/4 Pairs	111
9	Footprint of Nut on Plate	116
10	X-Ray Photographs of Contamination Transferred from Radioactive Plate to Mated Plate. 1/16, 1/4, 3/16, 1/4 Inch Pairs	117
11	Free Body Diagram for Two Plates in Contact	119
12	Single Plate Analysis-Midplane σ_z Stress Distribution	120
13	Single Plate Analysis-Midplane σ_z Stress Distribution	121
14	Single Plate Analysis-Midplane σ_z Stress Distribution	122

<u>Figure</u>		<u>Page</u>
15	Interface Pressure Distribution in a Bolted Joint	123
16	Interface Pressure Distribution in a Bolted Joint	124
17	Interface Pressure Distribution in a Bolted Joint	125
18	Finite Element Analysis Results for 1/4 Inch Plate Pair	126
19	Pressure in Joint, Triangular Loading	127
20	Variations of Loading and Boundary Conditions	128
21	Pressure in Joint, Uniform Displacement Under Nut	129
22	Deflection of Plate Under Nut	130
23	Finite Element Analysis Results for 3/16 Inch Plate Pair	131
24	Finite Element Analysis Results for 1/8 Inch Plate Pair	132
25	Gap Deformation for Free and Fixed Edges — Finite Element Analysis, 1/8 inch Plate Pair.	133
26	Finite Element Analysis Result for 1/16 Inch Plate Pair	134
27	Finite Element Analysis Results for 1/8 Inch Plate Mated With 1/4 Inch Plate	135
28	Comparison Between Tested and Measured Separation Radii	136
29	Location of Nodes — Steady State Heat Transfer Analysis	137

NOMENCLATURE

A, B, C	radii
D	thickness
E	modulus of elasticity
G	shear modulus
h_c, h_f	heat transfer coefficients
H	hardness
k, k_1, k_2	thermal conductivities
P, p	pressure
r	coordinate
R_o	radius of separation
u, w	displacement in r and z directions
x	coordinate
X_c	length of contact
y	coordinate
y'	slope
z	coordinate
δ	deflection
ϵ	dilation
$\epsilon_r, \epsilon_t, \epsilon_{rz}$	strains
$\sigma, \sigma_1, \sigma_2$	standard deviations
$\sigma_r, \sigma_t, \sigma_z$	stresses

λ, μ	Lame's constants
ν	Poisson's ratio
τ	shear stress
θ	angle

Subscripts

r	radial direction
t	tangential direction
z	z-direction

Chapter I

INTRODUCTION

When two plates are bolted (or riveted) together, these will be in contact in the immediate vicinity of the bolt heads and separated beyond it. The pressure distribution in the contact area and the separation of the plates is of considerable interest in the study of heat transfer across joints. Cooper, Mikic and Yovanovich [1] show that with assumed Gaussian distribution of surface heights, the microscopic contact conductance is related to the interface pressure, surface characteristics and the hardness of the softer material in

$$h_c = 1.45 \frac{\tan \theta}{\sigma} k \left(\frac{P}{H} \right)^{0.985} \quad (1.1)$$

where

$$k \equiv \frac{2k_1 k_2}{k_1 + k_2} \quad (1.2)$$

and k_1 and k_2 represent the thermal conductivities of two bodies in contact; σ is the combined standard deviation for the two surfaces which can be expressed as

$$\sigma = (\sigma_1^2 + \sigma_2^2)^{1/2} \quad (1.3)$$

where σ_1 and σ_2 are the individual standard deviation of height for the respective surfaces; $\tan \theta$ is the mean of the absolute value of slope for the combined profile and it is related, for normal distribution of slope, to the individual mean of absolute values of slopes as

$$\tan \theta = (\tan^2 \theta_1 + \tan^2 \theta_2)^{1/2} \quad (1.4)$$

where

$$\tan \theta_i = \lim_{L \rightarrow \infty} \frac{1}{L} \int_0^L |y'_i| dx; \quad i = 1, 2 \quad (1.5)$$

and y' is the slope of the respective surface profiles; P represents the local interface pressure; and H is the hardness of the softer material.

Relation (1.1), as written above, is applicable for contact in a vacuum. One can modify the expression by simply adding to it

$$h_f \equiv \frac{\text{conductivity of interstitial fluid}}{\text{average distance between the surfaces}} \quad (1.6)$$

in order to account approximately for the presence of the interstitial fluid.

All parameters in relation (1.1), except for the pressure, are functions of the material and geometry and can be easily obtained. The determination of the pressure distribution and the extent of the contact area between two plates present both mathematical and experimental

difficulties. From the mathematical point of view, the difficulty stems from the fact that the theory of elasticity will yield a three dimensional (axisymmetric) problem with mixed boundary conditions. Experimentally, the discrimination between contact and gaps of the order of millionths of an inch is required.

Roetscher [2] proposed in 1927, a rule of thumb that the pressure distribution of two bolted plates, Fig.1, is limited to the two frustums of the cones with a half cone angle of 45 degrees as shown in Fig. 2 and that at any level within the cone the pressure is constant. Also, for symmetric plates, according to Roetscher, separation will occur at the circle which is defined by the contact plane and the 45 degree truncated cone emanating from the outer radius of the bolt head.

Since 1961 Fernlund [3], Greenwood [4] and Lardner [5] among others reported solutions based upon the theory of elasticity. Although their solutions also yield separation radii at approximately 45 degrees as in Roetscher's rule, their solutions yield a much more reasonable pressure distribution as compared to Roetscher's constant pressure at each level of the frustrum. These investigators have made use of the Hankel transform method demonstrated by Sneddon [6] in his solution for the elastic stresses produced in a thick plate of infinite radius by the application of pressure to its free surfaces. The basic assumption in their approach is that two bolted plates can be represented by a single plate of the same thickness as the combined thickness of the two plates under the same external loading. It then follows that the z -stress distribution at the parting plane can be approximated by the z -stress distribution in the same plane of the single plate. It also follows that separation will occur at the smallest radius in that plane for which

the z -stress is tensile. In the case of two plates of equal thickness the σ_z stress at the midplane of the equivalent single plate is the stress of interest.

Fernlund [3], for example, used the method of superposition in the sequence shown in Figs. 3(a) to 3(c) to obtain annular loading. Then by superposition of shear and radial stresses at radius A , Figs. 3(d) and 3 (e), opposite in sign of those due to the annular loading at the free surfaces, Fernlund obtained the solution for a single plate with a hole under annular loading (Fig. 3(f)).

Experimental work in this area included Bradley's [7] measurements of the stress field by three dimensional photoelasticity techniques, and the use of introducing pressurized oil at various radii in the contact zone and measuring the pressure at which oil leaks out from the joint [3,8]. Both of these experimental methods have uncertainties as indicated by the authors.

Because of the cumbersomness of the Hankel transform solution and experimental difficulties, the body of work in this area has been very limited and definite verification of analytical results by experiment is not cited in the literature.

The research described in the succeeding chapters was undertaken with the following primary objectives:

- a) To provide a method of solution for the case of two bolted plates without the simplifying assumption of the single plate substitution.
- b) To devise a test to validate the two plate analysis.
- c) To test the validity of the single plate substitution.

A finite element computer program has been assembled for the analytical solution of two-plate problems. Experiments have been performed to verify the analytical results. Since in heat transfer calculations the extent of the radius of contact is of primary importance, and since by restricting the experimental effort to the verification of only this parameter, (rather than the verification of the entire pressure distribution,) many experimental uncertainties should be eliminated, the experiments were designed only for the determination of the contact area.

Agreement between analysis and experiment was obtained and the results show that the single plate substitution is not justified and the 45 degree rule is not valid for the flat and smooth surfaces studied.

Chapter II

ANALYSIS

A. Problem Statement

The objective of the analysis was to solve the linear elasticity problem of two plates in contact defined mathematically by the following equations for each plate:

The equations of equilibrium

$$\frac{\partial}{\partial r} (r \sigma_r) - \sigma_t + r \frac{\partial \tau}{\partial z} = 0 \quad (2.1)$$

$$\frac{\partial}{\partial r} (r \tau) + \frac{\partial}{\partial z} (r \sigma_z) = 0$$

where $\tau_{rz} = \tau_{zr} = \tau$ and $\tau_{rt} = \tau_{tr} = \tau_{zt} = \tau_{tz} = 0$.

The stress - strain relations, using standard notation for stress and strain,

$$\begin{aligned} \sigma_r &= \lambda \epsilon + 2 \mu \epsilon_r \\ \sigma_t &= \lambda \epsilon + 2 \mu \epsilon_t \\ \sigma_z &= \lambda \epsilon + 2 \mu \epsilon_z \\ \tau &= 2 \mu \epsilon_{rz} \end{aligned} \quad (2.2)$$

where λ and μ are Lamé's constants and

$$\lambda = \frac{2 G \nu}{1 - 2\nu} \quad (2.3)$$

$$\mu = G$$

if G is the modulus of elasticity in shear and ν is Poisson's ratio; and ϵ the volume expansion is defined by

$$\epsilon = \frac{\partial u}{\partial r} + \frac{u}{r} + \frac{\partial w}{\partial z} \quad (2.4)$$

where u is the displacement in the radial direction and w is the displacement in the axial direction.

The strain - displacement relations

$$\begin{aligned} \epsilon_r &= \frac{\partial u}{\partial r} \\ \epsilon_t &= \frac{u}{r} \\ \epsilon_z &= \frac{\partial w}{\partial z} \\ \epsilon_{rz} &= \frac{1}{2} \left(\frac{\partial u}{\partial z} + \frac{\partial w}{\partial r} \right) \end{aligned} \quad (2.5)$$

The above equations can be combined to yield the equilibrium equations in terms of displacements

$$\begin{aligned} \nabla^2 u - \frac{u}{r^2} + \frac{1}{1 - 2\nu} \frac{\partial \epsilon}{\partial r} &= 0 \\ \nabla^2 w + \frac{1}{1 - 2\nu} \frac{\partial \epsilon}{\partial z} &= 0 \end{aligned} \quad (2.6)$$

The applicable boundary conditions are (see Fig. 11)

$$\begin{aligned}
 \sigma_r^{(1)}(A,z) &= \sigma_r^{(2)}(A,z) = 0 \\
 \tau^{(1)}(A,z) &= \tau^{(2)}(A,z) = 0 \\
 \sigma_r^{(1)}(C,z) &= \sigma_r^{(2)}(C,z) = 0 \\
 \tau^{(1)}(C,z) &= \tau^{(2)}(C,z) = 0 \\
 \tau^{(1)}(r,D_1) &= \tau^{(2)}(r,-D_2) = 0, \\
 \tau^{(1)}(r,0) &= \tau^{(2)}(r,0), \quad A \leq r \leq R_0 \\
 \sigma_z^{(1)}(r,D_1) &= \sigma_z^{(2)}(r,-D_2) = 0, \quad B \leq r \leq C \\
 \tau^{(1)}(r,0) &= \tau^{(2)}(r,0) = 0, \quad R_0 \leq r \leq C \\
 \sigma_z^{(1)}(r,0) &= \sigma_z^{(2)}(r,0), \quad A \leq r \leq R_0 \\
 \sigma_z^{(1)}(r,0) &= \sigma_z^{(2)}(r,0) = 0, \quad R_0 \leq r \leq R \\
 \sigma_z^{(1)}(r,D_1) &= \sigma_z^{(2)}(r,-D_2) = P(r), \quad A \leq r \leq B \\
 w^{(1)}(r,0) &= w^{(2)}(r,0), \quad A \leq r \leq R_0
 \end{aligned} \tag{2.7}$$

$$2\pi \int_A^B Pr \, dr = 2\pi \int_A^{R_0} pr \, dr$$

Inspection of the above equations shows that the above constitutes a mixed boundary value problem and the most appropriate technique for solution is the finite element method.

B. Method of Analysis

A finite element computer program was assembled for the analytical solution of bolted plates. Descriptions of the finite element method are given in references [9,10], but for completeness, an outline of the mathematical formulation for this case is presented in Appendix A. A listing of the computer program and instructions for its use may be found in Appendix B. Appendix C contains user's instructions and a listing of the finite element program modified to include thermal strains.

As in the previous work axial symmetry and isotropic linear elastic material behavior were assumed. However, the computer programs accommodate plates with different material properties in a bolted pair.

The basic concept of the finite element method is that a body may be considered to be an assemblage of individual elements. The body then consists of a finite number of such elements interconnected at a finite number of nodal points or nodal circles. The finite character of the structural connectivity makes it possible to obtain a solution by means of simultaneous algebraic equations. When the problem, as is the case here, is expressed in a cylindrical coordinate system and in the presence of axial symmetry in geometry and load, tangential displacements do not exist, and the three-dimensional annular ring finite element is then reduced to the characteristics of a two-dimensional finite element.

The analysis consists of (a) structural idealization, (b) evaluation of the element properties, and (c) structural analysis of the assemblage of the elements. Items (b) and (c) are covered in the appendices and in the references quoted. The structural idealization and the criteria for acceptable solutions will be described in this chapter.

Fig. 4(a) shows two circular plates in contact under arbitrary axisymmetric loading. The plates are subdivided into a number of annular ring elements which are defined by the corner nodal circles (or node points when represented in a plane) as shown in Figs. 4(b) and 4(c). Unlike the cases described in Chapter I, which have been solved by the Hankel transform method, all plates solved by the finite element method have finite radii. The cross sections of each annular ring element is either a general quadrilateral or triangle. To improve accuracy smaller elements are used in zones where rapid variations in stress are anticipated than in zones of constant stress; thus the different size elements shown in Fig. 4(b). (However, the total number of elements allowable are subject to computer capacity.)

Figure 4(b) shows the two plates in contact for the radial distance X_c and separated beyond it. It is to be noted that the nodal points on the parting line and within the length of contact X_c are common to elements in both plates. The other elements adjacent to the parting line on each plate are separated from their corresponding elements in the mating plate and these elements have no common nodal points. Physically, it is equivalent to the welding together of the two plates in the contact zone. Mathematically, we are imposing the condition that

in the contact zone the displacements in the z and r directions be identical for both plates. In the case of bolted plates of equal thickness, i.e. in the presence of symmetry about the parting plane, these conditions apply exactly. Furthermore, because of this symmetry, one needs to analyze only one plate, as shown in Fig. 5(b), with the imposed boundary conditions on the contact zone of zero displacement in the z -direction and freedom to displace in the r -direction. It can also be observed that the solution of two plates with symmetry about the parting plane is equivalent to the solution of one of these plates under the same loading conditions, but resting on a frictionless infinitely rigid plane. Also, under the above conditions the shear stress in the contact zone is identically zero.

In the case of bolted plates of unequal thickness the model includes both plates as shown in Fig. 5(c). This model is an approximation because, in general, two plates of unequal thickness do not have the same displacement in the r -direction on the contact surface. The solution yields, therefore, a shearing stress distribution in the contact zone. The solution, however, should be exactly compatible with the physical model if the frictional forces in the joint prevent sliding.

The critical aspect of the approach used herein is the determination of the largest nodal circle on the parting plane which is common to an element on each plate. This nodal circle defines the contact zone and the radius, R_0 , at which separation occurs.

The output of the finite element computer program includes the displacement of each node in the r and z directions and the average

σ_z , σ_r , σ_t and τ_{rz} stresses for each element.

The computation is iterative and the objective is to achieve the lowest possible compressive σ_z stress in the outermost elements bordering the contact zone. Unacceptable solutions are shown in Fig. 6(a) and 6(b). If R_o for a given external load distribution is too small, then the solution will show that the two plates intersect (Fig. 6(a)). On the other hand, if R_o is assumed too large, the solution will show that the outer portion of the contact zone sustains a tensile σ_z stress (Fig. 6(b)). Neither of these two situations is physically feasible. In general, the procedure employed was to commence the iterations with a value for R_o which would yield a tensile σ_z stress in the outer elements adjacent to the contact zone and then move R_o inward. The iteration ended as soon as no tensile σ_z stress was present at the contact zone. For example, for the case shown in Fig. 5(b), if the σ_z stress for the element in the last row and to the left of the last roller is tensile, then the following iteration will proceed without the last roller. Thus, the resolution is one nodal interval. Finer resolution can be obtained by reducing the interval between nodal circles by introducing more elements or shifting the grid locally. The same criteria apply to the model shown in Fig. 5(c).

In the finite element analysis of the Fernlund (3) model, i.e. single plate with external loads at the faces $z = \pm D$ no iteration is required and the rollers shown in Fig. 5(c) would extend to the outer radius of the plate. (Although Fernlund's computations are based on infinite plates, computations show that there is no distinction between infinite plates and plates of radius greater than five times of the outer

radius, B , of the load. See Fig. 5(a).

Convergence was tested by subdividing elements further, with nodal points in the coarser grid remaining nodal points in the finer grid. Changing the mesh from 180 elements to 360 elements have shown no improvement in accuracy. Meshes from 180 to 300 elements were used in this analysis. Typical spacings between nodal points were 0.015 inch radially and 0.03 inch in the z -direction.

Chapter III

EXPERIMENTAL METHOD

The objective of the experiment was to determine the extent of contact between two plates when bolted together. Sixteen type 304 stainless steel plates, 4 inches in diameter, were machined to nominal thicknesses of 1/16, 1/8, 3/16 and 1/4 inch, 4 plates for each thickness. After rough machining these plates were stress relieved at 1875°F and ground flat to 0.0002 inch. One side of each plate was then lapped flat to better than one fringe of sodium light (11 micro-inches) in the case of the 1/8, 3/16 and 1/4 inch plates, and to better than two fringes in the case of the 1/16 inch plates. Disregarding scratches, the finish of the lapped surfaces was 5 micro-inches rms. Each plate had a central hole, 0.257 inch in diameter, for a 1/4 - 20 bolt, and two notches and two holes on the periphery (see Fig. 7). Two techniques were employed in determining the area of contact when two of these plates were bolted together. The first technique entailed the following procedure (see Fig. 7):

- (a) The plates were cleaned with alcohol and lens tissue.
- (b) One plate was placed on the base of the fixture shown in Fig. 7, lapped surface up and the two holes on the periphery of the plates engaged with two pins on the fixture. Spacers between the fixture base and plate prevented the pins from extending beyond the top surface of the plate.

- (c) A second plate was placed on top of the first plate, lapped surfaces mating. The notches on the two plates were lined up with each other and with notches in the base of the fixture. Thus, rotation of the plates was prevented.
- (d) A standard 1/4 - 20 hex-nut with its annular bearing surface (0.42 inch O.D.) lapped flat was engaged on a high strength 1/4 - 20 bolt. The nut was located about two threads away from the head of the bolt and served in lieu of the bolt head. The lapped surface of the nut faced away from the bolt head and since the nut was not sent home against the bolt head, the looseness of fit between nut and bolt offered a degree of self alignment.
- (e) The bolt and nut assembly described in (d) above was then inserted through the 1/4 inch central holes of the two plates and a second 1/4 - 20 lapped nut was engaged on the bolt. Thus the two plates were captured by the two 1/4 -20 nuts with the lapped surfaces of the nuts bearing against the plates.
- (f) With the torque wrench shown on the right in Fig. 7, the nuts were torqued down to 70 pound-inches of torque to yield a 1100 pound force in the bolt [11].
- (g) The position of the keys was changed to engage with only the lower plate and the fixture and a special spanner wrench, as shown in Fig. 7, was engaged with the top plate. The spanner wrench was restrained to move in the horizontal plane and it was set into motion by the screw pressing against the wrench handle.

- (h) With the aid of the spanner wrench the upper plate was rotated relative to the lower plate several times approximately ± 5 degrees.

Thus, the above procedure allowed for the rubbing of one plate relative to its mate while under a bolt force of approximately 1100 lbs. The remaining steps were the disassembly and the measurement of the extent of the contact zone which was defined by the shine due to the rubbing in the contact zone. It is to be noted that the boundaries of the contact zone as measured by the naked eye and by searching for marks of "polished" or "damaged" surface under a 10.5 power magnification are essentially the same.

The above test was performed on 5 pairs of specimen. These were

1. One 0.07 in. plate mated to a 0.65 in. plate
2. One 0.126 in. plate mated to a 0.126 in. plate
3. One 0.191 in. plate mated to a 0.192 in. plate
4. One 0.253 in. plate mated to a 0.256 in. plate
5. One 0.124 in. plate mated to a 0.257 in. plate

The identical tests were repeated for

1. One 0.124 in. plate mated to a 0.126 in. plate; and
2. One 0.191 in. plate mated to a 0.192 in. plate,

but in lieu of the 1/4 - 20 nuts in direct contact with the plates special washers, 1.000 in. O.D., 0.257 in. I.D. and 0.620 in. high, were interposed between the bolt head and nut.

The diameters of the contact zones were measured with a machinist ruler with 100 divisions to the inch and with a Jones and Lamston Vertac 14 Optical Comparator.

The second technique used the same parts and fixture, but it involved autoradiographic measurements.

Four plates, 1/4, 3/16, 1/8 and 1/16 inch thick were sent to Tracerlab, Inc., Waltham, Mass., for electrolytic plating with radioactive silver $\text{Ag } 110^{\text{M}}$ (half life of 8 months). Each plate was masked except for an area on the lapped face one inch in radius. The plates then received a plating of copper about 5 microinches thick and then approximately a 5 microinch plating of silver containing the radioactive isotope. The resultant activity on each plate was about 2 millicuries.

These plates were then mated to plates of equal thickness (not plated) and assembled in a shielded hood as indicated in steps (a) to (h) above except that in the case of the pair of 1/4 inch plates care was taken not to rotate the plates during and after assembly and in the remaining cases the rotation specified in step (h) was done only once in one direction.

The plates were then disassembled and the radioactive contamination on the plates which were in contact with the radioactive plates measured. The transferred activity was:

1/4 in. plate	approximately	0.05 microcuries
3/16 in. plate	approximately	3. microcuries
1/8 in. plate	approximately	0.1 microcuries
1/16 in. plate	approximately	0.4 microcuries

It was also observed in handling that the adhesion of the silver on the 3/16 in. plate was poor.

Kodak type R single coated industrial x-ray film was then placed on the contaminated plates under darkroom conditions. The sensitive side of the film was pressed against the radioactive sides of the plates with a uniform load of about five pounds and left for exposure for three days. After three days, the film was removed and developed. The results are shown in Fig. 10.

Chapter IV

RESULTS

A. Pressure Distribution and Radii of Separation from Single Plate and Two Plate Finite Element Models.

Using the finite element procedure described in Chapter II, the midplane stress distribution of single circular plates of thickness $2D$, outer radii of 1.54 in., inner radii of 0.1 in., Poisson ratio of 0.3, and loaded by a constant pressure between radii A and B , Fig. 3(f), was computed. Computations were performed for D values of 0.1, 0.1333 and 0.2 in. For each value of D the radius B , which defines the region of the symmetric external load, assumed the values of 0.31, 0.22, 0.16 and 0.13 in. The σ_z stress distribution at the midplane, from the inner radius to the radius at which the above stress is no longer compressive, is shown in Figs. 12, 13 and 14 as a function of radius.

The identical cases were then recomputed, using again the finite element method, in accordance with the two plate model shown in Figs. 4(b) and 5(b). These results are given in Figs. 15, 16 and 17.

Inspection of the above figures show that the two plate model yields a somewhat different stress distribution in the contact zone than the stress distribution approximated from the single plate model, and more significantly, from the heat transfer point of view, the two plate model yields a lower value for the radius of separation, R_o , which

results in a reduction in area for heat transfer. Table 1 gives a comparison of the values for R_0 obtained from the two models.

It may be observed that the single plate result of Fernlund (Ref. 3, pp. 56, 124) is in fair agreement with the finite element results obtained for the single plate model.

B. Radii of Separation from Experiment and Their Predicted Values from the Two Plate Finite Element Computation.

As described in Chapter III, stainless steel circular plate specimen (Fig. 7) were bolted together, rotated relative to each other with the bolt force acting, and after disassembly the contact area of the joint was determined by measuring the footprints (the shiny, polished areas) on each plate due to the plates rubbing against each other. Photographs of these footprints are shown in Fig. 8. Fig. 9 also shows a typical footprint of the annular bearing surface of the 1/4 - 20 nut against a plate. All plates tested were of 304 stainless steel, 4 inch O.D., .257 I.D., and the nominal thicknesses of the plates were 1/16, 1/8, 3/16 and 1/4 inch. In addition to the plates fastened with standard nuts which gave a loading circle of radius B (Fig. 5) of 0.211 inch, plates fastened by the special nuts described in Chapter III for which B was 0.5 inch were also tested.

Figure 10 shows the results of the autoradiographic tests described in Chapter III. For all plate pairs tested, i.e. 1/16, 1/8, 3/16 and 1/4 inch nominal, the value of B was 0.211 inch.

The pressure distributions and radii of separation for all the

above test cases were computed independently by the two plate model finite element analysis. Table 2 gives the test and analytical results for all test cases. The test results are an average of all measurements (minimum of six readings). A description of the analyses follows.

Figure 18 shows the results of a two plate and a single plate model analysis for the 0.253 inch bolted test specimen. For Figure 19 the external pressure distribution between radii A and B is triangular. (The total force, however, is equal to the force exerted in the case of uniform pressure.) In one case, the peak external pressure is at A, Fig. 20(a), and in the other case at B, Fig. 20(b). Results of another computation which assumed a uniform displacement of 50 microinches under each nut is shown in Fig. 21. It is interesting to note that the point of separation obtained by using the two plate model for all variations of loading given above occurs in the range of r/A values of 2.73 to 2.93 while the two plate model yields separation at a value for r/A of 3.5. The computed deflections under the nuts are given in Fig. 22.

The finite element analysis results for the 0.191 in. plate pair specimen are given in Fig. 23. Figures 24 and 25 show the computed pressure distribution and deflection patterns in the joint, respectively, for the 1/8 in. plate pair. In order to investigate the possible influence misalignments of the spanner wrench, i.e. vertical forces or restraints exerted at edge of plate, may have on the results of the experiment, the extreme case of fixing the outer edges of the plate as shown in Fig. 20(c) was considered. As Fig. 24 shows, within the

resolution of the finite element grid size, the effect is negligible. This model, Fig. 20(c), and result also indicate that the influence of additional fasteners 2 inches away would not have an influence on the contact zone for the geometry considered. (However, if the distance between bolts is considerably reduced, then the contact area should increase.) The computed results for the 1/16 inch plate pair is given in Fig. 26.

Figure 27 gives the finite element analysis results for the asymmetric case of a 1/8 in. plate bolted to a 1/4 in. plate. The model shown in Fig. 5(c) was used and as discussed in Chapter II, this model is strictly valid only if the friction in the joint prevents sliding between the plates. Nevertheless, the percent discrepancy between the computed value and tested value (see Table 2) falls within the range of the symmetric cases analyzed and tested.

In summary, the results obtained from the two plate finite element model and from experiment are in good agreement (Fig. 28).

Chapter V

APPLICATION

An application of the above results for the evaluation of the thermal contact conductance, h_c , and the determination of the heat transferred in a specific, but typical, lap joint section is illustrated in this chapter.

An aluminum lap joint in a vacuum environment, the relevant section and boundary conditions as shown in Fig. 29, was analyzed by means of a nodal analysis. The plate thickness was 0.1 in. and the hole diameter, 2A, was 0.2 in. The bearing surface of the bolt, 2B, was 0.26 in. in diameter. Because of the high conductivity and small thickness of the plates, no z dependence (see Fig. 29) was assumed for the temperature in the main body of the plate. However, heat flow in the z -direction in the nodes above and below the contact zone is considered. Qualitatively, the heat flow in the joint proceeds in the x - y plane from the left end (Fig. 29) toward the 0.2 in. diameter hole. In the vicinity of the hole, a macroscopic constriction for heat flow is encountered because the flow is being channeled toward the small contact zone. The flow of heat then encounters the microscopic constrictions at the contacting asperities (which determine h_c) in the contact zone; spreads out in the x - y directions in the second plate; and continues to the right edge of the lap joint.

The material properties assumed were (refer to equation 1.1):

$$\begin{aligned}
 H &= 150,000 \text{ psi} \\
 k &= 100 \text{ Btu/hr-}^\circ\text{F-ft} \quad (k_1 = k_2 = 100) \\
 \sigma &= 5.9 \times 10^{-6} \text{ ft.} \quad (\sigma_1 = \sigma_2 = 50 \times 10^{-6} \text{ in.}) \\
 \tan \theta &= 0.1
 \end{aligned}$$

Assuming further, a uniform load of 46,500 psi on the loading surface (#10 screw; 1000 lb. bolt force) and referring to Fig. 15, curve $\frac{B}{A} = 1.3$, the following interface stresses, σ_z , contact heat transfer coefficient, h_c , and conductance, (area) $\cdot(h_c)$, were obtained as a function of inner and outer radii. (These radii define increments of area, the sum of which define one quarter of the contact zone.):

$\frac{r_{\text{outer}}}{\text{inch}}$	$\frac{r_{\text{inner}}}{\text{inch}}$	$\frac{\sigma_z}{\text{psi}}$	$\frac{h_c}{\text{Btu/hr-}^\circ\text{F-ft}^2}$	Area x h_c $\text{Btu/hr-}^\circ\text{F-ft}^2$
.13	.1	27,900	446,000	16.6
.16	.13	14,000	223,000	10.6
.175	.16	3,950	63,100	1.7

The conductance between nodal points were then computed and with the aid of the steady state heat transfer program listed in Appendix D, the nodal temperatures for the conditions given in Fig. 29 were computed. The heat transferred from the edge maintained at 20°F to the edge at 0°F (Fig. 29) for this case was 2.88 Btu/hour. The same computation was repeated for the case of a bearing surface between the plate

and the bolt (2B) of 0.44 in. in diameter, but the bolt force was left unchanged. The heat transferred from the 20°F edge to the 0°F edge in this case was 3.15 Btu/hour. In the absence of the joint the heat transfer along an equivalent 7 inch length of solid aluminum would have been 3.58 Btu/hour. This data shows that the thermal resistance of the contact zone (not entire 7 inch lap joint) was decreased from 1.52 to 0.92 °F-hr/Btu by the increase of the effective bolt head diameter from .26 to .44 in. It should be observed that the change in thermal resistance of the joint is primarily due to the increase in contact area and the resulting decrease in macroscopic constriction resistance at the hole. Also, the heat flux in this example is mainly controlled by the 7 inch length and 0.1 inch thickness rather than the joint resistance. This emphasizes the importance of a balanced thermal design.

For large heat fluxes where thermal strains may have an influence on the radii of separation, the finite element program given in Appendix C may be used. Also, in a non-vacuum environment the effect of the interstitial fluid is added in two ways. Firstly, equation (1.6) is applied to account for the presence of interstitial fluid in the contact zone, and secondly, conduction across the gaps between the plates and convection from the plates is considered. (Radiation heat transfer, if applicable, should also be included.)

Chapter VI

CONCLUSIONS

The finite element technique used in this work for the analysis of the pressure distribution and deformation of smooth and flat bolted plates under conditions of axial symmetry predicts contact areas in joints considerably lower than reported previously in the literature. These results were verified experimentally. The discrepancy between the previously reported results and the results reported here is due to the simplifying assumption made by earlier researchers that a joint can be modeled as a single plate.

The computer programs listed in the appendices will also accommodate joints made up of plates of dissimilar materials and the presence of thermal gradients.

Of the eleven tests performed, only one (case 3, autoradiographic) yielded inconsistent results. (This data point could probably be ignored because of the poor adhesion of the plating material which manifested itself by the high radioactive contamination count during test.)

The finite element analysis performed for the test specimen show that the gap between the 1/4 inch bolted steel specimen is 98.6 microinches at the outer radius of the plate of 2 inches, and 1/32 of an inch away from the radius of separation (0.35 in.), the gap is

only 3 microinches for the test load. This data indicates the difficulties previous workers have encountered in their experiments. (This also explains the oval shape of several of the footprints.) Furthermore, this data shows that the effects of surface roughness and the lack of flatness could have a significant effect on the size of contour area.

An application of the above work to a heat transfer problem is illustrated in Chapter V.

REFERENCES

1. Cooper, M.G., Mikic, B.B., and Yovanovich, M.M., "Thermal Contact Conductance," International Journal of Heat and Mass Transfer, Vol. 12, No. 3 (March 1969), 279-300.
2. Roetscher, F., Die Maschinenelemente, Erster Band. Berlin: Julius Springer, 1927.
3. Fernlund, I., "A Method to Calculate the Pressure Between Bolted or Riveted Plates," Transactions of Chalmers, University of Technology. Gothenburg, Sweden, No. 245, 1961.
4. Greenwood, J.A., "The Elastic Stresses Produced in the Mid-Plane of a Slab by Pressure Applied Symmetrically at its Surface," Proc. Camb. Phil. Soc. Cambridge, England, Vol. 60, 1964, 159-169.
5. Lardner, T.J., "Stresses in a Thick Plate with Axially Symmetric Loading," J. of Applied Mechanics, Trans. ASME, Series E, Vol. 32, June 1965 (458-459).
6. Sneddon, I.N., "The Elastic Stresses Produced in a Thick Plate by the Application of Pressure to its Free Surfaces," Proc. Camb. Phil. Soc. Cambridge, England, Vol. 42, 1946 (260-271).
7. Bradley, T.L., "Stress Analysis for Thermal Contact Resistance Across Bolted Joints," M.S. Thesis, Massachusetts Institute of Technology, Mechanical Engineering Department, Cambridge, Mass. August 1968.
8. Louisiana State University, Division of Engineering Research, The Thermal Conductance of Bolted Joints. NASA Grant No. 19-001-035, C.A. Whitehurst, Dir. Baton Rouge: LSU Div. of Eng. Res., May 1968.
9. Zienkiewicz, O.C., The Finite Element Method in Structural and Continuum Mechanics. London: McGraw-Hill Publishing Co., Ltd., 1967.
10. Przemieniecki, J.S., Theory of Matrix Structural Analysis. New York: McGraw-Hill Book Co., 1968.
11. Cobb, B.J., "Preloading of Bolts," Product Engineering, August 19, 1963 (62-66).
12. Wilson, E.L., "Structural Analysis of Axisymmetric Solids," AIAA Journal, Vol. 3, No. 12, (Dec. 1965), 2269-2274.

13. Jones, R.M. and Crose, J.G., SAAS II Finite Element Stress Analysis of Axisymmetric Solids. United States Air Force Report No. SAMSOTR-68-455 (Sept. 1968).
14. Christian, J.T. and others, FEAST-1 and FEAST-3 Programs. Cambridge: Computer Program Library, M.I.T. Department of Civil Engineering, Soil Mechanics Division, 1969.
15. Clough, R.W., "The Finite Element Method in Structural Mechanics," Ch. 7, Stress Analysis, Zienkiewicz, O.C. and Holister, G.S., editors. London: John Wiley and Sons, Ltd., 1965.

APPENDIX A

FINITE ELEMENT ANALYSIS OF AXISYMMETRIC SOLIDS

The finite element method and the equations which govern the stresses and displacements in axisymmetric solids is given in the literature [9,10,12,13,15] and the procedure will be briefly summarized in this appendix.

The procedure for the standard stiffness analysis method is as follows [15]:

(a) The internal displacements, v , are expressed as

$$\{v(r,z)\} = [M(r,z)] \{\alpha\} \quad (A.1)$$

where M is a displacement function and α are the generalized coordinates representing the amplitudes of the displacement functions.

(b) The nodal displacements v_i are expressed in terms of the generalized coordinates

$$\{v_i\} = [A] \{\alpha\} \quad (A.2)$$

where A is obtained by substituting the coordinates of the nodal points into M .

(c) The generalized coordinates are expressed in terms of the nodal displacements

$$\{\alpha\} = [A]^{-1} \{v_i\} \quad (A.3)$$

(d) The element strains, ϵ , are evaluated

$$\{\epsilon\} = [B(r,z)] \{\alpha\} \quad (\text{A.4})$$

where B is obtained from the appropriate differentiation of M .

(e) The element stresses are expressed in terms of the stress-strain relation D

$$\{\sigma(r,z)\} = [D] \{\epsilon\} = [D] [B] \{\alpha\} \quad (\text{A.5})$$

(f) Assuming a virtual strain $\bar{\epsilon}$ and a generalized virtual coordinate displacement $\bar{\alpha}$ the internal virtual work, W_i , in the differential volume, dV , is given by

$$dW_i = \{\epsilon\}^T \{\sigma\} dV = \{\alpha\}^T [B]^T [D] [B] \{\alpha\} dV \quad (\text{A.6})$$

and the total internal virtual work is

$$W_i = \{\bar{\alpha}\}^T \left[\int_{Vol} [B]^T [D] [B] dV \right] \alpha \quad (\text{A.7})$$

(g) The external work, W_e , associated with the generalized displacement $\bar{\alpha}$ is

$$W_e = \{\alpha\}^T \{\beta\} \quad (\text{A.8})$$

where β are generalized forces corresponding with the displacements α .

(h) After equating W_i and W_e and setting the $\bar{\alpha}$ displacement to unity

$$\{\epsilon\} = \left[\int_{Vol} [B]^T [D] [B] \right] \alpha = [\bar{k}] \{\alpha\} \quad (A.9)$$

where $[\bar{k}] = \int_{Vol} [B]^T [D] [B] dV \quad (A.10)$

and which transforms to the nodal point surfaces

$$k = [A^{-1}] [\bar{k}] [A^{-1}] \quad (A.11)$$

(i) The stiffness matrix for the complete system is then

$$[K] = \sum_{m=1}^n [k]_m \quad (A.12)$$

where n equals the number of elements and the equilibrium relationship becomes

$$\{Q\} = [K] \{v_i\} \quad (A.13)$$

where

$$\{Q\} = \sum_{m=1}^n \{R\}_m \quad (A.14)$$

$$\{R\} = \int_{Area} [A^{-1}]^T [M]^T \{P\}_m dA \quad (A.15)$$

and P are the surface forces.

The above procedure applies with minor modification to problems with thermal and body force loading.

The expression

$$\{Q\} = [K] \{v_i\} \quad (A.16)$$

represents the relationship between all nodal point forces and all nodal point displacements. Mixed boundary conditions are considered by rewriting this equation in the partitioned form

$$\begin{Bmatrix} Q_a \\ Q_b \end{Bmatrix} = \begin{bmatrix} K_{aa} & K_{ab} \\ K_{ba} & K_{bb} \end{bmatrix} \begin{Bmatrix} u_a \\ u_b \end{Bmatrix} \quad (A.17)$$

where $v_i = u$.

The first part of the partitioned equation can be written as

$$\{Q_a\} = [K_{aa}] \{u_a\} + [K_{ab}] \{u_b\} \quad (A.18)$$

and then expressed in the reduced form

$$\{Q^*\} = [K_{aa}] \{u_a\} \quad (A.19)$$

where

$$\{Q^*\} = \{Q_a\} - [K_{ab}] \{u_b\} \quad (A.20)$$

The matrix equation (A.19) is solved for the nodal point displacements by standard techniques. Once the displacement are known the strains are evaluated from the strain displacement relationship and the stresses in turn are evaluated from the stress strain relations.

Both triangular and quadrilateral elements are used. The displacements in the $r-z$ plane in the element are assumed to be of the form

$$v_r = \alpha_1 + \alpha_2 r + \alpha_3 z \tag{A.21}$$

$$v_z = \alpha_4 + \alpha_5 r + \alpha_6 z$$

This linear displacement field assures continuity between elements since lines which are initially straight remain straight in their displaced position. Six equilibrium equations are developed for each triangular element.

A quadrilateral element is composed of four triangular elements and ten equilibrium equations correspond to each element.

APPENDIX B



FINITE ELEMENT PROGRAM FOR THE ANALYSIS OF ISOTROPIC
ELASTIC AXISYMMETRIC PLATES (ref. 13,14)

Input Instructions:

<u>Card Sequence</u>	<u>Item</u>	<u>Format</u>	<u>Columns</u>
1	Title	18A4	1-72
2	Total number of nodal points	I5	1-5
	Total number of elements	I5	6-10
	Total number of materials	I5	11-15
	Normalizing stress (NORM)	I5	16-20
	Number of pressure cards	I5	21-25
	(If NORM = 0, put in value of E in material card; if NORM = 1, put in value $E/\sigma_{\text{vertical}}$; if NORM = -1, put in value $E/\sigma_{\text{octahedral}}$; NOTE: Use NORM = 0 for this application.)		
3	(Material property cards - one set of (a) and (b) for each material)		
	(a) 1st card		
	Material No.	I5	1-5
	Initial σ_z stress	F10.0	6-15
	Initial σ_r stress	F10.0	16-25
	(b) Second Card		
	E	F10.0	1-10
	ν	F10.0	11-20

<u>Card Sequence</u>	<u>Item</u>	<u>Format</u>	<u>Column</u>
4	Nodal point information (One for each node)	2I5,4F10.0	
	Node number		1-5
	CODE		6-10
	r-coordinate		11-20
	z-coordinate		21-30
	XR		31-40
	XZ		41-50

If the number in column 10 is

		<u>Condition</u>
0	XR is the specified R-load and XZ is the specified Z-load	free
1	XR is the specified R-displacement and XZ is the specified Z-load	
2	XR is the specified R-load and XZ is the specified Z-displacement.	
3	XR is the specified R-displacement and XZ is the specified Z-displacement.	fixed

Remarks

The following restrictions are placed on the size of problems which can be handled by the program.

<u>Item</u>	<u>Maximum Number</u>
Nodal Points	450
Elements	450
Materials	25
Boundary Pressure Cards	200

All loads are considered to be total forces acting on a one radian segment. Nodal point cards must be in numerical sequence. If cards are omitted, the omitted nodal points are generated at equal intervals along a straight line between the defined nodal points. The boundary code (column 10), XR and XZ are set equal to zero.

If the number in columns 6-10 of the nodal point cards is other than 0, 1, 2 or 3, it is interpreted as the magnitude of an angle in degrees. The terms in columns 31-50 of the nodal point card are then interpreted as follows:

XR is the specified load in the s-direction

XZ is the specified displacement in the n-direction

The angle must always be input as a negative angle and may range from -.001 to -180 degrees. Hence, +1.0 degree is the same as -179.0 degrees. The displacements of these nodal points which are printed by the program are

u_r = the displacement in the s-direction

u_z = the displacement in the n-direction

Element cards must be in element number sequence. If element cards are omitted, the program automatically generates the omitted information by incrementing by one the preceding I, J, K and L. The material identification code for the generated cards is set equal to the value given on the last card. The last element card must always be supplied.

Triangular elements are also permissible; they are identified by repeating the last nodal point number (i.e. I, J, K, K).

One card for each boundary element which is subjected to a normal pressure is required. The boundary element must be on the left as one

progresses from I to J. Surface tensile force is input as a negative pressure.

Printed output includes:

1. Reprint of input data.
2. Nodal point displacement
3. Stresses at the center of each element.

Nodal point numbers must be entered counterclockwise around the element when coding element data.

The maximum difference between the nodal point numbers on an element must be less than 25. However, on a nodal diagram elements and nodes need not be numbered sequentially.

Listing:

```
C      *****
C      FINITE ELEMENT PROGRAM FOR THE ANALYSIS OF ISOTROPIC ELASTIC
C      AXYSYMMETRIC PLATES REF FEAST 1,3 SAAS 2
C      *****
C
C      IMPLICIT REAL*8 (A-H,O-Z)
C      IMPLICIT INTEGER*2(I-N)
C      COMMON      STTCP,HED(18),SIGIR(25),SIGI7(25),GAMMA(25),ZKNOT(25),
1 DEPTH(25),E(10,25),SIG(7),R(450),Z(450),UR(450),
2 UZ(450),STOTAL(450,4),KSW
C      COMMON /INTEGR/ NUMNP,NUMEL,NUMMAT,NDEPTH,NORM,MTYPE,ICODE(450)
C      COMMON /ARG/ RRR(5),ZZZ(5),S(10,10),P(10),LM(4),DD(3,3),
1 HH(6,10),RR(4),ZZ(4),C(4,4),H(6,10),D(6,6),F(6,10),TP(6),XI(6),
2 FE(10),IX(450,5)
C      COMMON /BANARG/ B(900),A(900,54),MBAND
C      COMMON/PRESS/ IBC(200),JBC(200),PR(200),NUMPC
C      DATA STRS /'*****'/
C      *****
C      READ AND PRINT CONTROL INFORMATION
C      *****
50 READ (5,1000,END=950) HED
WRITE (6,2000) HED
C
C      READ(5,1001) NUMNP,NUMEL,NUMMAT,NORM,NUMPC
WRITE (6,2006) NUMNP,NUMEL
IF (NORM) 65,65,66
66 WRITE (6,2041)
C      *****
C      READ AND PRINT MATERIAL PROPERTIES
C      *****
65 CONTINUE
C
C      DO 80 M=1,NUMMAT
C      READ (5,1002) MTYPE, SIGIZ(MTYPE),SIGIR(MTYPE)
C      WRITE (6,2007) MTYPE,SIGIZ(MTYPE),SIGIR(MTYPE)
C      READ (5,1003) (E(J,MTYPE),J=1,2)
C      FENT0001
C      FENT0002
C      FENT0003
C      FENT0004
C      FENT0005
C      FENT0006
C      FENT0007
C      FENT0008
C      FENT0009
C      FENT0010
C      FENT0011
C      FENT0012
C      FENT0013
C      FENT0014
C      FENT0015
C      FENT0016
C      FENT0017
C      FENT0018
C      FENT0019
C      FENT0020
C      FENT0021
C      FENT0022
C      FENT0023
C      FENT0024
C      FENT0025
C      FENT0026
C      FENT0027
C      FENT0028
C      FENT0029
C      FENT0030
C      FENT0031
C      FENT0032
C      FENT0033
C      FENT0034
C      FENT0035
C      FENT0036
```

	WRITE (6,2051) (E(J,MTYPE),J=1,2)	FENT0037
80	CONTINUE	FENT0038
C	*****	FENT0039
C	READ AND PRINT NODAL POINT DATA	FENT0040
C	*****	FENT0041
100	WRITE (6,2013)	FENT0042
	L=0	FENT0043
105	READ (5,1006) N,ICODE(N),R(N),Z(N),UR(N),UZ(N)	FENT0044
106	NL=L+1	FENT0045
	IF (L.EQ.0) GO TO 110	FENT0046
	ZX=N-L	FENT0047
	DR=(R(N)-R(L))/ZX	FENT0048
	DZ=(Z(N)-Z(L))/ZX	FENT0049
110	L=L+1	FENT0050
	IF (N-L) 113,112,111	FENT0051
111	ICODE(L)=0	FENT0052
	R(L)=R(L-1)+DR	FENT0053
	Z(L)=Z(L-1)+DZ	FENT0054
	UR(L)=0.0	FENT0055
	UZ(L)=0.0	FENT0056
	GO TO 110	FENT0057
112	WRITE (6,2014) (K,ICODE(K),R(K),Z(K),UR(K),UZ(K),K=NL,N)	FENT0058
	IF (NUMNP-N) 113,120,105	FENT0059
113	WRITE (6,2015) N	FENT0060
	GO TO 900	FENT0061
C	*****	FENT0062
C	READ AND PRINT ELEMENT PROPERTIES	FENT0063
C	*****	FENT0064
120	WRITE (6,2016)	FENT0065
	N=0	FENT0066
130	READ (5,1007) M,(IX(M,I),I=1,5)	FENT0067
140	N=N+1	FENT0068
	IF (M-N) 170,170,150	FENT0069
150	IX(N,1)=IX(N-1,1)+1	FENT0070
	IX(N,2)=IX(N-1,2)+1	FENT0071
	IX(N,3)=IX(N-1,3)+1	FENT0072

	IX(N,4)=IX(N-1,4)+1	FENT0073
	IX(N,5)=IX(N-1,5)	FENT0074
170	WRITE (6,2017) N,(IX(N,I),I=1,5)	FENT0075
	IF (M-N) 180,180,140	FENT0076
180	IF (NUMEL-N) 300,300,130	FENT0077
C	*****	FENT0078
C	READ AND PRINT THE PRESSURE CARDS	FENT0079
C	*****	FENT0080
300	IF(NUMPC) 290,210,290	FENT0081
290	WRITE(6,9000)	FENT0082
	DO 200 L=1,NUMPC	FENT0083
	READ(5,9001) IRC(L),JBC(L),PR(L)	FENT0084
200	WRITE(6,9002) IRC(L),JBC(L),PR(L)	FENT0085
210	CONTINUE	FENT0086
C	*****	FENT0087
C	DETERMINE PAND WIDTH	FENT0088
C	*****	FENT0089
	J=0	FENT0090
	DO 340 N=1,NUMEL	FENT0091
	DO 340 I=1,4	FENT0092
	DO 325 L=1,4	FENT0093
	KK=IX(N,I)-IX(N,L)	FENT0094
	IF (KK.LT.0) KK=-KK	FENT0095
	IF (KK.GT.J) J=KK	FENT0096
325	CONTINUE	FENT0097
340	CONTINUE	FENT0098
	MRAND=2*J+2	FENT0099
C	*****	FENT0100
C	SOLVE FOR DISPLACEMENTS AND STRESSES	FENT0101
C	*****	FENT0102
	KSW=0	FENT0103
	CALL STIFF	FENT0104
	IF (KSW.NE.0) GO TO 900	FENT0105
C		FENT0106
	CALL BANSCL	FENT0107
	WRITE(6,2052)	FENT0108

```

WRITE (6,2025) (N,B      (2*N-1),B      (2*N),N=1,NUMNP)
C
450 CALL STRESS(SPLOT)
C *****
C PROCESS ALL DFCKS EVEN IF ERROR
C *****
GO TO 910
900 WRITE (6,4000)
910 WRITE (6,4001) HED
C
920 READ (5,1000) CHK
IF (CHK.NE.STRS) GO TO 920
GO TO 50
950 CONTINUE
WRITE (6,4002)
CALL EXIT
C *****
C *****
1000 FORMAT (18A4)
1001 FORMAT (12I5)
1002 FORMAT ( 15,2F10.0)
1003 FORMAT(2F10.0)
1004 FORMAT (2F10.0)
1005 FORMAT (3F10.0)
1006 FORMAT (2I5,4F10.0)
1007 FORMAT (6I5)
C *****
2000 FORMAT (1H1,20A4)
2006 FORMAT (28HNUMBER OF NODAL POINTS----- I3/
1 28H NUMBER OF ELEMENTS----- I3)
2007 FORMAT (20HOMATERIAL NUMBER---- I3/
1 25H INITIAL VERTICAL STRESS= F10.3 ,5X,
2 26HINITIAL HORIZONTAL STRESS= F10.3)
2013 FORMAT (12HINODAL POINT ,4X, 4HTYPE ,4X, 10HR-ORDINATE ,4X,
1 10HZ-ORDINATE ,10X, 6HR-LOAD ,10X, 6HZ-LOAD )
2014 FORMAT (I12,I8,2F14.3,2E16.5)

```

```

FENTO109
FENTO110
FENTO111
FENTO112
FENTO113
FENTO114
FENTO115
FENTO116
FENTO117
FENTO118
FENTO119
FENTO120
FENTO121
FENTO122
FENTO123
FENTO124
FENTO125
FENTO126
FENTO127
FENTO128
FENTO129
FENTO130
FENTO131
FENTO132
FENTO133
FENTO134
FENTO135
FENTO136
FENTO137
FENTO138
FENTO139
FENTO140
FENTO141
FENTO142
FENTO143
FENTO144

```

```

2015 FORMAT (26NODAL POINT CARD ERROR N= I5)
2016 FORMAT (49HELEMENT NO.      I      J      K      L      MATERIAL  )
2017 FORMAT (I113,4I6,1I12)
2025 FORMAT (12NODAL POINT ,6X, 14HR-DISPLACEMENT ,6X, 14HZ-DISPLACEM
1ENT / (I12,1P2D20.7))
2041 FORMAT (76MODULUS AND YIELD STRESS NORMALIZED WITH RESPECT TO IN
1ITIAL VERTICAL STRESS )
2051 FORMAT(1H0,10X,'E',8X,'NU',/,3X,F11.1,F10.4/)
2052 FORMAT(1H1)
C *****
3003 FORMAT (16I5)
C *****
4000 FORMAT (//// ' ABNORMAL TERMINATION')
4001 FORMAT (//// ' END OF PROBLEM ' 20A4)
4002 FORMAT (//// ' END OF JOB')
C *****
9000 FORMAT(29HOPRESSURE BOUNDARY CONDITIONS/ 24H      I      J      PRESSU
1RE )
9001 FORMAT(2I5,F10.0)
9002 FORMAT(2I6,F12.3)
      END
      SUBROUTINE STIFF
C
      IMPLICIT REAL*8 (A-H,O-Z)
      IMPLICIT INTEGER*2(I-N)
      COMMON      STTCP,HED(18),SIGIR(25),SIGIZ(25),GAMMA(25),ZKNOT(25),
1 DEPTH(25),E(10,25),SIG(7),R(450),Z(450),UR(450),
2 UZ(450),STOTAL(450,4),KSW
      COMMON /INTGR/ NUMNP,NUMEL,NUMMAT,NDEPTH,NORM,MTYPE,ICODE(450)
      COMMON /ARG/ RRR(5),ZZZ(5),S(10,10),P(10),LM(4),DD(3,3),
1 HH(6,10),RR(4),ZZ(4),C(4,4),H(6,10),D(6,6),F(6,10),TP(6),XI(6),
2 EE(10),IX(450,5)
      COMMON /BANARG/ B(900),A(900,54),MBAND
      COMMON/PRESS/ IBC(200),JBC(200),PR(200),NUMPC
      DIMENSION CODE(450)
C *****

```

```

FENTO145
FENTO146
FENTO147
FENTO148
FENTO149
FENTO150
FENTO151
FENTO152
FENTO153
FENTO154
FENTO155
FENTO156
FENTO157
FENTO158
FENTO159
FENTO160
FENTO161
FENTO162
FENTO163
FENTO164
FENTO165
FENTO166
FENTO167
FENTO168
FENTO169
FENTO170
FENTO171
FENTO172
FENTO173
FENTO174
FENTO175
FENTO176
FENTO177
FENTO178
FENTO179
FENTO180

```

C	INITIALIZATION	FENT0181
C	*****	FENT0182
	NB=27	FENT0183
	ND=2*NB	FENT0184
	ND2=2*NUMNP	FENT0185
	DO 50 N=1,ND2	FENT0186
	B(N)=0.0	FENT0187
	DO 50 M=1,ND	FENT0188
50	A(N,M)=0.0	FENT0189
C	*****	FENT0190
C	FORM STIFFNESS MATRIX	FENT0191
C	*****	FENT0192
	DO 210 N=1,NUMEL	FENT0193
C		FENT0194
C		FENT0195
	90 CALL QUAD(N,VOL)	FENT0196
	IF (VOL) 142,142,144	FENT0197
142	WRITE (6,2003) N	FENT0198
	KSW=1	FENT0199
	GO TO 210	FENT0200
C		FENT0201
	144 IF (IX(N,3)-IX(N,4)) 145,165,145	FENT0202
145	DO 150 II=1,9	FENT0203
	CC=S(II,10)/S(10,10)	FENT0204
	DO 150 JJ=1,9	FENT0205
150	S(II,JJ)=S(II,JJ)-CC*S(10,JJ)	FENT0206
C		FENT0207
	DO 160 II=1,8	FENT0208
	CC=S(II,9)/S(9,9)	FENT0209
	DO 160 JJ=1,8	FENT0210
160	S(II,JJ)=S(II,JJ)-CC*S(9,JJ)	FENT0211
C		FENT0212
C	ADD ELEMENT STIFFNESS TO TOTAL STIFFNESS	FENT0213
C		FENT0214
	165 DO 166 I=1,4	FENT0215
166	LM(I)=2*IX(N,I)-2	FENT0216

C		FENT0217
	DO 200 I=1,4	FENT0218
	DO 200 K=1,2	FENT0219
	II=LM(I)+K	FENT0220
	KK=2*I-2+K	FENT0221
	DO 200 J=1,4	FENT0222
	DO 200 L=1,2	FENT0223
	JJ=LM(J)+L-II+1	FENT0224
	LL=2*J-2+L	FENT0225
	IF (JJ) 200,200,175	FENT0226
175	IF (ND-JJ) 180,195,195	FENT0227
180	WRITE (6,2004) N	FENT0228
	KSW=1	FENT0229
	GO TO 210	FENT0230
195	A(II,JJ)=A(II,JJ)+S(KK,LL)	FENT0231
200	CONTINUE	FENT0232
210	CONTINUE	FENT0233
	IF(KSW.EQ.1) GO TO 500	FENT0234
C		FENT0235
C	ADD CONCENTRATED FORCES	FENT0236
C		FENT0237
	DO 250 N=1,NUMNP	FENT0238
	K=2*N	FENT0239
	B(K)=P(K)+U7(N)	FENT0240
	B(K-1)=B(K-1)+UR(N)	FENT0241
250	CONTINUE	FENT0242
C		FENT0243
C		FENT0244
C	PRESSURE BOUNDARY CONDITIONS	FENT0245
C		FENT0246
	IF(NUMPC) 260,310,260	FENT0247
260	DO 300 L=1,NUMPC	FENT0248
	I=IBC(L)	FENT0249
	J=JBC(L)	FENT0250
	CODE(I)=ICODE(I)	FENT0251
	CODE(J)=ICODE(J)	FENT0252

	PP=PR(L)/6.	FENT0253
	DZ=(Z(I)-Z(J))*PP	FENT0254
	DR=(R(J)-R(I))*PP	FENT0255
	RX=2.0*R(I)+R(J)	FENT0256
	ZX=R(I)+2.0*R(J)	FENT0257
264	II=2*I	FENT0258
	JJ=2*J	FENT0259
270	SINA=0.0	FENT0260
	COSA=1.0	FENT0261
	IF(CODE(I)) 271,272,272	FENT0262
271	SINA=DSIN(CODE(I))	FENT0263
	COSA=DCOS(CODE(I))	FENT0264
272	B(II-1)=B(II-1)+RX*(COSA*DZ+SINA*DR)	FENT0265
	B(II)=B(II)-RX*(SINA*DZ-COSA*DR)	FENT0266
290	SINA=0.0	FENT0267
	COSA=1.0	FENT0268
	IF(CODE(J)) 291,292,292	FENT0269
291	SINA=DSIN(CODE(I))	FENT0270
	COSA=DCOS(CODE(I))	FENT0271
292	B(JJ-1)=B(JJ-1)+ZX*(COSA*DZ+SINA*DR)	FENT0272
	B(JJ)=B(JJ)-ZX*(SINA*DZ-COSA*DR)	FENT0273
300	CONTINUE	FENT0274
310	CONTINUE	FENT0275
C	DISPLACEMENT B.C.	FENT0276
C		FENT0277
	DO 400 M=1,NUMNP	FENT0278
	U=UR(M)	FENT0279
	N=2*M-1	FENT0280
	KX=ICODE(M)+1	FENT0281
	GO TO (400,370,390,380),KX	FENT0282
370	CALL MODIFY(N,U,ND2)	FENT0283
	GO TO 400	FENT0284
380	CALL MODIFY(N,U,ND2)	FENT0285
390	U=UZ(M)	FENT0286
	N=N+1	FENT0287
	CALL MODIFY(N,U,ND2)	FENT0288

400	CONTINUE	FENT0289
C		FENT0290
500	RETURN	FENT0291
C	*****	FENT0292
2003	FORMAT (26HNEGATIVE AREA ELEMENT NO. I4)	FENT0293
2004	FORMAT (29HOBAND WIDTH EXCEEDS ALLOWABLE I4)	FENT0294
C	*****	FENT0295
	END	FENT0296
	SUBROUTINE QUAD(N,VOL)	FENT0297
C		FENT0298
	IMPLICIT REAL*8 (A-H,O-Z)	FENT0299
	IMPLICIT INTEGER*2 (I-N)	FENT0300
	COMMON STTOP,HED(18),SIGIR(25),SIGIZ(25),GAMMA(25),ZKNOT(25),	FENT0301
	1 DEPTH(25),E(10,25),SIG(7),R(450),Z(450),UR(450),	FENT0302
	2 UZ(450),STOTAL(450,4),KSW	FENT0303
	COMMON /INTEGR/ NUMNP,NUMEL,NUMMAT,NDEPTH,NORM,MTYPE,ICODE(450)	FENT0304
	COMMON /ARG/ RRR(5),ZZZ(5),S(10,10),P(10),LM(4),DD(3,3),	FENT0305
	1 HH(5,10),RR(4),ZZ(4),C(4,4),H(6,10),D(6,6),F(6,10),TP(6),XI(6),	FENT0306
	2 FE(10),IX(450,5)	FENT0307
	COMMON /BANARG/ B(900),A(900,54),MBAND	FENT0308
C	*****	FENT0309
	I=IX(N,1)	FENT0310
	J=IX(N,2)	FENT0311
	K=IX(N,3)	FENT0312
	L=IX(N,4)	FENT0313
C		FENT0314
	I1=1	FENT0315
	I2=2	FENT0316
	I3=3	FENT0317
	I4=4	FENT0318
	I5=5	FENT0319
C	*****	FENT0320
C	DETERMINE ELASTIC CONSTANTS AND STRESS-STRAIN RELATIONSHIP	FENT0321
C	*****	FENT0322
C		FENT0323
	CALL MPROP(N)	FENT0324

C		FENT0325
C	*****	FENT0326
C	FORM QUADRILATERAL STIFFNESS MATRIX	FENT0327
C	*****	FENT0328
	210 RRR(5)=(R(I)+R(J)+R(K)+R(L))/4.0	FENT0329
	ZZZ(5)=(Z(I)+Z(J)+Z(K)+Z(L))/4.0	FENT0330
	DO 94 M=1,4	FENT0331
	MM=IX(N,M)	FENT0332
	IF(R(MM).EQ.0..AND.ICODE(MM).EQ.0) ICODE(MM)=1	FENT0333
	93 RRR(M)=R(MM)	FENT0334
	94 ZZZ(M)=Z(MM)	FENT0335
C		FENT0336
	DO 100 II=1,10	FENT0337
	DO 95 JJ=1,6	FENT0338
	95 HH(JJ,II)=0.0	FENT0339
	DO 100 JJ=1,10	FENT0340
	100 S(II,JJ)=0.0	FENT0341
	IF (K-L) 125,120,125	FENT0342
	120 CALL TRISTF(I1,I2,I3)	FENT0343
	RRR(5)=(RRR(1)+RRR(2)+RRR(3))/3.0	FENT0344
	ZZZ(5)=(ZZZ(1)+ZZZ(2)+ZZZ(3))/3.0	FENT0345
	VOL=XI(1)	FENT0346
	GO TO 160	FENT0347
	125 VOL=0.0	FENT0348
	CALL TRISTF(I4,I1,I5)	FENT0349
	IF(XI(1).EQ.0.) WRITE(6,2000) N	FENT0350
	VOL=VOL+XI(1)	FENT0351
	CALL TRISTF(I1,I2,I5)	FENT0352
	IF(XI(1).EQ.0) WRITE(6,2000) N	FENT0353
	VOL=VOL+XI(1)	FENT0354
	CALL TRISTF(I3,I4,I5)	FENT0355
	IF(XI(1).EQ.0) WRITE(6,2000) N	FENT0356
	VOL=VOL+XI(1)	FENT0357
	CALL TRISTF(I2,I3,I5)	FENT0358
	IF(XI(1).EQ.0) WRITE(6,2000) N	FENT0359
	VOL=VOL+XI(1)	FENT0360

C	DO 140 II=1,6	FENTO361
	DO 140 JJ=1,10	FENTO362
	140 HH(II,JJ)=HH(II,JJ)/4.0	FENTO363
C		FENTO364
C		FENTO365
	160 RETURN	FENTO366
C	****	FENTO367
	2000 FORMAT (' ZERO AREA ELEMENT',I5)	FENTO368
	END	FENTO369
	SUBROUTINE TRISTF(II,JJ,KK)	FENTO370
	IMPLICIT REAL*8 (A-H,C-Z)	FENTO371
	IMPLICIT INTEGER*2(I-N)	FENTO372
	COMMON STTOP,HED(18),SIGIR(25),SIGIZ(25),GAMMA(25),ZKNOT(25),	FENTO373
	1 DEPTH(25),E(10,25),SIG(7),R(450),Z(450),UR(450),	FENTO374
	2 UZ(450),STOTAL(450,4),KSW	FENTO375
	COMMON /INTEGR/ NUMNP,NUMEL,NUMMAT,NDEPTH,NORM,MTYPE,ICODE(450)	FENTO376
	COMMON /ARG/ RRR(5),ZZZ(5),S(10,10),P(10),LM(4),DD(3,3),	FENTO377
	1 HH(6,10),RR(4),Z7(4),C(4,4),H(6,10),D(6,6),F(6,10),TP(6),XI(6),	FENTO378
	2 EE(10),IX(450,5)	FENTO379
	COMMON /BANARG/ B(900),A(900,54),MBAND	FENTO380
C	*****	FENTO381
C	INITIALIZATION	FENTO382
C		FENTO383
	LM(1)=II	FENTO384
	LM(2)=JJ	FENTO385
	LM(3)=KK	FENTO386
C		FENTO387
	RR(1)=RRR(II)	FENTO388
	RR(2)=RRR(JJ)	FENTO389
	RR(3)=RRR(KK)	FENTO390
	RR(4)=RRR(II)	FENTO391
	Z7(1)=Z77(II)	FENTO392
	ZZ(2)=ZZ7(JJ)	FENTO393
	Z7(3)=Z77(KK)	FENTO394
	Z7(4)=Z77(II)	FENTO395
		FENTO396

C		FENT0397
	85 DO 100 I=1,6	FENT0398
	DO 90 J=1,10	FENT0399
	F(I,J)=0.0	FENT0400
	90 H(I,J)=0.0	FENT0401
	DO 100 J=1,6	FENT0402
	100 D(I,J)=0.0	FENT0403
C		FENT0404
C	FORM INTEGRAL (G)T*(C)*(G)	FENT0405
	CALL INTER(XI,RR,ZZ)	FENT0406
C		FENT0407
	D(2,6)=XI(1)*(C(1,2)+C(2,3))	FENT0408
	D(3,5)=XI(1)*C(4,4)	FENT0409
	D(5,5)=D(3,5)	FENT0410
	D(6,6)=XI(1)*C(2,2)	FENT0411
	D(1,1)=XI(3)*C(3,3)	FENT0412
	D(1,2)=XI(2)*(C(1,3)+C(3,3))	FENT0413
	D(1,3)=XI(5)*C(3,3)	FENT0414
	D(1,6)=XI(2)*C(2,3)	FENT0415
	D(2,2)=XI(1)*(C(1,1)+2.0*C(1,3)+C(3,3))	FENT0416
	D(2,3)=XI(4)*(C(1,3)+C(3,3))	FENT0417
	D(3,3)=XI(6)*C(3,3)+XI(1)*C(4,4)	FENT0418
	D(3,6)=XI(4)*C(2,3)	FENT0419
	DO 110 I=1,6	FENT0420
	DO 110 J=1,6	FENT0421
	110 D(J,I)=D(I,J)	FENT0422
C		FENT0423
C		FENT0424
C	FORM COEFFICIENT-DISPLACEMENT MATRIX	FENT0425
C		FENT0426
	COMM=RR(2)*(ZZ(3)-ZZ(1))+RR(1)*(ZZ(2)-ZZ(3))+RR(3)*(ZZ(1)-ZZ(2))	FENT0427
	DD(1,1)=(RR(2)*ZZ(3)-RR(3)*ZZ(2))/COMM	FENT0428
	DD(1,2)=(RR(3)*ZZ(1)-RR(1)*ZZ(3))/COMM	FENT0429
	DD(1,3)=(RR(1)*ZZ(2)-RR(2)*ZZ(1))/COMM	FENT0430
	DD(2,1)=(ZZ(2)-ZZ(3))/COMM	FENT0431
	DD(2,2)=(ZZ(3)-ZZ(1))/COMM	FENT0432

	DD(2,3)=(ZZ(1)-ZZ(2))/COMM	FENT0433
	DD(3,1)=(RR(3)-RR(2))/COMM	FENT0434
	DD(3,2)=(RR(1)-RR(3))/COMM	FENT0435
	DD(3,3)=(RR(2)-RR(1))/COMM	FENT0436
C		FENT0437
	DO 120 I=1,3	FENT0438
	J=2*LM(I)-1	FENT0439
	H(1,J)=DD(1,I)	FENT0440
	H(2,J)=DD(2,I)	FENT0441
	H(3,J)=DD(3,I)	FENT0442
	H(4,J+1)=DD(1,I)	FENT0443
	H(5,J+1)=DD(2,I)	FENT0444
120	H(6,J+1)=DD(3,I)	FENT0445
C		FENT0446
C	FORM STIFFNESS MATRIX (H)T*(D)*(H)	FENT0447
C		FENT0448
	DO 130 J=1,10	FENT0449
	DO 130 K=1,6	FENT0450
	IF (H(K,J)) 128,130,128	FENT0451
128	DO 129 I=1,6	FENT0452
129	F(I,J)=F(I,J)+D(I,K)*H(K,J)	FENT0453
130	CONTINUE	FENT0454
C		FENT0455
	DO 140 I=1,10	FENT0456
	DO 140 K=1,6	FENT0457
	IF (H(K,I)) 138,140,138	FENT0458
138	DO 139 J=1,10	FENT0459
139	S(I,J)=S(I,J)+H(K,I)*F(K,J)	FENT0460
140	CONTINUE	FENT0461
C		FENT0462
C	FORM STRAIN TRANSFORMATION MATRIX	FENT0463
C		FENT0464
	DO 410 I=1,6	FENT0465
	DO 410 J=1,10	FENT0466
410	HH(I,J)=HH(I,J)+H(I,J)	FENT0467
C		FENT0468

C	500 RETURN	FENT0469
	FND	FENT0470
	SUBROUTINE MPRCP(N)	FENT0471
	IMPLICIT REAL*8 (A-H,O-Z)	FENT0472
	IMPLICIT INTEGER*2(I-N)	FENT0473
	COMMON STDP,HED(18),SIGIR(25),SIGIZ(25),GAMMA(25),ZKNOT(25),	FENT0474
	1 DEPTH(25),E(10,25),SIG(7),R(450),Z(450),UR(450),	FENT0475
	2 UZ(450),STOTAL(450,4),KSW	FENT0476
	COMMON /INTEGR/ NUMNP,NUMEL,NUMMAT,NDEPTH,NORM,MTYPE,ICODE(450)	FENT0477
	COMMON /ARG/ RRR(5),ZZZ(5),S(10,10),P(10),LM(4),DD(3,3),	FENT0478
	1 HH(6,10),RR(4),ZZ(4),C(4,4),H(6,10),D(6,6),F(6,10),TP(6),XI(6),	FENT0479
	2 EE(10),IX(450,5)	FENT0480
	COMMON /BANARG/ B(900),A(900,54),MBAND	FENT0481
C	*****	FENT0482
	I=IX(N,1)	FENT0483
	J=IX(N,2)	FENT0484
	K=IX(N,3)	FENT0485
	L=IX(N,4)	FENT0486
	MTYPE=IX(N,5)	FENT0487
C		FENT0488
	DO 5 II=1,4	FENT0489
	DO 5 JJ=1,4	FENT0490
	5 C(II,JJ)=0.0	FENT0491
C	*****	FENT0492
C	DETERMINE ELASTIC CONSTANTS	FENT0493
C	*****	FENT0494
C		FENT0495
	40 DO 55 KK=1,2	FENT0496
	55 EF(KK)=E(KK,MTYPE)	FENT0497
	60 IF (NORM) 65,75,65	FENT0498
	65 FF(1)=EE(1)*SIGIZ(MTYPE)	FENT0499
C	*****	FENT0500
C	FORM STRESS STRAIN RELATIONSHIP	FENT0501
C	*****	FENT0502
	75 COFF=EE(1)/(1.-EE(2)-2.*EE(2)*FF(2))	FENT0503
		FENT0504

	C(1,1)=COEF*(1.-EE(2))	FENT0505
	C(1,2)=COEF*EE(2)	FENT0506
	C(1,3)=EE(2)*COEF	FENT0507
	C(2,1)=C(1,2)	FENT0508
	C(2,2)=C(1,1)	FENT0509
	C(2,3)=C(1,2)	FENT0510
	C(3,1)=C(1,3)	FENT0511
	C(3,2)=C(1,2)	FENT0512
	C(3,3)=C(1,1)	FENT0513
	C(4,4)=COEF*(0.5-EE(2))	FENT0514
	RETURN	FENT0515
	END	FENT0516
	SUBROUTINE MODIFY(N,U,ND2)	FENT0517
C		FENT0518
	IMPLICIT REAL*8 (A-H,O-Z)	FENT0519
	IMPLICIT INTEGER*2(I-N)	FENT0520
	COMMON /BANARG/ R(900),A(900,54),MBAND	FENT0521
	DD 250 M=2,MBAND	FENT0522
	K=N-M+1	FENT0523
	IF (K) 235,235,230	FENT0524
230	B(K)=B(K)-A(K,M)*U	FENT0525
	A(K,M)=0.0	FENT0526
235	K=N+M-1	FENT0527
	IF (ND2-K) 250,240,240	FENT0528
240	B(K)=B(K)-A(N,M)*U	FENT0529
	A(N,M)=0.0	FENT0530
250	CONTINUE	FENT0531
	A(N,1)=1.0	FENT0532
	B(N)=U	FENT0533
	RETURN	FENT0534
	FND	FENT0535
	SUBROUTINE BANSOL	FENT0536
C		FENT0537
	IMPLICIT REAL*8 (A-H,O-Z)	FENT0538
	IMPLICIT INTEGER*2(I-N)	FENT0539
	COMMON STTCP,HED(18),SIGIR(25),SIGIZ(25),GAMMA(25),ZKNOT(25),	FENT0540

	1 DEPTH(25),E(10,25),SIG(7),R(450),7(450),UR(450),	FENT0541
	2 UZ(450),STOTAL(450,4),KSW	FENT0542
	COMMON /INTEGR/ NUMNP,NUMEL,NUMMAT,NDEPTH,NORM,MTYPE,ICCODE(450)	FENT0543
	COMMON /BANARG/ B(900),A(900,54),MBAND	FENT0544
	ND2=2*NUMNP	FENT0545
C		FENT0546
	DO 280 N=1,ND2	FENT0547
	DO 260 L=2,MBAND	FENT0548
	C=A(N,L)/A(N,1)	FENT0549
	I=N+L-1	FENT0550
C		FENT0551
	IF (ND2.LT.I) GO TO 260	FENT0552
C		FENT0553
	J=0	FENT0554
	DO 250 K=L,MBAND	FENT0555
	J=J+1	FENT0556
	250 A(I,J)=A(I,J)-C*A(N,K)	FENT0557
	B(I)=B(I)-C*B(N)	FENT0558
	260 A(N,L)=C	FENT0559
	280 B(N)=B(N)/A(N,1)	FENT0560
C		FENT0561
C	BACKSUBSTITUTION	FENT0562
C		FENT0563
	N=ND2	FENT0564
	300 N=N-1	FENT0565
C		FENT0566
	IF (N.LE.0) GO TO 500	FENT0567
	DO 400 K=2,MBAND	FENT0568
	L=N+K-1	FENT0569
	IF (ND2.LT.L) GO TO 400	FENT0570
	B(N)=B(N)-A(N,K)*B(L)	FENT0571
	400 CONTINUE	FENT0572
C		FENT0573
	GO TO 300	FENT0574
C		FENT0575
	500 RETURN	FENT0576

END	FENT0577
SUBROUTINE STRESS(SPLOTT)	FENT0578
IMPLICIT REAL*8 (A-H,O-Z)	FENT0579
IMPLICIT INTEGER*2(I-N)	FENT0580
COMMON STTOP,HFD(18),SIGIR(25),SIGIZ(25),GAMMA(25),ZKNOT(25),	FENT0581
1 DEPTH(25),E(10,25),SIG(7),R(450),Z(450),UR(450),	FENT0582
2 UZ(450),STOTAL(450,4),KSW	FENT0583
COMMON /INTEGR/ NUMNP,NUMEL,NUMMAT,NDEPTH,NORM,MTYPE,ICODE(450)	FENT0584
COMMON /ARG/ RRR(5),ZZZ(5),S(10,10),P(10),LM(4),DD(3,3),	FENT0585
1 HH(6,10),RR(4),ZZ(4),C(4,4),H(6,10),D(6,6),F(6,10),TP(6),XI(6),	FENT0586
2 EE(10),IX(450,5)	FENT0587
COMMON /BANARG/ B(900),A(900,54),MBAND	FENT0588
C *****	FENT0589
C COMPUTE ELEMENT STRESSES AND STRAINS	FENT0590
C *****	FENT0591
DO 300 N=1,NUMEL	FENT0592
CALL QUAD(N,VOL)	FENT0593
C	FENT0594
C FIND ELEMENT COORDINATES	FENT0595
C	FENT0596
I1=IX(N,1)	FENT0597
J1=IX(N,2)	FENT0598
K1=IX(N,3)	FENT0599
L1=IX(N,4)	FENT0600
C	FENT0601
IF (K1-L1,EQ.0) GO TO 50	FENT0602
RRP(5)=(R(I1)+P(J1)+P(K1)+R(L1))/4.0	FENT0603
ZZZ(5)=(Z(I1)+Z(J1)+Z(K1)+Z(L1))/4.0	FENT0604
GO TO 100	FENT0605
50 RRR(5)=(R(I1)+R(J1)+R(K1))/3.0	FENT0606
ZZZ(5)=(Z(I1)+Z(J1)+Z(K1))/3.0	FENT0607
C	FENT0608
C COMPUTE STRAINS	FENT0609
C	FENT0610
100 DO 120 I=1,4	FENT0611
II=2*I	FENT0612

	JJ=2*IX(N,I)	FENT0613
	P(II-1)=B(JJ-1)	FENT0614
120	P(II)=B(JJ)	FENT0615
C		FENT0616
	P(9)=0.0	FENT0617
	P(10)=0.0	FENT0618
130	DO 150 I=1,2	FENT0619
	RR(I)=P(I+8)	FENT0620
	DO 150 K=1,8	FENT0621
150	RR(I)=RR(I)-S(I+8,K)*P(K)	FENT0622
C		FENT0623
	COMM=S(9,9)*S(10,10)-S(9,10)*S(10,9)	FENT0624
	IF (COMM) 155,160,155	FENT0625
155	P(9)=(S(10,10)*RR(1)-S(9,10)*RR(2))/COMM	FENT0626
	P(10)=(-S(10,9)*RR(1)+S(9,9)*RR(2))/COMM	FENT0627
C		FENT0628
160	DO 170 I=1,6	FENT0629
	TP(I)=0.0	FENT0630
	DO 170 K=1,10	FENT0631
170	TP(I)=TP(I)+HH(I,K)*P(K)	FENT0632
C		FENT0633
	RR(1)=TP(2)	FENT0634
	RR(2)=TP(6)	FENT0635
	RR(3)=(TP(1)+TP(2)*RRR(5)+TP(3)*ZZZ(5))/RRR(5)	FENT0636
	RR(4)=TP(3)+TP(5)	FENT0637
C		FENT0638
C	COMPUTE STRESSES	FENT0639
C		FENT0640
	DO 180 I=1,4	FENT0641
	SIG(I)=0.0	FENT0642
	DO 180 K=1,4	FENT0643
180	SIG(I)=SIG(I)+C(I,K)*RR(K)	FENT0644
C		FENT0645
C	COMPUTE PRINCIPLE STRESSES	FENT0646
C		FENT0647
	CC=(SIG(1)+SIG(2))/2.0	FENT0648

```

      BB=(SIG(1)-SIG(2))/2.0
      CR=DSQRT(BB**2+SIG(3)**2)
      SIG(5)=CC+CR
      SIG(6)=CC-CR
C     ****
C     CALCULATE ROTATION OF PRINCIPLE PLANES
C     ****
500  IF(DABS(SIG(4)).LT.1.0E-09) SIG(4)=0.0
      IF(DABS(BB).GT.1.0E-09) GO TO 510
      BB=0.0
510  IF ((SIG(4).NE.0.).OR.(BB.NE.0.)) GO TO 520
      ANG=0.0
      GO TO 530
520  ANG=DATAN2(SIG(4),BB)/2.0
530  SIG(8)=57.396*ANG
      SIG(7)=(SIG(5)-SIG(6))/2.0
C     ****
C     OUTPUT STRESSES
C     ****
      IF(N.NE.1) GO TO 615
      WRITE (6,2000)
615  WRITE (6,2001) N,RRR(5),ZZZ(5),(SIG(I),I=1,4)
300  CONTINUE
2000 FORMAT (8H1ELEMENT,8X,'R',8X,'Z',6X,'SIG(R)',6X,'SIG(Z)',5X,'SIG(T
1)',4X,'TAU(RZ)')
2001 FORMAT (I8,2F9.3, 1P7D12.3,          OP1F10.2)
      RETURN
      END
SUBROUTINE INTER(XI,RR,ZZ)
      IMPLICIT REAL*8 (A-H,C-Z)
      IMPLICIT INTEGER*2(I-N)
      DIMENSION RR(1),ZZ(1),XI(1)
      DIMENSION XM(7),R(7),Z(7),XX(9)
C
      XX(1)=.1259391805448
      XX(2)=XX(1)

```

```

FENT0649
FENT0650
FENT0651
FENT0652
FENT0653
FENT0654
FENT0655
FENT0656
FENT0657
FENT0658
FENT0659
FENT0660
FENT0661
FENT0662
FENT0663
FENT0664
FENT0665
FENT0666
FENT0667
FENT0668
FENT0669
FENT0670
FENT0671
FENT0672
FENT0673
FENT0674
FENT0675
FENT0676
FENT0677
FENT0678
FENT0679
FENT0680
FENT0681
FENT0682
FENT0683
FENT0684

```

	XX(3)=XX(1)	FENT0685
	XX(4)=.1323941527884	FENT0686
	XX(5)=XX(4)	FENT0687
	XX(6)=XX(4)	FENT0688
	XX(7)=.225	FENT0689
	XX(8)=.696140478028	FENT0690
	XX(9)=.410426192314	FENT0691
	R(7)=(RR(1)+RR(2)+RR(3))/3.	FENT0692
	Z(7)=(ZZ(1)+ZZ(2)+ZZ(3))/3.	FENT0693
C		FENT0694
	DO 100 I=1,3	FENT0695
	J=I+3	FENT0696
	R(I)=XX(8)*RR(I)+(1.-XX(8))*R(7)	FENT0697
	R(J)=XX(9)*RR(I)+(1.-XX(9))*R(7)	FENT0698
	Z(I)=XX(8)*ZZ(I)+(1.-XX(8))*Z(7)	FENT0699
100	Z(J)=XX(9)*ZZ(I)+(1.-XX(9))*Z(7)	FENT0700
C		FENT0701
	DO 200 I=1,7	FENT0702
200	XM(I)=XX(I)*R(I)	FENT0703
C		FENT0704
	DO 300 I=1,6	FENT0705
300	XI(I)=0.	FENT0706
C		FENT0707
	AREA=.5*(RR(1)*(ZZ(2)-ZZ(3))+RR(2)*(ZZ(3)-ZZ(1))+RR(3)*(ZZ(1)-ZZ(2)))	FENT0708
C		FENT0709
	DO 400 I=1,7	FENT0710
	XI(1)=XI(1)+XM(I)	FENT0711
	XI(2)=XI(2)+XM(I)/R(I)	FENT0712
	XI(3)=XI(3)+XM(I)/(R(I)**2)	FENT0713
	XI(4)=XI(4)+XM(I)*Z(I)/R(I)	FENT0714
	XI(5)=XI(5)+XM(I)*Z(I)/(R(I)**2)	FENT0715
400	XI(6)=XI(6)+XM(I)*(Z(I)**2)/(R(I)**2)	FENT0716
C		FENT0717
	DO 500 I=1,6	FENT0718
500	XI(I)=XI(I)*AREA	FENT0719
		FENT0720

C

RETURN
FND

FENT0721
FENT0722
FENT0723

|
|

APPENDIX C

FINITE ELEMENT PROGRAM FOR THE ANALYSIS OF ISOTROPIC
ELASTIC AXISYMMETRIC PLATES - THERMAL STRAINS INCLUDED (Ref. 13, 14)

Program Capabilities:

The following restrictions are placed on the size of problems which can be handled by the program.

<u>Item</u>	<u>Maximum Number</u>
Nodal Points	450
Elements	450
Materials	25
Boundary Pressure Cards	200

Printed output includes:

1. Reprint of Input Data
2. Nodal Point Displacements
3. Stresses at the center of each element.

Input Data Format:

- A. Identification card - (18A4)
Columns 1 to 72 of this card contain information to be printed with results.
- B. Control card - (5I5,F10.0)
- | | | |
|---------|---------|-------------------------------|
| Columns | 1 - 5 | Number of nodal points |
| | 6 - 10 | Number of elements |
| | 11 - 15 | Number of different materials |

- 16 - 20 Normalizing stress (see NORM, Appendix B)
- 21 - 25 Number of boundary pressure cards
- 26 - 35 Reference temperature (stress free temperature)

C. Material Property information

The following group of cards must be supplied for each different material:

First Card - (2I5, 2F10.0)

- Columns 1 - 5 Materials identification - any number from 1 to 12.
- 6 - 10 Number of different temperatures for which properties are given = 8 maximum.
- 11 - 20 Initial Z stress.
- 21 - 30 Initial R stress.

Following Cards - (4F10.0) One card for each temperature



- Columns 1 - 10 Temperature
- 11 - 20 Modulus of elasticity - E
- 21 - 30 Poisson's ratio - ν
- 31 - 40 Coefficient of thermal expansion

D. Nodal Point Cards - (2I5, 5F10.0)

One card for each nodal point with the following information:

- Columns 1 - 5 Nodal point number
- 10 Number which indicates if displacements or forces are to be specified.
- 11 - 20 R - ordinate
- 21 - 30 Z - ordinate
- 31 - 40 XR
- 41 - 50 XZ
- 51 - 60 Temperature

If the number in column 10 is

		<u>Condition</u>
0	XR is the specified R-load and XZ is the specified Z - load	free
1	XR is the specified R-displacement and XZ is the specified Z-load.	
2.	XR is the specified R-load and XZ is the specified Z-displacement.	
3	XR is the specified R-displacement and XZ is the specified Z- displacement.	fixed

All loads are considered to be total forces acting on a one radian segment. Nodal point cards must be in numerical sequence. If cards are omitted, the omitted nodal points are generated at equal intervals along a straight line between the defined nodal points. The necessary temperatures are determined by linear interpolation. The boundary code (column 10), XR and XZ are set equal to zero.

Skew Boundaries:

If the number in columns 5-10 of the nodal point cards is other than 0, 1, 2 or 3, it is interpreted as the magnitude of an angle in degrees. The terms in columns 31-50 of the nodal point card are then interpreted as follows:

XR is the specified load in the s-direction

XZ is the specified displacement in the n-direction

The angle must always be input as a negative angle and may range from -.001 to -180 degrees. Hence, +1.0 degree is the same as -179.0 degrees.

The displacements of these nodal points which are printed by the program are

u_r = the displacement in the s-direction

u_z = the displacement in the n-direction

E. Element Cards - (6I5)

One card for each element

Columns	1 - 5	Element number	1. Order nodal points counter-clockwise around element.
	6 - 10	Nodal Point I	
	11 - 15	Nodal Point J	
	16 - 20	Nodal Point K	2. Maximum difference between nodal point I.D. must be less than 25.
	21 - 25	Nodal Point L	
	26 - 30	Material Identification	

Element cards must be in element number sequence. If element cards are omitted, the program automatically generates the omitted information by incrementing by one the preceding I, J, K and L. The material identification code for the generated cards is set equal to the value given on the last card. The last element card must always be supplied.

Triangular elements are also permissible; they are identified by repeating the last nodal point number (i.e., I, J, K, K).

F. Pressure Cards - (2I5, 1F10.0)

One card for each boundary element which is subjected to a normal pressure.

Columns	1 - 5	Nodal Point I
	6 - 10	Nodal Point J
	11 - 20	Normal Pressure

The boundary element must be on the left as one progresses from I to J. Surface tensile force is input as a negative pressure.

Listing:

```
C      *****
C      FINITE ELEMENT PROGRAM FOR THE ANALYSIS OF ISCTROPIC ELASTIC
C      AXYSYMMETRIC PLATFS RFF FEAST 1,3 SAAS 2
C      *****
C
C      IMPLICIT REAL*8 (A-H,O-Z)
C      IMPLICIT INTEGER*2(I-N)
C      COMMON      STTOP,HED(18),SIGIR(25),SIGIZ(25),GAMMA(25),ZKNOT(25),
1 DEPTH(25),F(8,4,25),SIG(7),R(450),Z(450),UR(450),TT(3),
2 U7(450),STOTAL(450,4),
3 T(450),TFMP,Q,KSW
C      COMMON /INTEGR/ NUMNP,NUMEL,NUMMAT,NDEPTH,NORM,MTYPE,ICODE(450)
C      COMMON /ARG/ RRR(5),ZZZ(5),S(10,10),P(10),LM(4),DD(3,3),
1 HH(6,10),RR(4),ZZ(4),C(4,4),H(6,10),D(6,6),F(6,10),TP(6),XI(6),
2 EE(10),IX(450,5)
C      COMMON /BANARG/ R(900),A(900,54),MBAND
C      COMMON/PRESS/ IBC(200),JBC(200),PR(200),NUMPC
C      DATA STRS /'*****'/
C      *****
C      READ AND PRINT CONTROL INFORMATION
C      *****
50 READ (5,1000,END=950) HED
   WRITE (6,2000) HED
C
C      READ(5,1001) NUMNP,NUMEL,NUMMAT,NORM,NUMPC,Q
C      WRITE(6,2006) NUMNP,NUMEL,NUMMAT,NUMPC,Q
C      IF (NORM) 65,65,66
66 WRITE (6,2041)
C      *****
C      READ AND PRINT MATERIAL PROPERTIES
C      *****
65 CONTINUE
C
C      DO 80 M=1,NUMMAT
C      READ(5,1012) MTYPE,NUMTC,SIGIZ(MTYPE),SIGIR(MTYPE)
C      WRITE(6,2011) MTYPE,NUMTC,SIGIZ(MTYPE),SIGIR(MTYPE)
```

```
FEWT0001
FEWT0002
FEWT0003
FEWT0004
FEWT0005
FEWT0006
FEWT0007
FEWT0008
FEWT0009
FEWT0010
FEWT0011
FEWT0012
FEWT0013
FEWT0014
FEWT0015
FEWT0016
FEWT0017
FEWT0018
FEWT0019
FEWT0020
FEWT0021
FEWT0022
FEWT0023
FEWT0024
FEWT0025
FEWT0026
FEWT0027
FEWT0028
FEWT0029
FEWT0030
FEWT0031
FEWT0032
FEWT0033
FEWT0034
FEWT0035
FEWT0036
```

	READ(5,1011) ((E(I,J,MTYPE),J=1,4),I=1,NUMTC)	FEWT0037
	WRITE(6,2010) ((E(I,J,MTYPE),J=1,4),I=1,NUMTC)	FEWT0038
	DO 81 I=NUMTC,8	FEWT0039
	DO 81 J=1,4	FEWT0040
	81 E(I,J,MTYPE)=E(NUMTC,J,MTYPE)	FEWT0041
	80 CONTINUE	FEWT0042
C	*****	FEWT0043
C	READ AND PRINT NODAL POINT DATA	FEWT0044
C	*****	FEWT0045
	100 WRITE (6,2013)	FEWT0046
	L=0	FEWT0047
	105 READ(5,1006) N,ICDDE(N),R(N),Z(N),UR(N),UZ(N),T(N)	FEWT0048
	106 NL=L+1	FEWT0049
	IF (L.EQ.0) GO TO 110	FEWT0050
	ZX=N-L	FEWT0051
	DR=(R(N)-R(L))/ZX	FEWT0052
	DZ=(Z(N)-Z(L))/ZX	FEWT0053
	DT=(T(N)-T(L))/ZX	FEWT0054
	110 L=L+1	FEWT0055
	IF (N-L) 113,112,111	FEWT0056
	111 ICODE(L)=0	FEWT0057
	R(L)=R(L-1)+DR	FEWT0058
	Z(L)=Z(L-1)+DZ	FEWT0059
	T(L)=T(L-1)+DT	FEWT0060
	UP(L)=0.0	FEWT0061
	UZ(L)=0.0	FEWT0062
	GO TO 110	FEWT0063
	112 WRITE(6,2014) (K,ICDDE(K),R(K),Z(K),UR(K),UZ(K),T(K),K=NL,N)	FEWT0064
	IF (NUMNP-N) 113,120,105	FEWT0065
	113 WRITE (6,2015) N	FEWT0066
	GO TO 900	FEWT0067
C	*****	FEWT0068
C	READ AND PRINT ELEMENT PROPERTIES	FEWT0069
C	*****	FEWT0070
	120 WRITE (6,2016)	FEWT0071
	N=0	FEWT0072

130	READ (5,10C7) M,(IX(M,I),I=1,5)	FEWT0073
140	N=N+1	FEWT0074
	IF (M-N) 170,170,150	FEWT0075
150	IX(N,1)=IX(N-1,1)+1	FEWT0076
	IX(N,2)=IX(N-1,2)+1	FEWT0077
	IX(N,3)=IX(N-1,3)+1	FEWT0078
	IX(N,4)=IX(N-1,4)+1	FEWT0079
	IX(N,5)=IX(N-1,5)	FEWT0080
170	WRITE (6,20C17) N,(IX(N,I),I=1,5)	FEWT0081
	IF (M-N) 180,180,140	FEWT0082
180	IF (NUMEL-N) 300,300,130	FEWT0083
C	*****	FEWT0084
C	READ AND PRINT THE PRESSURE CARDS	FEWT0085
C	*****	FEWT0086
300	IF(NUMPC) 290,210,290	FEWT0087
290	WRITE(6,9000)	FEWT0088
	DO 200 L=1,NUMPC	FEWT0089
	READ(5,9001) IBC(L),JBC(L),PR(L)	FEWT0090
200	WRITE(6,9002) IBC(L),JBC(L),PR(L)	FEWT0091
210	CONTINUE	FEWT0092
C	*****	FEWT0093
C	DETERMINE BAND WIDTH	FEWT0094
C	*****	FEWT0095
	J=0	FEWT0096
	DO 340 N=1,NUMEL	FEWT0097
	DO 340 I=1,4	FEWT0098
	DO 325 L=1,4	FEWT0099
	KK=IX(N,I)-IX(N,L)	FEWT0100
	IF (KK.LT.0) KK=-KK	FEWT0101
	IF (KK.GT.J) J=KK	FEWT0102
325	CONTINUE	FEWT0103
340	CONTINUE	FEWT0104
	MRAND=2*J+2	FEWT0105
C	*****	FEWT0106
C	SOLVE FOR DISPLACEMENTS AND STRESSES	FEWT0107
C	*****	FEWT0108

```

KSW=0
CALL STIFF
IF (KSW.NE.0) GO TO 900
C
CALL BANSOL
WRITE(6,2052)
WRITE (6,2025) (N,B      (2*N-1),B      (2*N),N=1,NUMNP)
C
450 CALL STRESS(SPLOT)
C *****
C  PROCSS ALL DECKS EVEN IF FRROR
C *****
GO TO 910
900 WRITE (6,4000)
910 WRITE (6,4001) HED
C
920 READ (5,1000) CHK
IF (CHK.NE.STRS) GO TO 920
GO TO 50
950 CONTINUE
WRITE (6,4002)
CALL EXIT
C *****
C *****
1000 FORMAT (18A4)
1001 FORMAT(5I5,F10.0)
1002 FORMAT ( 15,2F10.0)
1003 FORMAT(2F10.0)
1004 FORMAT (2F10.0)
1005 FORMAT (3F10.0)
1006 FORMAT(2I5,5F10.0)
1007 FORMAT (6I5)
1011 FORMAT(4F10.0)
1012 FORMAT(2I5,2F10.0)
C *****
2000 FORMAT (1H1,20A4)

```

```

FEWT0109
FEWT0110
FEWT0111
FEWT0112
FEWT0113
FEWT0114
FEWT0115
FEWT0116
FEWT0117
FEWT0118
FEWT0119
FEWT0120
FEWT0121
FEWT0122
FEWT0123
FEWT0124
FEWT0125
FEWT0126
FEWT0127
FEWT0128
FEWT0129
FEWT0130
FEWT0131
FEWT0132
FEWT0133
FEWT0134
FEWT0135
FEWT0136
FEWT0137
FEWT0138
FEWT0139
FEWT0140
FEWT0141
FEWT0142
FEWT0143
FEWT0144

```


144	IF (IX(N,3)-IX(N,4))	145,165,145	FEWT0217
145	DO 150 II=1,9		FEWT0218
	CC=S(II,10)/S(10,10)		FEWT0219
	P(II)=P(II)-CC*P(10)		FEWT0220
	DO 150 JJ=1,9		FEWT0221
150	S(II, JJ)=S(II, JJ)-CC*S(10, JJ)		FEWT0222
C			FEWT0223
	DO 160 II=1,8		FEWT0224
	CC=S(II,9)/S(9,9)		FEWT0225
	P(II)=P(II)-CC*P(9)		FEWT0226
	DO 160 JJ=1,8		FEWT0227
160	S(II, JJ)=S(II, JJ)-CC*S(9, JJ)		FEWT0228
C			FEWT0229
C	ADD ELEMENT STIFFNESS TO TOTAL STIFFNESS		FEWT0230
C			FEWT0231
165	DO 166 I=1,4		FEWT0232
166	LM(I)=2*IX(N, I)-2		FEWT0233
C			FEWT0234
	DO 200 I=1,4		FEWT0235
	DO 200 K=1,2		FEWT0236
	II=LM(I)+K		FEWT0237
	KK=2*I-2+K		FEWT0238
	B(II)=R(II)+P(KK)		FEWT0239
	DO 200 J=1,4		FEWT0240
	DO 200 L=1,2		FEWT0241
	JJ=LM(J)+L-II+1		FEWT0242
	LL=2*J-2+L		FEWT0243
	IF (JJ) 200,200,175		FEWT0244
175	IF (ND-JJ) 180,195,195		FEWT0245
180	WRITE (6,2004) N		FEWT0246
	KSW=1		FEWT0247
	GO TO 210		FEWT0248
195	A(II, JJ)=A(II, JJ)+S(KK, LL)		FEWT0249
200	CONTINUE		FEWT0250
210	CONTINUE		FEWT0251
	IF(KSW.EQ.1) GO TO 500		FEWT0252

C		FEWT0253
C	ADD CONCENTRATED FORCES	FEWT0254
C		FEWT0255
	DO 250 N=1,NUMNP	FEWT0256
	K=2*N	FEWT0257
	B(K)=B(K)+UZ(N)	FEWT0258
	B(K-1)=B(K-1)+UR(N)	FEWT0259
	250 CONTINUE	FEWT0260
C		FEWT0261
C		FEWT0262
C	PRESSURE BOUNDARY CONDITIONS	FEWT0263
C		FEWT0264
	IF(NUMPC) 260,310,260	FEWT0265
260	DO 300 L=1,NUMPC	FEWT0266
	I=IRC(L)	FEWT0267
	J=JBC(L)	FEWT0268
	CODE(I)=ICODE(I)	FEWT0269
	CODE(J)=ICODE(J)	FEWT0270
	PP=PR(L)/6.	FEWT0271
	DZ=(Z(I)-Z(J))*PP	FEWT0272
	DR=(R(J)-R(I))*PP	FEWT0273
	RX=2.0*R(I)+R(J)	FEWT0274
	RJ=R(I)+2.0*R(J)	FEWT0275
264	II=2*I	FEWT0276
	JJ=2*J	FEWT0277
270	SINA=0.0	FEWT0278
	COSA=1.0	FEWT0279
	IF(CODE(I)) 271,272,272	FEWT0280
271	SINA=DSIN(CODE(I))	FEWT0281
	COSA=DCOS(CODE(I))	FEWT0282
272	B(II-1)=B(II-1)+RX*(COSA*DZ+SINA*DR)	FEWT0283
	B(JJ)=B(JJ)-RX*(SINA*DZ-COSA*DR)	FEWT0284
290	SINA=0.0	FEWT0285
	COSA=1.0	FEWT0286
	IF(CODE(J)) 291,292,292	FEWT0287
291	SINA=DSIN(CODE(I))	FEWT0288

	COSA=DCOS(CODE(I))	FEWT0289
292	B(JJ-1)=R(JJ-1)+ZX*(COSA*DZ+SINA*DR)	FEWT0290
	B(JJ)=B(JJ)-ZX*(SINA*DZ-COSA*DR)	FEWT0291
300	CONTINUE	FEWT0292
310	CONTINUE	FEWT0293
C	DISPLACEMENT B.C.	FEWT0294
C		FEWT0295
	DO 400 M=1,NUMNP	FEWT0296
	U=UR(M)	FEWT0297
	N=2*M-1	FEWT0298
	KX=ICODE(M)+1	FEWT0299
	GO TO (400,370,390,380),KX	FEWT0300
370	CALL MODIFY(N,U,ND2)	FEWT0301
	GO TO 400	FEWT0302
380	CALL MODIFY(N,U,ND2)	FEWT0303
390	U=UZ(M)	FEWT0304
	N=N+1	FEWT0305
	CALL MODIFY(N,U,ND2)	FEWT0306
400	CONTINUE	FEWT0307
C		FEWT0308
	500 RETURN	FEWT0309
C	*****	FEWT0310
2003	FORMAT (26HNEGATIVE AREA ELEMENT NO. I4)	FEWT0311
2004	FORMAT (29HORAND WIDTH EXCEEDS ALLOWABLE I4)	FEWT0312
C	*****	FEWT0313
	END	FEWT0314
	SUBROUTINE QUAD(N,VCL)	FEWT0315
C		FEWT0316
	IMPLICIT REAL*8 (A-H,O-Z)	FEWT0317
	IMPLICIT INTEGER*2 (I-N)	FEWT0318
	COMMON STTOP,HED(18),SIGIR(25),SIGIZ(25),GAMMA(25),ZKNOT(25),	FEWT0319
	1DEPTH(25),E(8,4,25),SIG(7),R(450),Z(450),UR(450),TT(3),	FEWT0320
	2 UZ(450),STOTAL(450,4),	FEWT0321
	3 T(450),TEMP,Q,KSW	FEWT0322
	COMMON /INTEGR/ NUMNP,NUMEL,NUMMAT,NDEPTH,NORM,MTYPE,ICODE(450)	FEWT0323
	COMMON /ARG/ RRR(5),ZZZ(5),S(10,10),P(10),LM(4),DD(3,3),	FEWT0324

	1	HH(6,10),RR(4),ZZ(4),C(4,4),H(6,10),D(6,6),F(6,10),TP(6),XI(6),	FEWT0325
	2	EE(10),IX(450,5)	FEWT0326
		COMMON /BANARG/ B(900),A(900,54),MBAND	FEWT0327
C		*****	FEWT0328
		I=IX(N,1)	FEWT0329
		J=IX(N,2)	FEWT0330
		K=IX(N,3)	FEWT0331
		L=IX(N,4)	FEWT0332
C			FEWT0333
		I1=1	FEWT0334
		I2=2	FEWT0335
		I3=3	FEWT0336
		I4=4	FEWT0337
		I5=5	FEWT0338
C		THERMAL STRESSES	FEWT0339
		TEMP=(T(I)+T(J)+T(K)+T(L))/4.0	FEWT0340
		DO 103 M=2,8	FEWT0341
		IF(E(M,1,MTYPE)-TEMP) 103,104,104	FEWT0342
	103	CONTINUE	FEWT0343
	104	RATIO=0.0	FEWT0344
		DEN=E(M,1,MTYPE)-E(M-1,1,MTYPE)	FEWT0345
		IF(DEN) 70,71,70	FEWT0346
	70	RATIO=(TEMP-E(M-1,1,MTYPE))/DEN	FEWT0347
	71	DO 105 KK=1,3	FEWT0348
	105	FF(KK)=E(M-1,KK+1,MTYPE)+RATIO*(E(M,KK+1,MTYPE)-E(M-1,KK+1,MTYPE))	FEWT0349
		TEMP=TEMP-Q	FEWT0350
C		*****	FEWT0351
C		DETERMINE ELASTIC CONSTANTS AND STRESS-STRAIN RELATIONSHIP	FEWT0352
C		*****	FEWT0353
C			FEWT0354
		CALL MPROP(N)	FEWT0355
C			FEWT0356
	88	DO 110 M=1,3	FEWT0357
	110	TT(M)=(C(M,1)+C(M,2)+C(M,3))*EE(3)*TEMP	FEWT0358
C		*****	FEWT0359
C		FCRM QUADRILATERAL STIFFNESS MATRIX	FEWT0360

C	*****	FEWT0361
210	RRR(5)=(R(I)+R(J)+R(K)+R(L))/4.0	FEWT0362
	ZZZ(5)=(Z(I)+Z(J)+Z(K)+Z(L))/4.0	FEWT0363
	DD 94 M=1.4	FEWT0364
	MM=IX(N,M)	FEWT0365
	IF(R(MM).EQ.0..AND.ICODE(MM).EQ.0) ICODE(MM)=1	FEWT0366
93	RRR(M)=R(MM)	FEWT0367
94	ZZZ(M)=Z(MM)	FEWT0368
C		FEWT0369
	DD 100 II=1,10	FEWT0370
	P(II)=0.0	FEWT0371
	DD 95 JJ=1,6	FEWT0372
95	HH(JJ,II)=0.0	FEWT0373
	DD 100 JJ=1,10	FEWT0374
100	S(II,JJ)=0.0	FEWT0375
	IF (K-L) 125,120,125	FEWT0376
120	CALL TRISTF(I1,I2,I3)	FEWT0377
	RRR(5)=(RRR(1)+RRR(2)+RRR(3))/3.0	FEWT0378
	ZZZ(5)=(ZZZ(1)+ZZZ(2)+ZZZ(3))/3.0	FEWT0379
	VOL=XI(1)	FEWT0380
	GO TO 160	FEWT0381
125	VOL=0.0	FEWT0382
	CALL TRISTF(I4,I1,I5)	FEWT0383
	IF(XI(1).EQ.0.) WRITE(6,2000) N	FEWT0384
	VOL=VOL+XI(1)	FEWT0385
	CALL TRISTF(I1,I2,I5)	FEWT0386
	IF(XI(1).EQ.0) WRITE(6,2000) N	FEWT0387
	VOL=VOL+XI(1)	FEWT0388
	CALL TRISTF(I3,I4,I5)	FEWT0389
	IF(XI(1).EQ.0) WRITE(6,2000) N	FEWT0390
	VOL=VOL+XI(1)	FEWT0391
	CALL TRISTF(I2,I3,I5)	FEWT0392
	IF(XI(1).EQ.0) WRITE(6,2000) N	FEWT0393
	VOL=VOL+XI(1)	FEWT0394
C		FEWT0395
	DD 140 II=1,6	FEWT0396

85	DO 100 I=1,6	FEWT0433
	DO 90 J=1,10	FEWT0434
	F(I,J)=0.0	FEWT0435
90	H(I,J)=0.0	FEWT0436
	DO 100 J=1,6	FEWT0437
100	D(I,J)=0.0	FEWT0438
C		FEWT0439
C	FORM INTEGRAL (G)T*(C)*(G)	FEWT0440
	CALL INTER(XI,RR,ZZ)	FEWT0441
C		FEWT0442
	D(2,6)=XI(1)*(C(1,2)+C(2,3))	FEWT0443
	D(3,5)=XI(1)*C(4,4)	FEWT0444
	D(5,5)=D(3,5)	FEWT0445
	D(6,6)=XI(1)*C(2,2)	FEWT0446
	D(1,1)=XI(3)*C(3,3)	FEWT0447
	D(1,2)=XI(2)*(C(1,3)+C(3,3))	FEWT0448
	D(1,3)=XI(5)*C(3,3)	FEWT0449
	D(1,6)=XI(2)*C(2,3)	FEWT0450
	D(2,2)=XI(1)*(C(1,1)+2.0*C(1,3)+C(3,3))	FEWT0451
	D(2,3)=XI(4)*(C(1,3)+C(3,3))	FEWT0452
	D(3,3)=XI(6)*C(3,3)+XI(1)*C(4,4)	FEWT0453
	D(3,6)=XI(4)*C(2,3)	FEWT0454
	DO 110 I=1,6	FEWT0455
	DO 110 J=1,6	FEWT0456
110	D(J,I)=D(I,J)	FEWT0457
C		FEWT0458
C		FEWT0459
C	FORM COEFFICIENT-DISPLACEMENT MATRIX	FEWT0460
C		FEWT0461
	COMM=RR(2)*(ZZ(3)-ZZ(1))+RR(1)*(ZZ(2)-ZZ(3))+RR(3)*(ZZ(1)-ZZ(2))	FEWT0462
	DD(1,1)=(RR(2)*ZZ(3)-RR(3)*ZZ(2))/COMM	FEWT0463
	DD(1,2)=(RR(3)*ZZ(1)-RR(1)*ZZ(3))/COMM	FEWT0464
	DD(1,3)=(RR(1)*ZZ(2)-RR(2)*ZZ(1))/COMM	FEWT0465
	DD(2,1)=(ZZ(2)-ZZ(3))/COMM	FEWT0466
	DD(2,2)=(ZZ(3)-ZZ(1))/COMM	FEWT0467
	DD(2,3)=(ZZ(1)-ZZ(2))/COMM	FEWT0468

```

DD(3,1)=(RR(3)-RR(2))/COMM
DD(3,2)=(RR(1)-RR(3))/COMM
DD(3,3)=(RR(2)-RR(1))/COMM
C
DO 120 I=1,3
J=2*LM(I)-1
H(1,J)=DD(1,I)
H(2,J)=DD(2,I)
H(3,J)=DD(3,I)
H(4,J+1)=DD(1,I)
H(5,J+1)=DD(2,I)
120 H(6,J+1)=DD(3,I)
C
FORM STIFFNESS MATRIX (H)T*(D)*(H)
C
DO 130 J=1,10
DO 130 K=1,6
IF (H(K,J)) 128,130,128
128 DO 129 I=1,6
129 F(I,J)=F(I,J)+D(I,K)*H(K,J)
130 CONTINUE
C
DO 140 I=1,10
DO 140 K=1,6
IF (H(K,I)) 138,140,138
138 DO 139 J=1,10
139 S(I,J)=S(I,J)+H(K,I)*F(K,J)
140 CONTINUE
TP(1)=XI(2)*TT(3)
TP(2)=XI(1)*(TT(1)+TT(3))
TP(3)=XI(4)*TT(3)
TP(4)=0.0
TP(5)=0.0
TP(6)=XI(1)*TT(2)
DO 160 I=1,10
DO 160 K=1,6

```

```

FEWT0469
FEWT0470
FEWT0471
FEWT0472
FEWT0473
FEWT0474
FEWT0475
FEWT0476
FEWT0477
FEWT0478
FEWT0479
FEWT0480
FEWT0481
FEWT0482
FEWT0483
FEWT0484
FEWT0485
FEWT0486
FEWT0487
FEWT0488
FEWT0489
FEWT0490
FEWT0491
FEWT0492
FEWT0493
FEWT0494
FEWT0495
FEWT0496
FEWT0497
FEWT0498
FEWT0499
FEWT0500
FEWT0501
FEWT0502
FEWT0503
FEWT0504

```

```

160 P(I)=P(I)+H(K,I)*TP(K)
C
C   FORM STRAIN TRANSFORMATION MATRIX
C
      DO 410 I=1,6
      DO 410 J=1,10
410 HH(I,J)=HF(I,J)+H(I,J)
C
C
500 RETURN
      FND
      SUBROUTINE MPROP(N)
      IMPLICIT REAL*8 (A-H,C-7)
      IMPLICIT INTEGER*2(I-N)
      COMMON      STTOP,HED(18),SIGIR(25),SIGIZ(25),GAMMA(25),ZKNOT(25),
1DFPTH(25),E(8,4,25),SIG(7),R(450),Z(450),UR(450),TT(3),
2 UZ(450),STOTAL(450,4),
3 T(450),TEMP,Q,KSW
      COMMON /INTEGR/ NUMNP,NUMEL,NUMMAT,NDEPTH,NORM,MTYPE,ICODE(450)
      COMMON /ARG/ RRR(5),ZZZ(5),S(10,10),P(10),LM(4),DD(3,3),
1 HH(6,10),RR(4),ZZ(4),C(4,4),H(6,10),D(6,6),F(6,10),TP(6),XI(6),
2 EE(10),IX(450,5)
      COMMON /BANARG/ B(900),A(900,54),MBAND
C   *****
      I=IX(N,1)
      J=IX(N,2)
      K=IX(N,3)
      L=IX(N,4)
      MTYPE=IX(N,5)
C
      DO 5 II=1,4
      DO 5 JJ=1,4
5 C(II,JJ)=0.0
C   *****
C   DETERMINE FLASTIC CONSTANTS
C   *****

```

```

FEWT0505
FEWT0506
FEWT0507
FEWT0508
FEWT0509
FEWT0510
FEWT0511
FEWT0512
FEWT0513
FEWT0514
FEWT0515
FEWT0516
FEWT0517
FEWT0518
FEWT0519
FEWT0520
FEWT0521
FEWT0522
FEWT0523
FEWT0524
FEWT0525
FEWT0526
FEWT0527
FEWT0528
FEWT0529
FEWT0530
FEWT0531
FEWT0532
FEWT0533
FEWT0534
FEWT0535
FEWT0536
FEWT0537
FEWT0538
FEWT0539
FEWT0540

```

C		FEWT0541
	60 IF (NORM) 65,75,65	FEWT0542
	65 FE(1)=EE(1)*SIGIZ(MTYPE)	FEWT0543
C	*****	FEWT0544
C	FORM STRESS STRAIN RELATIONSHIP	FEWT0545
C	*****	FEWT0546
	75 COEF=EE(1)/(1.-EE(2)-2.*EE(2)*EE(2))	FEWT0547
	C(1,1)=COEF*(1.-EE(2))	FEWT0548
	C(1,2)=COEF*EE(2)	FEWT0549
	C(1,3)=EE(2)*COEF	FEWT0550
	C(2,1)=C(1,2)	FEWT0551
	C(2,2)=C(1,1)	FEWT0552
	C(2,3)=C(1,2)	FEWT0553
	C(3,1)=C(1,3)	FEWT0554
	C(3,2)=C(1,2)	FEWT0555
	C(3,3)=C(1,1)	FEWT0556
	C(4,4)=COEF*(0.5-EE(2))	FEWT0557
	RETURN	FEWT0558
	END	FEWT0559
	SUBROUTINE MODIFY(N,U,ND2)	FEWT0560
C		FEWT0561
	IMPLICIT REAL*8 (A-H,O-Z)	FEWT0562
	IMPLICIT INTEGER*2(I-N)	FEWT0563
	COMMON /BANARG/ B(900),A(900,54),MBAND	FEWT0564
	DO 250 M=2,MBAND	FEWT0565
	K=N-M+1	FEWT0566
	IF (K) 235,235,230	FEWT0567
230	B(K)=B(K)-A(K,M)*U	FEWT0568
	A(K,M)=0.0	FEWT0569
235	K=N+M-1	FEWT0570
	IF (ND2-K) 250,240,240	FEWT0571
240	B(K)=B(K)-A(N,M)*U	FEWT0572
	A(N,M)=0.0	FEWT0573
250	CONTINUE	FEWT0574
	A(N,1)=1.0	FEWT0575
	B(N)=U	FEWT0576

```

RETURN
END
SUBROUTINE BANSOL
C
  IMPLICIT REAL*8 (A-H,O-Z)
  IMPLICIT INTEGER*2(I-N)
  COMMON      SITOP,HED(18),SIGIR(25),SIGIZ(25),GAMMA(25),ZKNCT(25),
1 DEPTH(25),E(8,4,25),SIG(7),R(450),Z(450),UR(450),TT(3),
2 UZ(450),STOTAL(450,4),
3 T(450),TEMP,Q,KS
  COMMON /INTEGR/ NUMNP,NUMEL,NUMMAT,NDEPTH,NORM,MTYPE,ICODE(450)
  COMMON /BANARG/ B(900),A(900,54),MBAND
  ND2=2*NUMNP
C
  DO 280 N=1,ND2
  DO 260 L=2,MBAND
  C=A(N,L)/A(N,1)
  I=N+L-1
C
  IF (ND2.LT.I) GO TO 260
C
  J=0
  DO 250 K=L,MBAND
  J=J+1
250 A(I,J)=A(I,J)-C*A(N,K)
  R(I)=B(I)-C*B(N)
260 A(N,L)=C
280 B(N)=B(N)/A(N,1)
C
  BACKSUBSTITUTION
C
  N=ND2
300 N=N-1
C
  IF (N.LE.0) GO TO 500
  DO 400 K=2,MBAND

```

```

FEWT0577
FEWT0578
FEWT0579
FEWT0580
FEWT0581
FEWT0582
FEWT0583
FEWT0584
FEWT0585
FEWT0586
FEWT0587
FEWT0588
FEWT0589
FEWT0590
FEWT0591
FEWT0592
FEWT0593
FEWT0594
FEWT0595
FEWT0596
FEWT0597
FEWT0598
FEWT0599
FEWT0600
FEWT0601
FEWT0602
FEWT0603
FEWT0604
FEWT0605
FEWT0606
FEWT0607
FEWT0608
FEWT0609
FEWT0610
FEWT0611
FEWT0612

```

```

L=N+K-1
IF (ND2.LT.L) GO TO 400
B(N)=B(N)-A(N,K)*B(L)
400 CONTINUE
C
GO TO 300
C
500 RETURN
END
SUBROUTINE STRESS(SPLOT)
IMPLICIT REAL*8 (A-H,O-Z)
IMPLICIT INTEGER*2(I-N)
COMMON STTOP,HED(18),SIGIR(25),SIGIZ(25),GAMMA(25),ZKNOT(25),
1DEPTH(25),E(8,4,25),SIG(7),R(450),Z(450),UR(450),TT(3),
2 UZ(450),STOTAL(450,4),
3 T(450),TEMP,C,KSW
COMMON /INTEGR/ NUMNP,NUMEL,NUMMAT,NDEPTH,NORM,MTYPE,ICODE(450)
COMMON /ARG/ RRR(5),ZZZ(5),S(10,10),P(10),LM(4),DD(3,3),
1 HH(6,10),RR(4),ZZ(4),C(4,4),H(6,10),D(6,6),F(6,10),TP(6),XI(6),
2 EE(10),IX(450,5)
COMMON /BANARG/ B(900),A(900,54),MBAND
*****
C COMPUTE ELEMENT STRESSES AND STRAINS
C *****
DO 300 N=1,NUMEL
CALL QUAD(N,VOL)
C
C FIND ELEMENT CCORDINATES
C
I1=IX(N,1)
J1=IX(N,2)
K1=IX(N,3)
L1=IX(N,4)
C
IF (K1-L1.EQ.0) GO TO 50
RRR(5)=(R(I1)+R(J1)+R(K1)+R(L1))/4.0

```

```

FEWT0613
FEWT0614
FEWT0615
FEWT0616
FEWT0617
FEWT0618
FEWT0619
FEWT0620
FEWT0621
FEWT0622
FEWT0623
FEWT0624
FEWT0625
FEWT0626
FEWT0627
FEWT0628
FEWT0629
FEWT0630
FEWT0631
FEWT0632
FEWT0633
FEWT0634
FEWT0635
FEWT0636
FEWT0637
FEWT0638
FEWT0639
FEWT0640
FEWT0641
FEWT0642
FEWT0643
FEWT0644
FEWT0645
FEWT0646
FEWT0647
FEWT0648

```

	ZZZ(5)=(Z(I1)+Z(J1)+Z(K1)+Z(L1))/4.0	FEWT0649
	GO TO 100	FEWT0650
50	RRR(5)=(P(I1)+R(J1)+R(K1))/3.0	FEWT0651
	ZZZ(5)=(Z(I1)+Z(J1)+Z(K1))/3.0	FEWT0652
C		FEWT0653
C	COMPUTE STRAINS	FEWT0654
C		FEWT0655
100	DO 120 I=1,4	FEWT0656
	II=2*I	FEWT0657
	JJ=2*IX(N,I)	FEWT0658
	P(II-1)=B(JJ-1)	FEWT0659
120	P(II)=B(JJ)	FEWT0660
C		FEWT0661
	P(9)=0.0	FEWT0662
	P(10)=0.0	FEWT0663
130	DO 150 I=1,2	FEWT0664
	RR(I)=P(I+8)	FEWT0665
	DO 150 K=1,8	FEWT0666
150	RR(I)=RR(I)-S(I+8,K)*P(K)	FEWT0667
C		FEWT0668
	COMM=S(9,9)*S(10,10)-S(9,10)*S(10,9)	FEWT0669
	IF (COMM) 155,160,155	FEWT0670
155	P(9)=(S(10,10)*RR(1)-S(9,10)*RR(2))/COMM	FEWT0671
	P(10)=(-S(10,9)*RR(1)+S(9,9)*RR(2))/COMM	FEWT0672
C		FEWT0673
160	DO 170 I=1,6	FEWT0674
	TP(I)=0.0	FEWT0675
	DO 170 K=1,10	FEWT0676
170	TP(I)=TP(I)+HH(I,K)*P(K)	FEWT0677
C		FEWT0678
	RR(1)=TP(2)	FEWT0679
	RR(2)=TP(6)	FEWT0680
	RR(3)=(TP(1)+TP(2)*RRR(5)+TP(3)*ZZZ(5))/RRR(5)	FEWT0681
	RR(4)=TP(3)+TP(5)	FEWT0682
C		FEWT0683
C	COMPUTE STRESSES	FEWT0684

```

C
DO 180 I=1,4
SIG(I)=0.0
DO 180 K=1,4
180 SIG(I)=SIG(I)+C(I,K)*RR(K)
C
C COMPUTE PRINCIPLE STRESSES
C
CC=(SIG(1)+SIG(2))/2.0
BB=(SIG(1)-SIG(2))/2.0
CR=DSQRT(BB**2+SIG(3)**2)
SIG(5)=CC+CR
SIG(6)=CC-CR
C
*****
C CALCULATE ROTATION OF PRINCIPLE PLANES
C
*****
500 IF (DABS(SIG(4)).LT.1.0E-09) SIG(4)=0.0
IF (DABS(BB).GT.1.0E-09) GO TO 510
BB=0.0
510 IF ((SIG(4).NE.0.).OR.(BB.NE.0.)) GO TO 520
ANG=0.0
GO TO 530
520 ANG=ATAN2(SIG(4),BB)/2.0
530 SIG(8)=57.396*ANG
SIG(7)=(SIG(5)-SIG(6))/2.0
C
*****
C OUTPUT STRESSES
C
*****
IF(N.NE.1) GO TO 615
WRITE (6,2000)
615 WRITE (6,2001) N,RRR(5),Z7Z(5),(SIG(I),I=1,4)
300 CONTINUE
2000 FORMAT (8H1ELEMENT,8X,'R',8X,'Z',6X,'SIG(R)',6X,'SIG(Z)',5X,'SIG(T
1)',4X,'TAU(RZ)')
2001 FORMAT (I8,2F9.3, 1P7D12.3, CP1F10.2)
RETURN

```

```

FEWT0685
FEWT0686
FEWT0687
FEWT0688
FEWT0689
FEWT0690
FEWT0691
FEWT0692
FEWT0693
FEWT0694
FEWT0695
FEWT0696
FEWT0697
FEWT0698
FEWT0699
FEWT0700
FEWT0701
FEWT0702
FEWT0703
FEWT0704
FEWT0705
FEWT0706
FEWT0707
FEWT0708
FEWT0709
FEWT0710
FEWT0711
FEWT0712
FEWT0713
FEWT0714
FEWT0715
FEWT0716
FEWT0717
FEWT0718
FEWT0719
FEWT0720

```

```

      FND
      SUBROUTINE INTER(XI,RR,ZZ)
      IMPLICIT REAL*8 (A-H,C-Z)
      IMPLICIT INTEGER*2(I-N)
      DIMENSION RR(1),ZZ(1),XI(1)
      DIMENSION XM(7),R(7),Z(7),XX(9)

```

```

C
      XX(1)=.1259391805448
      XX(2)=XX(1)
      XX(3)=XX(1)
      XX(4)=.1323941527884
      XX(5)=XX(4)
      XX(6)=XX(4)
      XX(7)=.225
      XX(8)=.696140478028
      XX(9)=.410426192314
      R(7)=(RR(1)+RR(2)+RR(3))/3.
      Z(7)=(ZZ(1)+ZZ(2)+ZZ(3))/3.
C
      DO 100 I=1,3
      J=I+3
      R(I)=XX(8)*RR(I)+(1.-XX(8))*R(7)
      R(J)=XX(9)*RR(I)+(1.-XX(9))*R(7)
      Z(I)=XX(8)*ZZ(I)+(1.-XX(8))*Z(7)
100 Z(J)=XX(9)*ZZ(I)+(1.-XX(9))*Z(7)
C
      DO 200 I=1,7
200 XM(I)=XX(I)*R(I)
C
      DO 300 I=1,6
300 XI(I)=0.
C
      AREA=.5*(RR(1)*(ZZ(2)-ZZ(3))+RR(2)*(ZZ(3)-ZZ(1))+RR(3)*(ZZ(1)-ZZ(2)
1)))
C
      DO 400 I=1,7

```

```

FEWT0721
FEWT0722
FEWT0723
FEWT0724
FEWT0725
FEWT0726
FEWT0727
FEWT0728
FEWT0729
FEWT0730
FEWT0731
FEWT0732
FEWT0733
FEWT0734
FEWT0735
FEWT0736
FEWT0737
FEWT0738
FEWT0739
FEWT0740
FEWT0741
FEWT0742
FEWT0743
FEWT0744
FEWT0745
FEWT0746
FEWT0747
FEWT0748
FEWT0749
FEWT0750
FEWT0751
FEWT0752
FEWT0753
FEWT0754
FEWT0755
FEWT0756

```

	XI(1)=XI(1)+XM(I)	FEWT0757
	XI(2)=XI(2)+XM(I)/R(I)	FEWT0758
	XI(3)=XI(3)+XM(I)/(R(I)**2)	FEWT0759
	XI(4)=XI(4)+XM(I)*Z(I)/R(I)	FEWT0760
	XI(5)=XI(5)+XM(I)*Z(I)/(R(I)**2)	FEWT0761
400	XI(6)=XI(6)+XM(I)*(Z(I)**2)/(R(I)**2)	FEWT0762
C		FEWT0763
	DO 500 I=1,6	FEWT0764
500	XI(I)=XI(I)*AREA	FEWT0765
C		FEWT0766
	RETURN	FEWT0767
	END	FEWT0768

APPENDIX D

STEADY STATE HEAT TRANSFER PROGRAM FOR BOLTED JOINT

Program Capacity: 50 nodal points

Output Data:

- (a) Input data
- (b) Inverse of matrix
- (c) Nodal temperature
- (d) Given and calculated augmenting vector and residual error

Input Data Sequence:

- A. Case identification (12A4) followed by two blank cards
- B. Card (I1) with a 1
- C. Card (I7) with dimension of matrix
- D. Card (I1) with a 1
- E. Cards (I1, 3(2I3, E15.8)) with node indices started in the first I3 field followed by conductance between these nodes. Only input from lower node number to higher node number required (since the conductance from node i to j equals the conductance from j to i.) Each card has three groups of z node numbers followed by a conductance value except the last card. Last card could have 1, 2 or 3 groups and has a 1 in column 1.
- F. Cards (I1, 3(I6, E15.8)) with number of node followed by conductance from the node to ground node which is at specified temperature. Each card has 3 groups of node number followed by conductance. The I1 field is skipped except for the last card for ground conductances which can have 1, 2 or 3 fields and the first column has a 1. A

node can be connected to only one ground node.

- G. Same as F above, but code temperature specified for ground node instead of the conductance value.
- H. Same as F above, but code internal power dissipation for the particular node instead of the conductance value.

Listing:

C	STFADY STATE HEAT TRANSFER PROGRAM	BOLTED JOINT	SSHT0001
	DIMENSION IDENT(12),A(050,050),AA(050,050),B(50),BI(50),		SSHT0002
	IBC(50),RES(50),ACON(50),TACCN(50),Q(50)		SSHT0003
101	WRITE(6,23)		SSHT0004
41	READ(5,51) K,IDENT		SSHT0005
51	FORMAT(I1,12A4)		SSHT0006
	WRITE(6,111) IDENT		SSHT0007
111	FORMAT(12A6)		SSHT0008
	IF(K .NE. 1) GO TO 41		SSHT0009
	READ(5,55) N,K		SSHT0010
55	FORMAT(I7/I1)		SSHT0011
	M = N+1		SSHT0012
	DO 3 I = 1,N		SSHT0013
	DO 3 J = 1,N		SSHT0014
	AA(I,J) = 0.0		SSHT0015
	ACON(I)=0.		SSHT0016
	Q(I) = 0.		SSHT0017
	TACCN(I) = 0.		SSHT0018
3	CONTINUE		SSHT0019
C	READ IN COEFF. MATRIX ELEMENTS		SSHT0020
42	READ(5,52) K,(I,J,AA(I,J),JM=1,3)		SSHT0021
52	FORMAT(I1,3(2I3,E15.8))		SSHT0022
	IF(K .NE. 1) GO TO 42		SSHT0023
43	READ(5,53) K,(I,ACON(I),JM=1,3)		SSHT0024
	IF(K .NE. 1) GO TO 43		SSHT0025
44	READ(5,53) K,(I,TACON(I),JM=1,3)		SSHT0026
	IF(K .NE. 1) GO TO 44		SSHT0027
45	READ(5,53) K,(I,Q(I),JM=1,3)		SSHT0028
	IF(K .NE. 1) GO TO 45		SSHT0029
53	FORMAT(I1,3(I6,E15.8))		SSHT0030
	DO 500 I=1,N		SSHT0031
500	B(I) = -(Q(I) + ACON(I) * TACCN(I))		SSHT0032
	DO 1000 I=1,N		SSHT0033
	DO 1000 J=I,N		SSHT0034
1000	AA(J,I) = AA(I,J)		SSHT0035
	DO 3000 I=1,N		SSHT0036

```

IN=I
AA(I,I) = 0.
DO 2001 J=1,N
JN=J
IF (JN .EQ. IN) GO TO 2001
2000 AA(I,I) = AA(I,I) + AA(I,J)
2001 CONTINUE
3000 AA(I,I) =(AA(I,I)+ACCN(I)) * (-1.)
WRITE(6,26)
26 FORMAT(1H1,27X,1H1,12X,1HQ,15X,1CHGRD. CCND.,1CX,1CHGRD. TEMP.//)
WRITE(6,25)(I,Q(I),ACCN(I),TACCN(I),I=1,N)
25 FORMAT(1H ,26X,I3,7X,F10.5,10X,F10.5,10X,F10.5,10X)
MM = 1
DO 4 I=1,N
DO 4 J = 1,N
A(I,J) = AA(I,J)
4 CONTINUE
WRITE(6,5)
5 FORMAT(1H1,39X17HA = COEFF. MATRIX //
1 40X21HB = AUGMENTING VECTOR //
2 40X19HT = SOLUTION VECTOR //
3 40X16HAI= INVERSE OF A //
4 40X33HBC = AUGMENTING VECTOR CALCULATED //
5 40X21H( A ) * ( T ) = ( R ) /// )
DO 7 I = 1,N
7 WRITE(6,6)( I,J,A(I,J), J = 1,N )
6 FORMAT(1H / (4( 5H A(I3,1H,I3,2H)=F10.5,5X)))
DO 8 I = 1,N
BI(I) = B(I)
8 CONTINUE
CALL MAT(N,M,A,B )
WRITE(6,22)
22 FORMAT(1H1 )
C WRITE INVERSE MATRIX
DO 9 I = 1,N
9 WRITE(6,10)( I,J,A(I,J), J = 1,N )

```

```

SSHT0037
SSHT0038
SSHT0039
SSHT0040
SSHT0041
SSHT0042
SSHT0043
SSHT0044
SSHT0045
SSHT0046
SSHT0047
SSHT0048
SSHT0049
SSHT0050
SSHT0051
SSHT0052
SSHT0053
SSHT0054
SSHT0055
SSHT0056
SSHT0057
SSHT0058
SSHT0059
SSHT0060
SSHT0061
SSHT0062
SSHT0063
SSHT0064
SSHT0065
SSHT0066
SSHT0067
SSHT0068
SSHT0069
SSHT0070
SSHT0071
SSHT0072

```

10	FORMAT(1H / (4(5H AI(I3,1H,I3,2H)=E15.8)))	SSHTC073
	WRITE(6,23)	SSHT0074
23	FORMAT(1H1)	SSHT0075
C	WRITE SOLUTION VECTOR	SSHT0076
12	WRITE(6,11)(J, B(J) ,J = 1,N)	SSHT0077
11	FORMAT(1H / 4(5H T(I3,2H)=F10.5,9X))	SSHT0078
	DO 13 I = 1,N	SSHT0079
	BC(I) = 0.0	SSHT0080
	DO 13 J = 1,N	SSHT0081
	BC(I) = BC(I) + (AA(I,J) * B(J))	SSHT0082
13	CONTINUE	SSHT0083
	DO 15 J = 1,N	SSHT0084
	RES(J) = ABS(BI(J)) - ABS(BC(J))	SSHT0085
15	CONTINUE	SSHT0086
	WRITE(6,16)	SSHT0087
16	FORMAT(1H1,30X76H AUGMENTING VECTOR CALCU.AUGMENTING VECTOR	SSHT0088
1	RESIDUAL ERROR //)	SSHT0089
17	WRITE (6,18) (J,I,BI(J),J,I,BC(J),RES(J),J=1,N)	SSHT0090
18	FORMAT(25X4H B(I3,1H, I3,2H)=E15.8,2X4H BC(I3,1H,I3,2H)=E15.8,	SSHTC091
1	6XE15.8 /)	SSHT0092
	GO TO 101	SSHT0093
	END	SSHT0094
	SUBROUTINE MAT (N,M,A,B)	SSHT0095
C	M = N + 1	SSHT0096
C	N = SIZE OF MATRIX TO BE INVERTED	SSHTC097
C	TO SOLVE AX = B, WHERE INPUT A = A, INPUT B = B	SSHT0098
C	OUTPUT B= X, OUTPUTA = A INVERSE	SSHT0099
	DIMENSION A(50,50),B(50)	SSHT0100
	N1 = N - 1	SSHT0101
	TEMP 15 = A(1,1)	SSHT0102
	A(M,N) = 1.0 / TEMP 15	SSHT0103
	B(M) = A(1,2) / TEMP 15	SSHT0104
	DO 1 I=2,N1	SSHTC105
	A(M,I-1)= A(1,I+1) / TEMP 15	SSHT0106
1	CONTINUE	SSHT0107
	A(M,N1) = B(1) / TEMP 15	SSHT0108

```

DO 10 I=1,N1
TEMP 6 = A(I+1,1)
B(I) = A(I+1,2) - TEMP 6 * B(M)
DO 5 J=2,N1
A(I,J-1)= A(I+1,J+1) - TEMP 6 * A(M,J-1)
5 CONTINUE
A(I,N1) = B(I+1) - TEMP 6 * A(M,N1)
A(I,N) = -TEMP6 / TEMP 15
10 CONTINUE
B(N) = B(M)
DO 15 I=1,N
A(N,I) = A(M,I)
15 CONTINUE
C REPEATS N - 1 TIMES
DO 100 K=1,N1
TEMP 15 = B(1)
A(M,N) = 1.0 / TEMP 15
B(M) = A(1,1) / TEMP 15
DO 51 I=2,N
A(M,I-1)= A(1,I) / TEMP 15
51 CONTINUE
DO 60 I =1,N1
TEMP 6 = B(I+1)
B(I) = A(I+1,1) - TEMP 6 * B(M)
DO 55 J=2,N
A(I,J-1)= A(I+1,J) - TEMP 6* A(M,J-1)
55 CONTINUE
A(I,N) = -TEMP 6 / TEMP 15
60 CONTINUE
B(N) = B(M)
DO 65 I=1,N
A(N,I) = A(M,I)
65 CONTINUE
100 CONTINUE
RETURN
END

```

```

SSHT0109
SSHT0110
SSHT0111
SSHTC112
SSHT0113
SSHT0114
SSHT0115
SSHT0116
SSHT0117
SSHT0118
SSHT0119
SSHTC120
SSHT0121
SSHT0122
SSHT0123
SSHTC124
SSHT0125
SSHTC126
SSHT0127
SSHT0128
SSHT0129
SSHT0130
SSHT0131
SSHTC132
SSHT0133
SSHTC134
SSHT0135
SSHTC136
SSHT0137
SSHT0138
SSHT0139
SSHTC140
SSHTC141
SSHT0142
SSHT0143
SSHT0144

```

TABLE 1

Separation Radius Comparison - Single and Two Plate Models

(see Figs. 12 - 17)

$\frac{A}{B}$	$\frac{B}{A}$	R_o/A		Percent Discrepancy Between Models
		Single Plate Model	Two Plate Model	
1	3.1	4.2	3.7	13.5
	2.2	3.3	2.7	22.2
	1.6	2.7	2.1	28.6
	1.3	2.4	1.7	41.7
.75	3.1	4.5	3.8	18.5
	2.2	3.6	2.8	28.9
	1.6	3.0	2.2	36.4
	1.3	2.7	2.0	35.0
.5	3.1	5.1	4.1	24.4
	2.2	4.2	3.2	31.3
	1.6	3.6	2.8	28.6
	1.3	3.3	2.5	32.0

TABLE 2

Test and Analytical Results for Radii of Separation of Bolted Plates (see Fig. 5)

Case	D in.	2B in.	Separation Diameters, $2 R_o$ - in.				% Discrepancy Between Computed Values and Tested Values		
			"Rubbing Test"		Autoradiographic Test		Computed	Rub. Test	Autorad. Test
			Range	Average	Range	Average			
1	.065	.422	.42-.48	.45	.41-.46	.44	.488	7.8	9.8
2	.124	.422	.50-.53	.51	.4 - .6	.55	.554	7.9	.7
3	.191	.422	.58-.64	.62	.76-.81	.78*	.620	0	25.8
4	.253	.422	.70-.76	.72	.68-.73	.7**	.700	2.9	0
5.	Unmatch- ed Pair .124/ .257	.422	.54-.58	.56	—	—	.588	4.8	—
6.	.124	1.0	1.06-1.10	1.09	—	—	1.104	1.3	—
7.	.191	1.0	1.11-1.17	1.16	—	—	1.210	4.1	—

* Original x-ray film shows hole in plate and 0.6 inch diameter zone more distinctly than remainder of area sensitized by the radioactive contamination. Loose radiographic contamination observed during test.

** Assembled and disassembled radioactive and non-radioactive plates without rotating plates relative to each other.

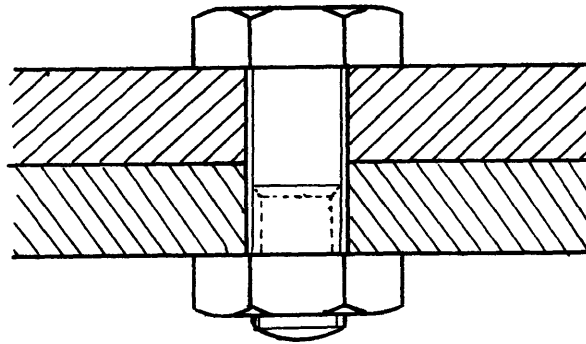


FIG. 1. BOLTED JOINT

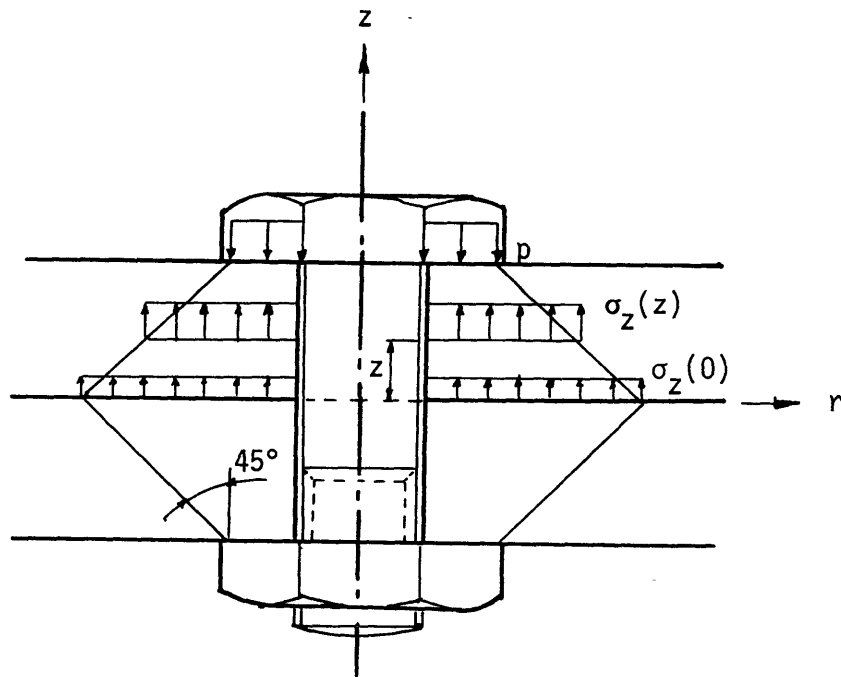


FIG. 2. ROETSCHER'S RULE OF THUMB FOR PRESSURE DISTRIBUTION IN A BOLTED JOINT

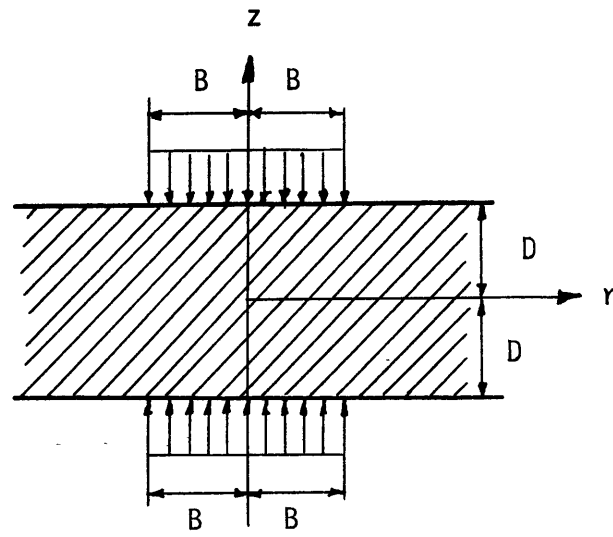


FIG. 3(a)

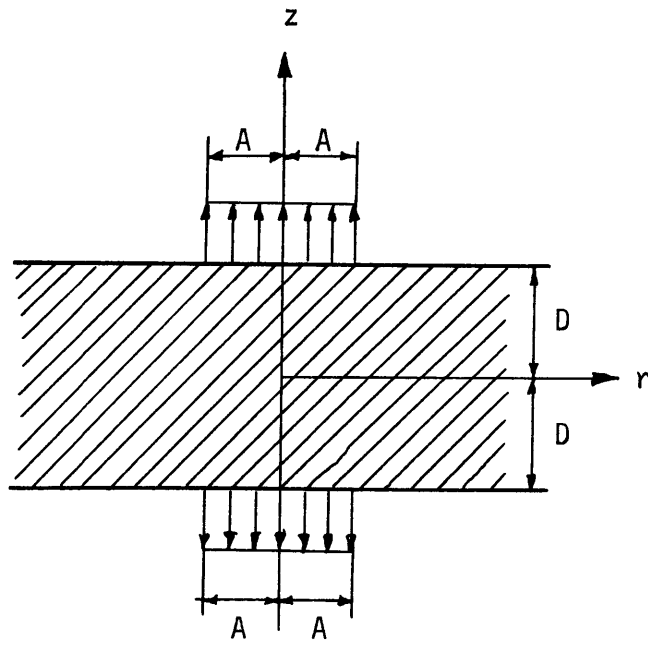


FIG. 3(b)

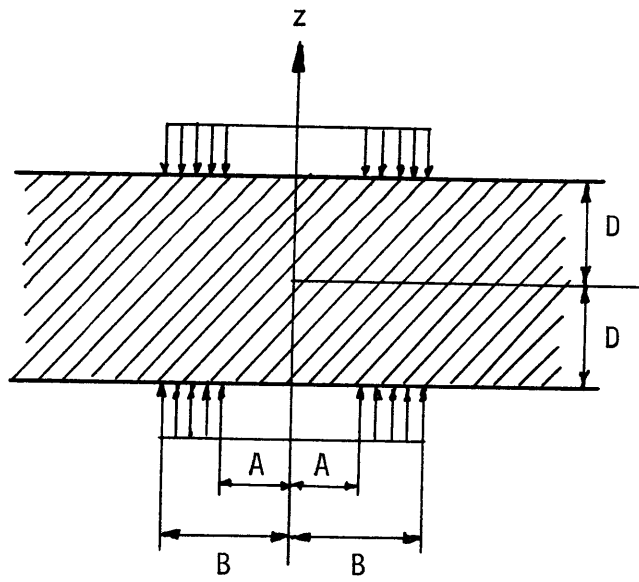


FIG. 3(c)

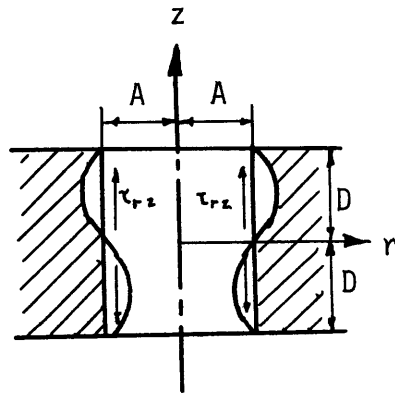


FIG. 3(d)

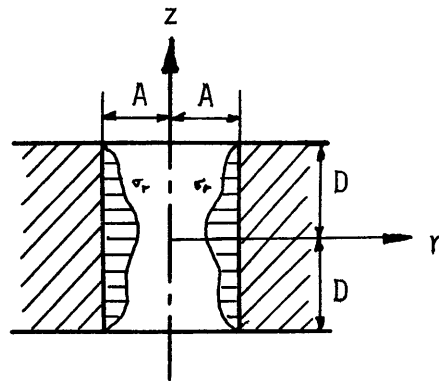


FIG. 3(e)

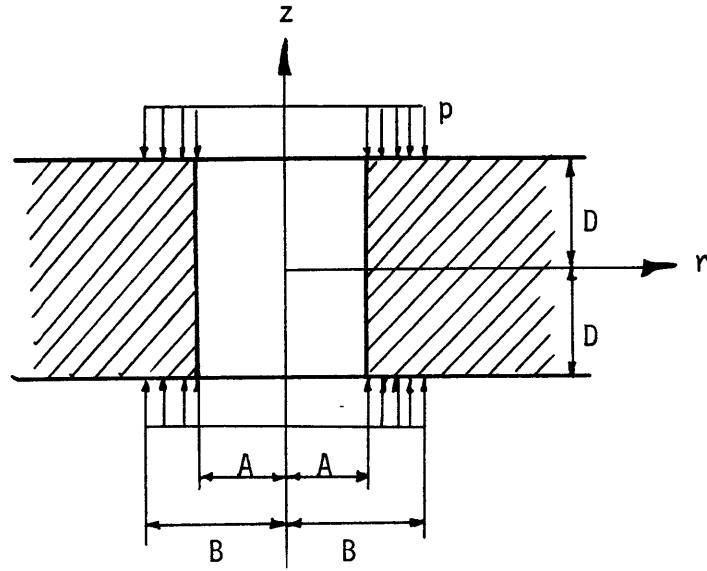
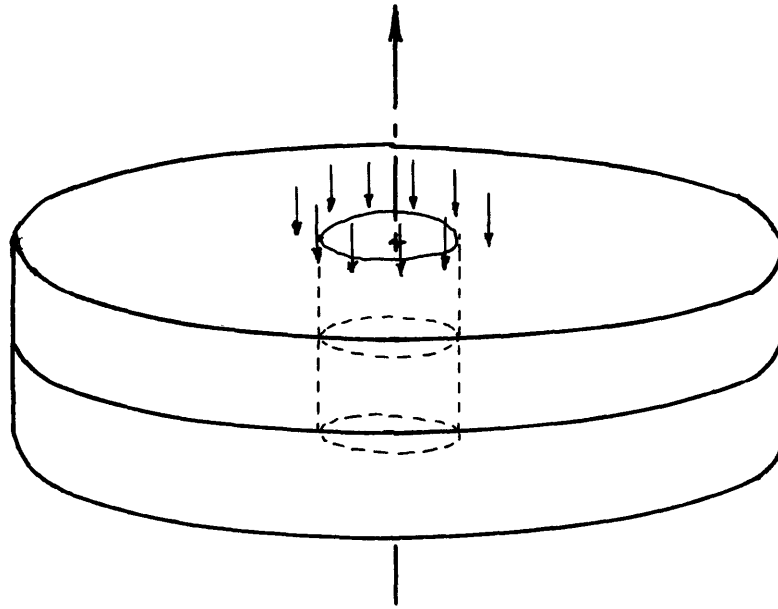


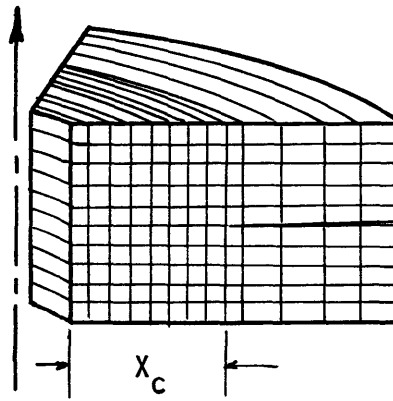
FIG. 3(f)

FIG. 3. FERNLUND'S SEQUENCE OF SUPERPOSITION



(a) Actual Plates

(b) Finite Element
Idealization



(c) Single Annular Ring
Element

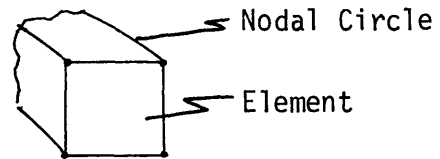
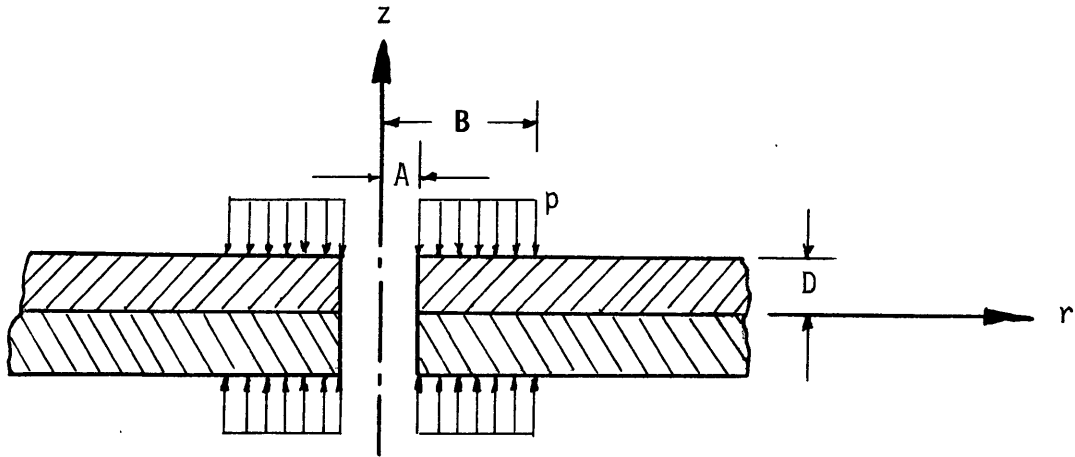
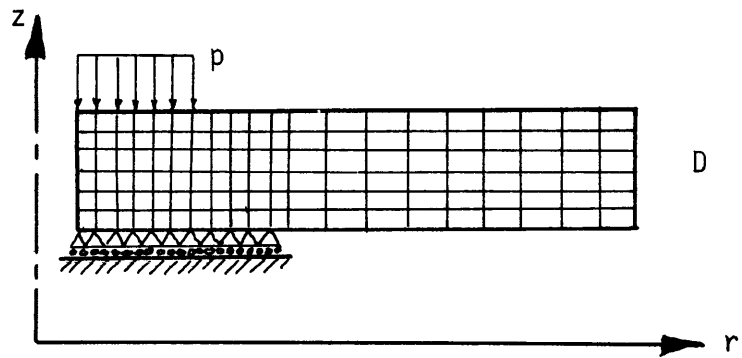


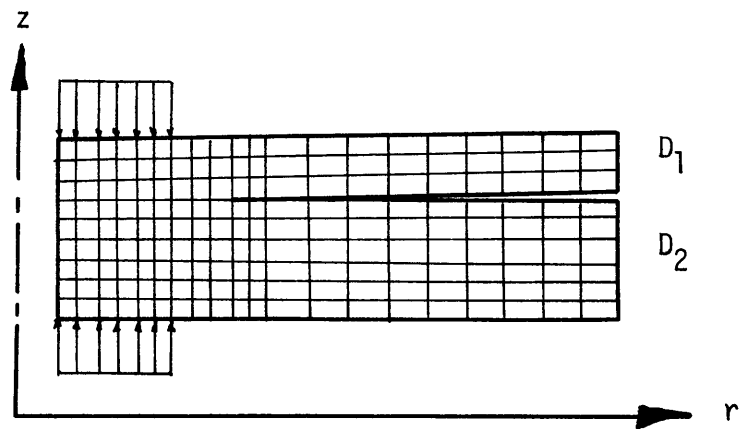
FIG. 4. FINITE ELEMENT IDEALIZATION OF TWO PLATES IN CONTACT



(a) Plates of Equal Thickness Under Load

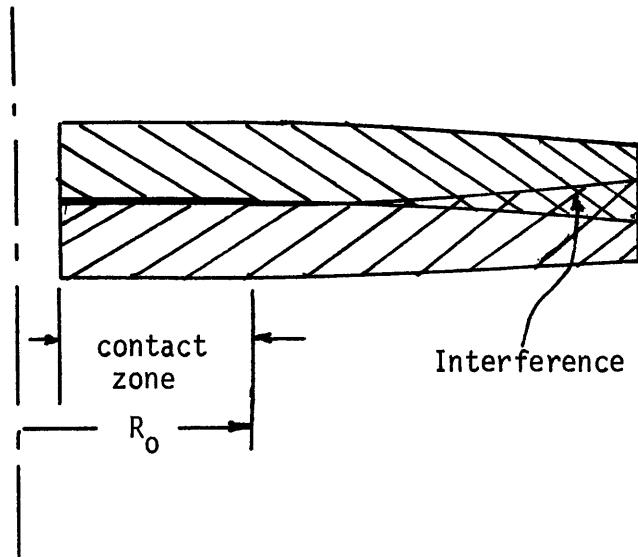


(b) Finite Element Model for Plates of Equal Thickness

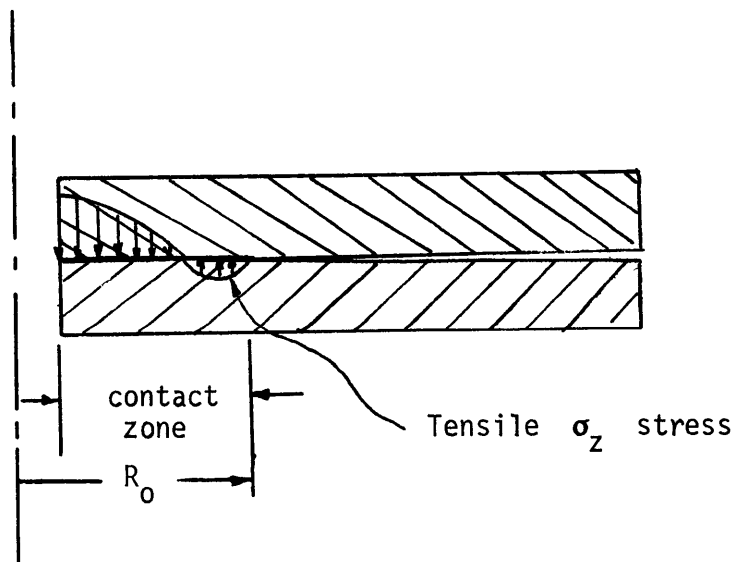


(c) Finite Element Model for Plates of Unequal Thickness

FIG. 5. FINITE ELEMENT MODELS



(a) Plates Intersect, R_0 too small



(b) Contact Zone Sustains Tension, R_0 too large

FIG. 6. EXAMPLES OF UNACCEPTABLE SOLUTIONS

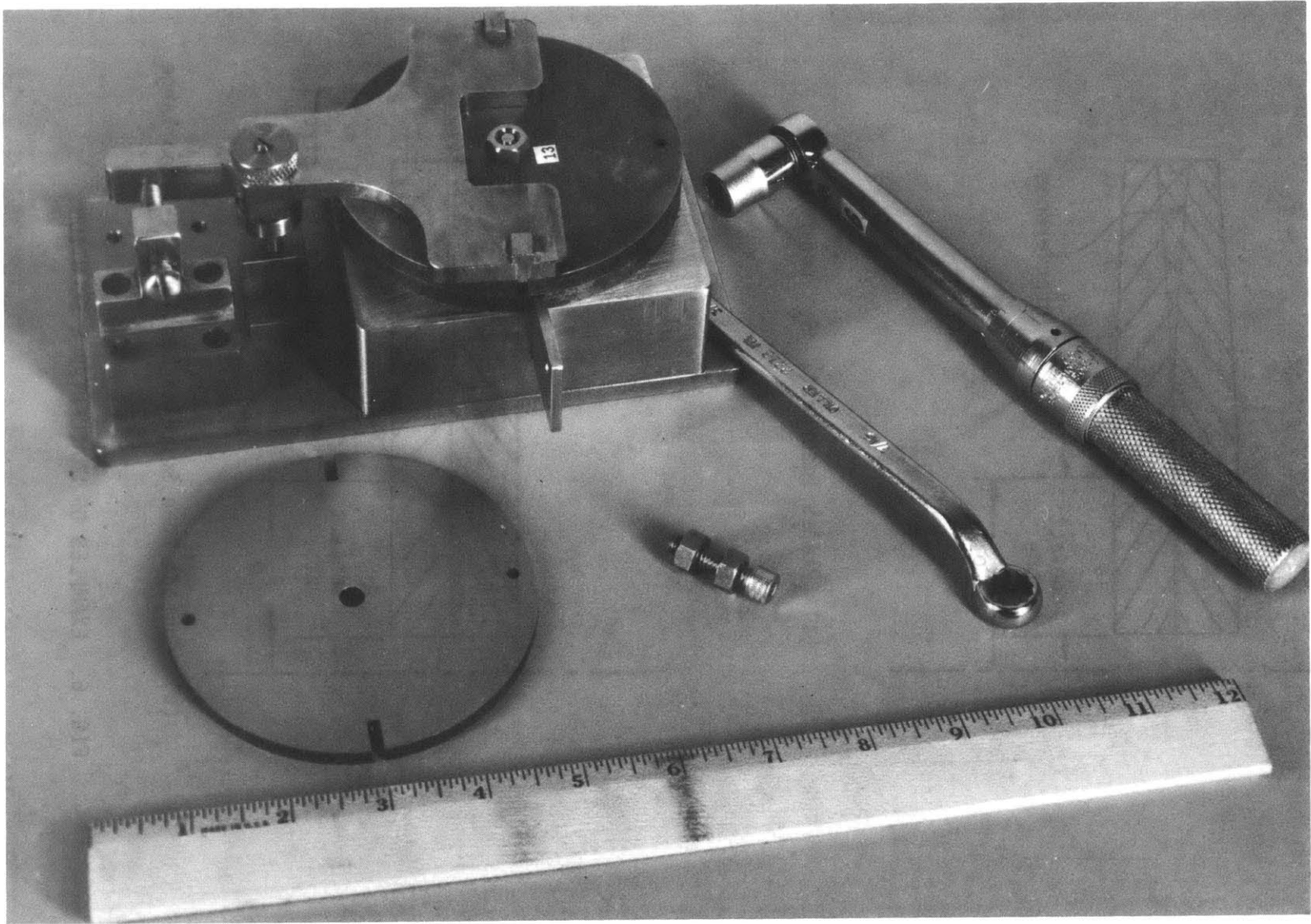


FIG. 7. PLATE SPECIMEN, BOLT AND NUTS, FIXTURE AND TOOLS.

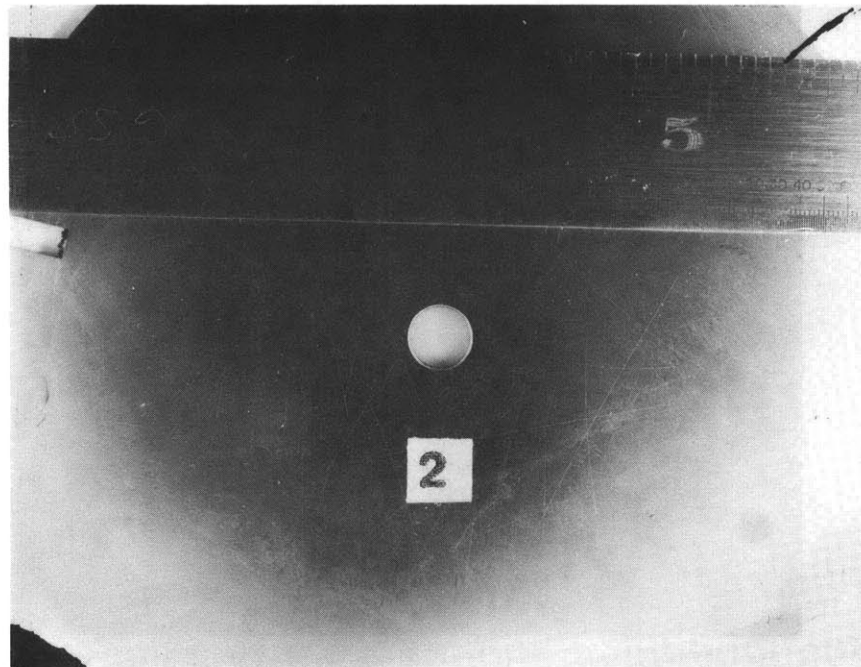
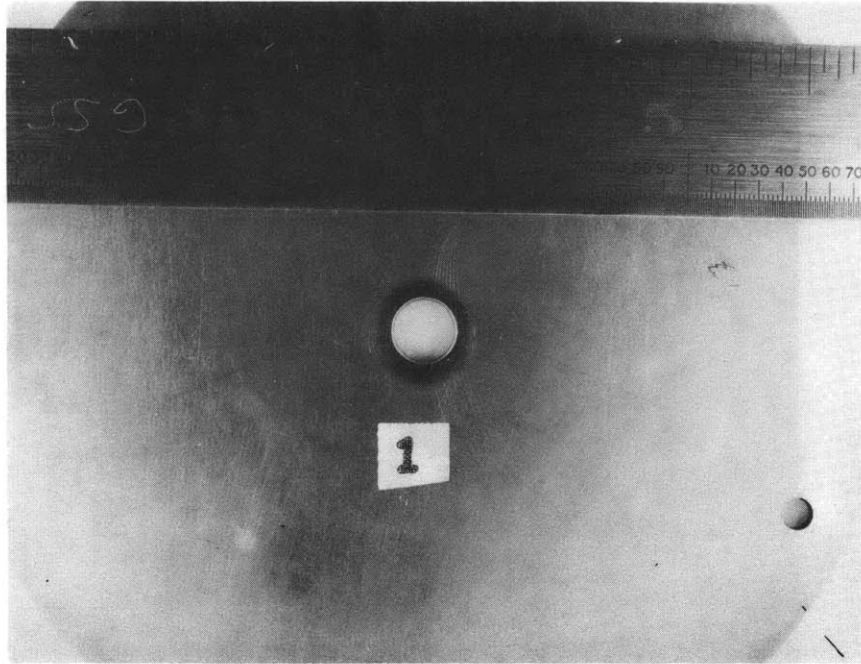


FIG. 8(a). FOOTPRINTS ON MATED PAIR OF 1/16 INCH PLATES.

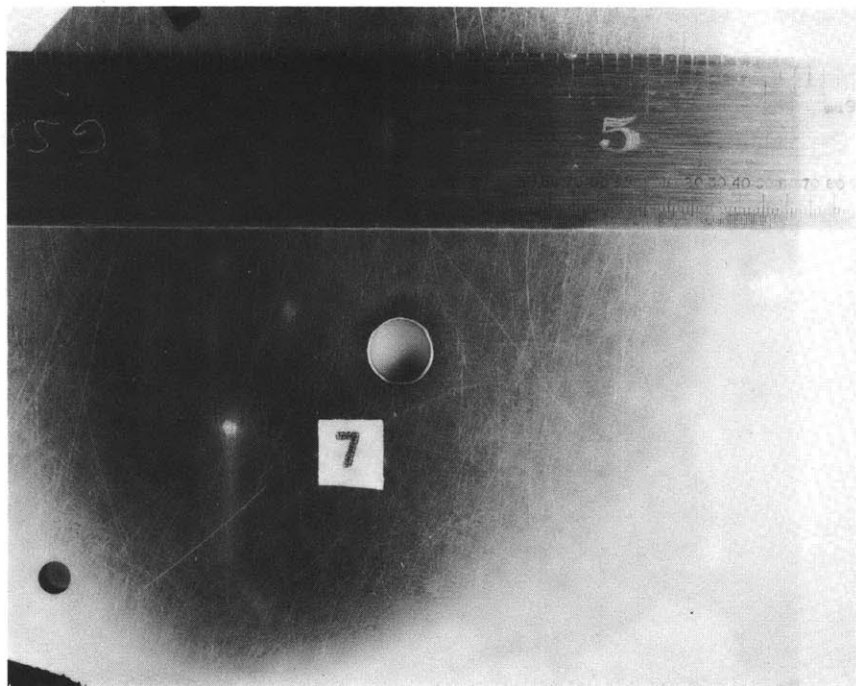
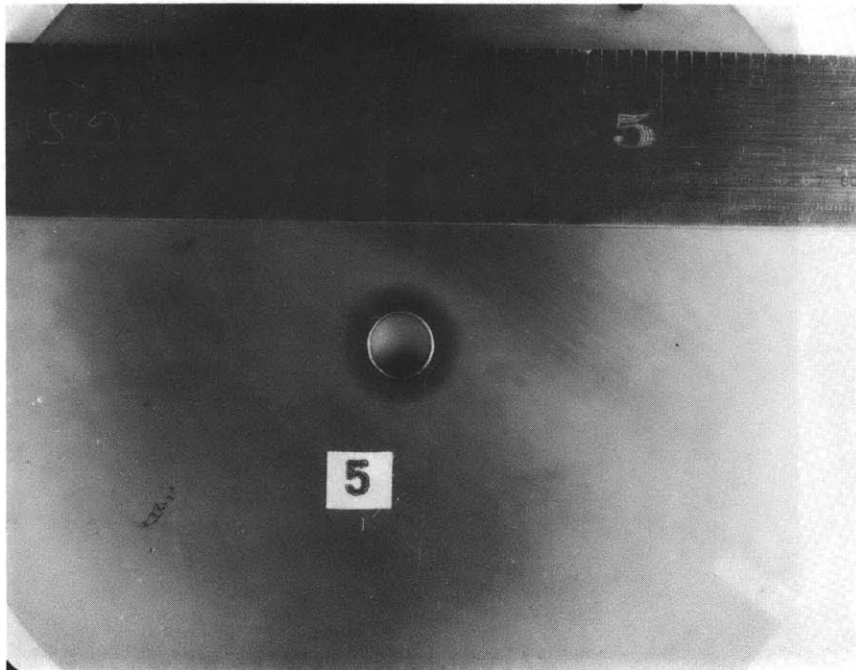


FIG. 8(b). FOOTPRINTS ON MATED PAIR OF 1/8 INCH PLATES.

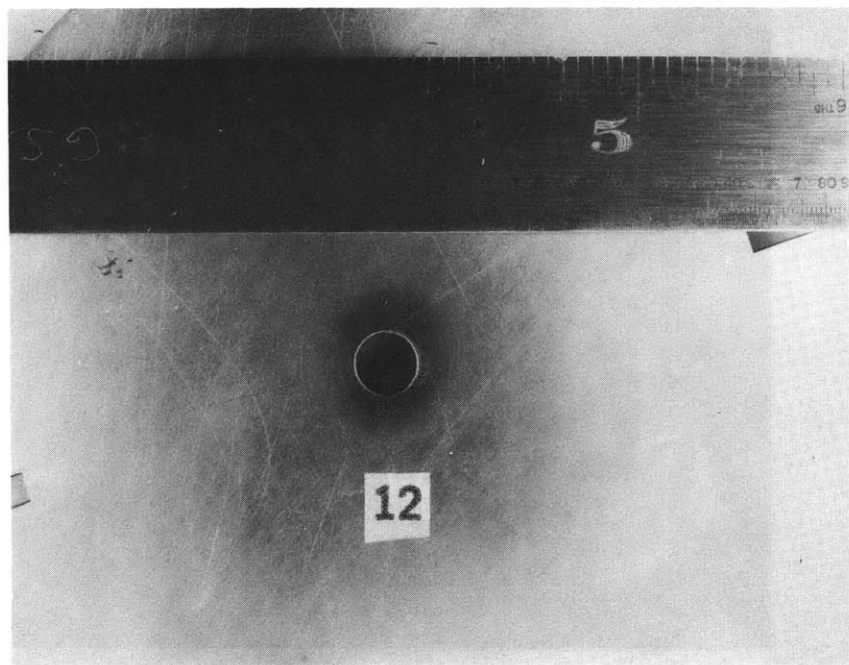
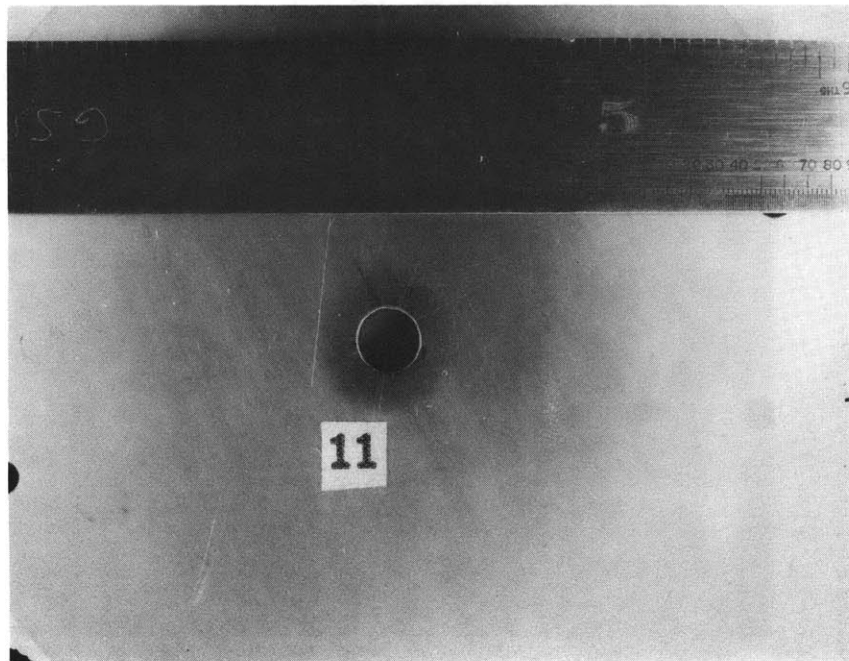


FIG. 8(c). FOOTPRINTS ON MATED PAIR OF 3/16 INCH PLATES.

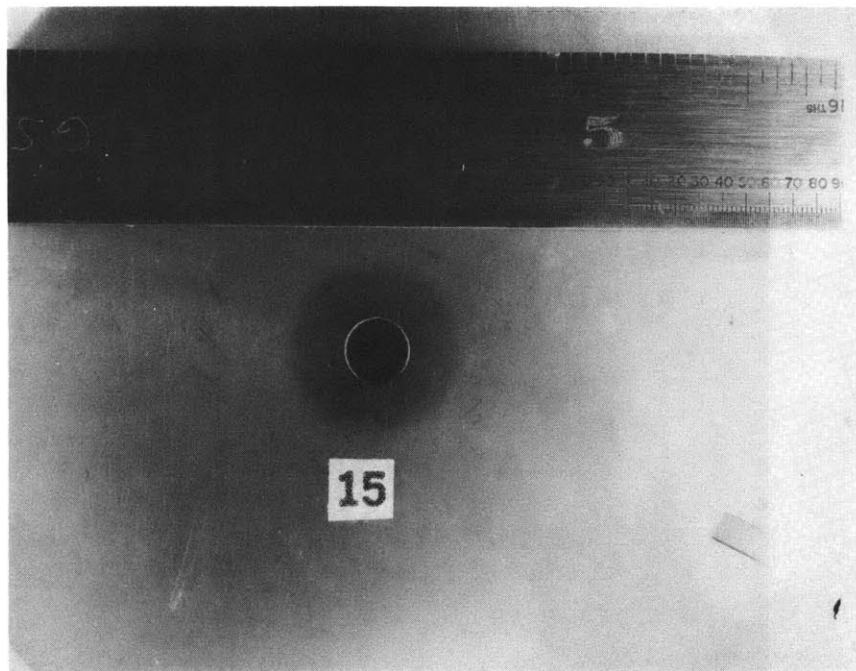
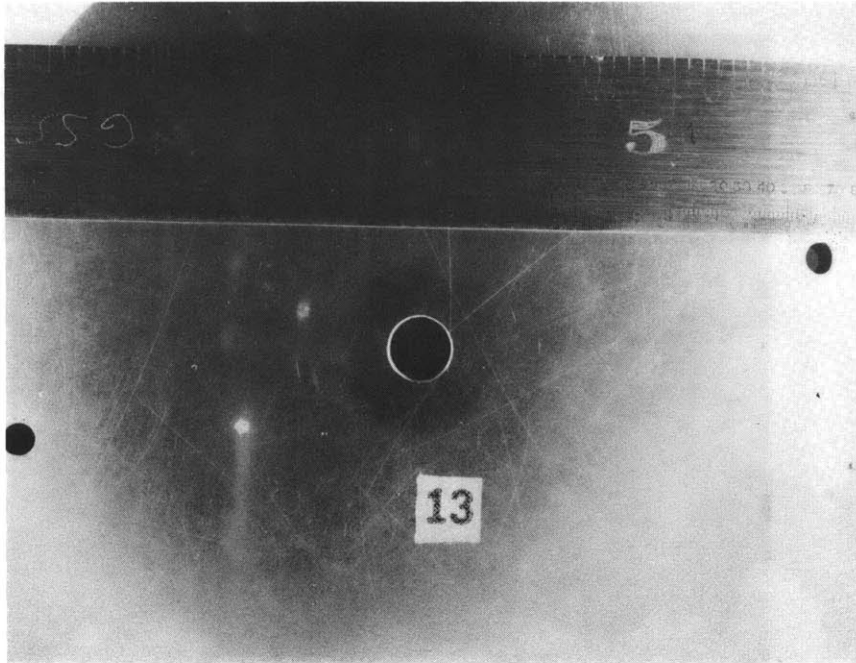


FIG. 8(d). FOOTPRINTS ON MATED PAIR OF 1/4 INCH PLATES.

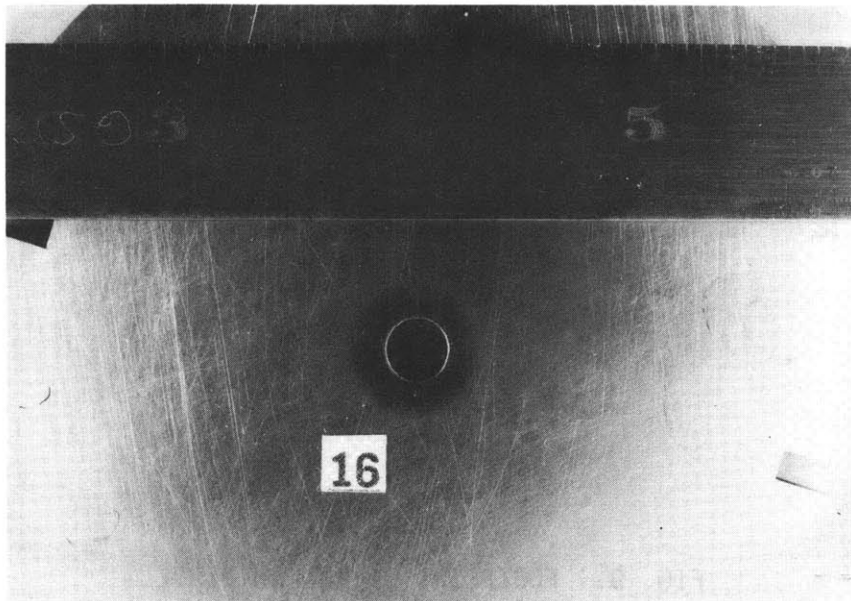
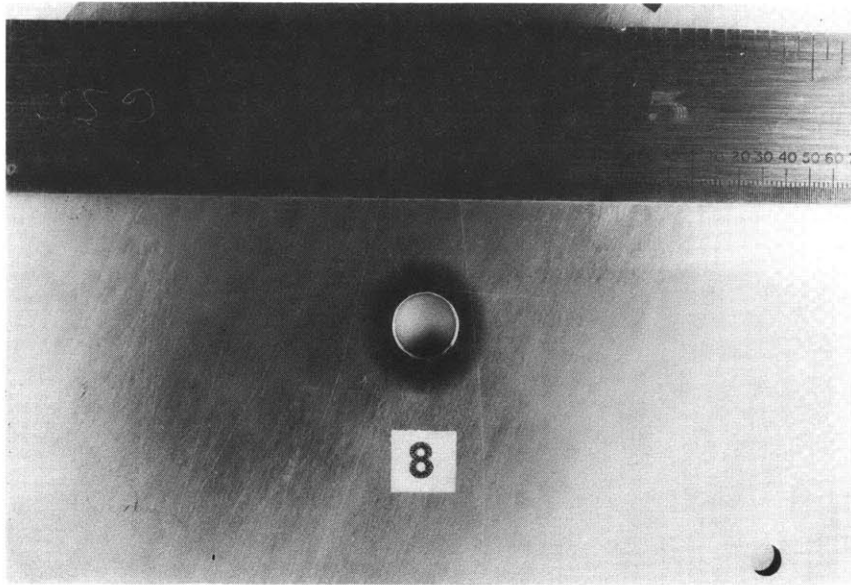


FIG. 8(e). FOOTPRINTS ON MATED PAIR OF 1/8 AND 1/4 INCH PLATES.

FIG. 8. FOOTPRINTS ON THE MATING SURFACES OF 1/16 - 1/16,
1/8 - 1/8, 3/16 - 3/16, 1/4 - 1/4, and 1/8 - 1/4
PAIRS. (A = .128, B = .21)

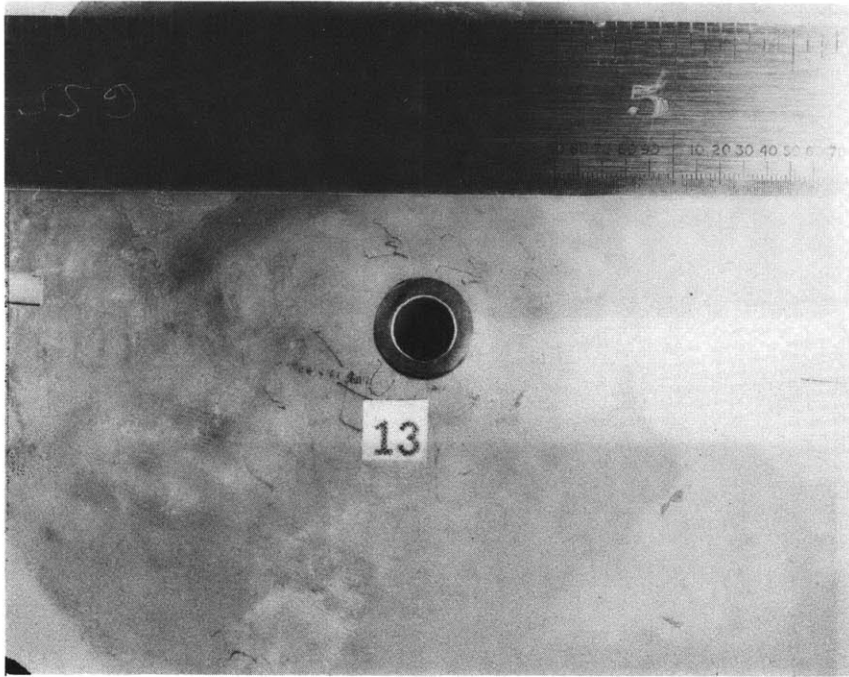


FIG. 9. FOOTPRINT OF NUT ON PLATE.

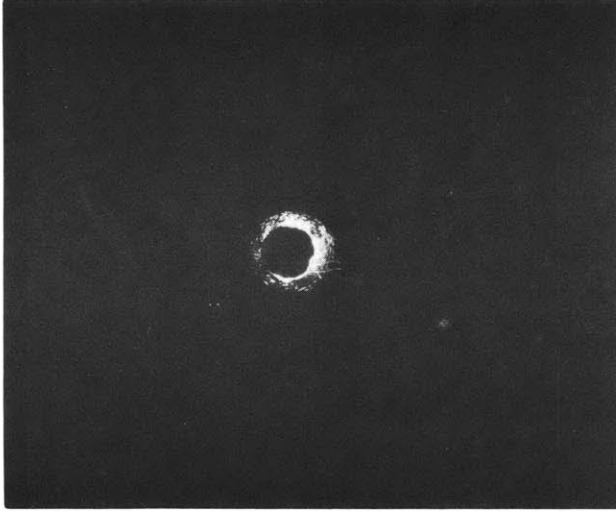


FIG. 10 (a). 1/16 INCH
PAIR

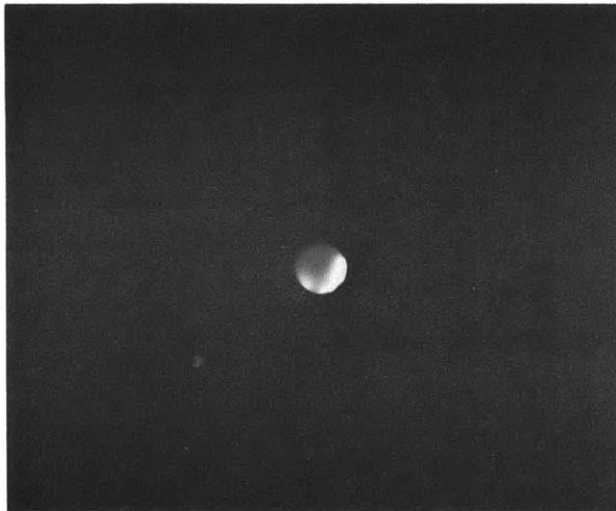


FIG. 10(b). 1/8 INCH
PAIR

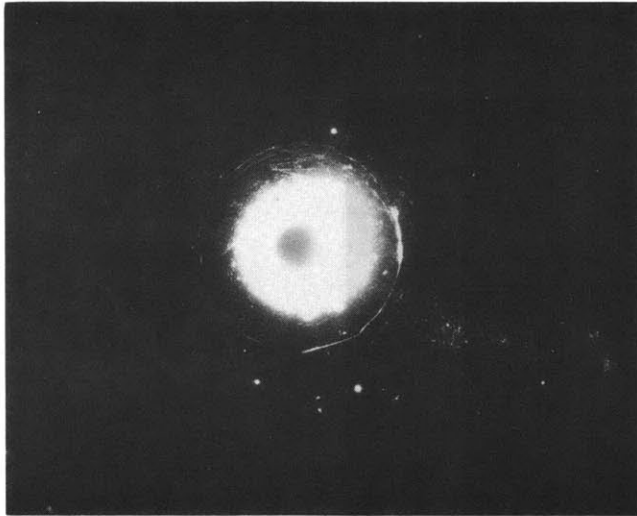


FIG. 10(c). 3/16 INCH
PAIR



FIG. 10(d). 1/4 INCH
PAIR

FIG. 10. X-RAY PHOTOGRAPHS OF CONTAMINATION TRANSFERRED
FROM RADIOACTIVE PLATE TO MATED PLATE. 1/16, 1/4,
3/16, 1/4 INCH PAIRS. (A = .128 in., B = .21 in.)

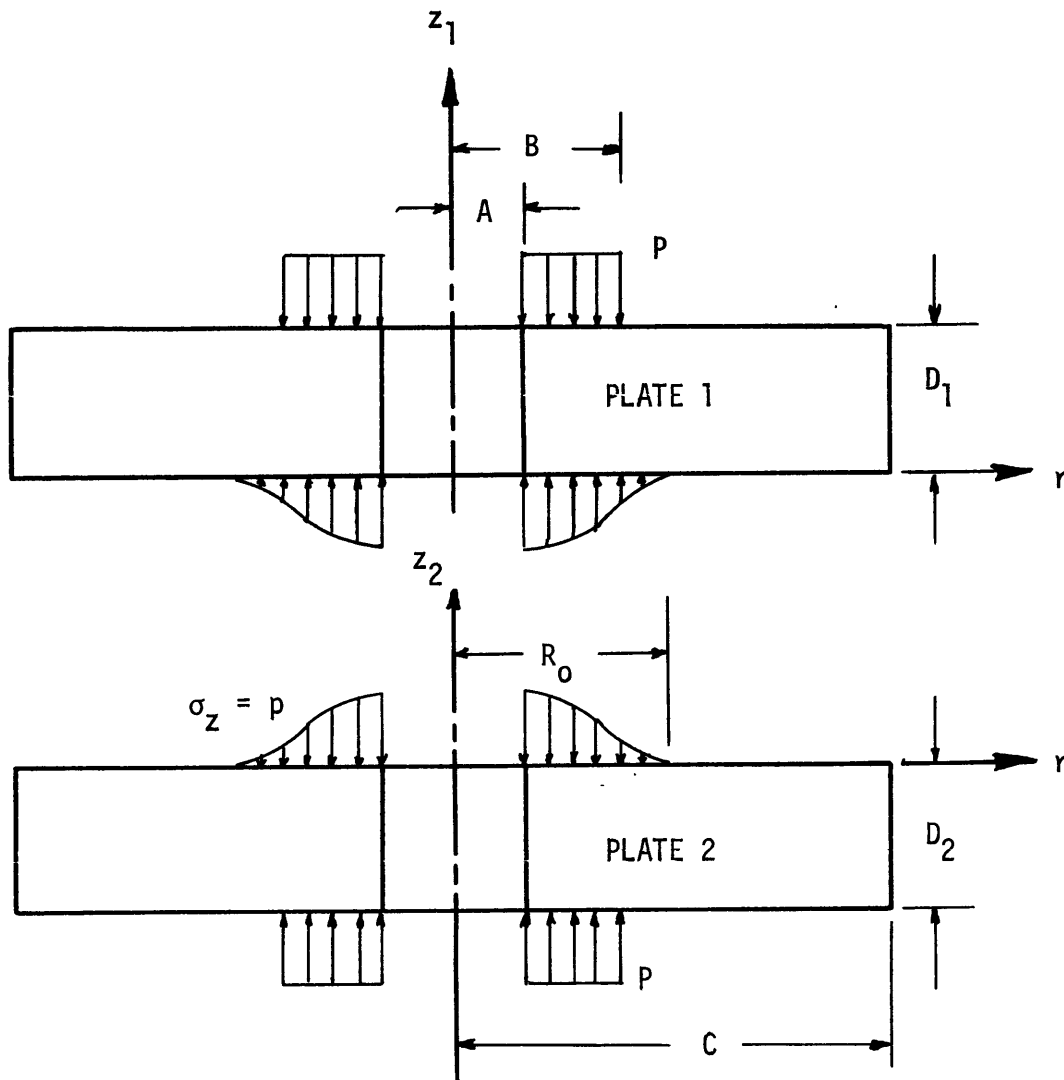


FIG. 11. FREE BODY DIAGRAM FOR TWO PLATES IN CONTACT.

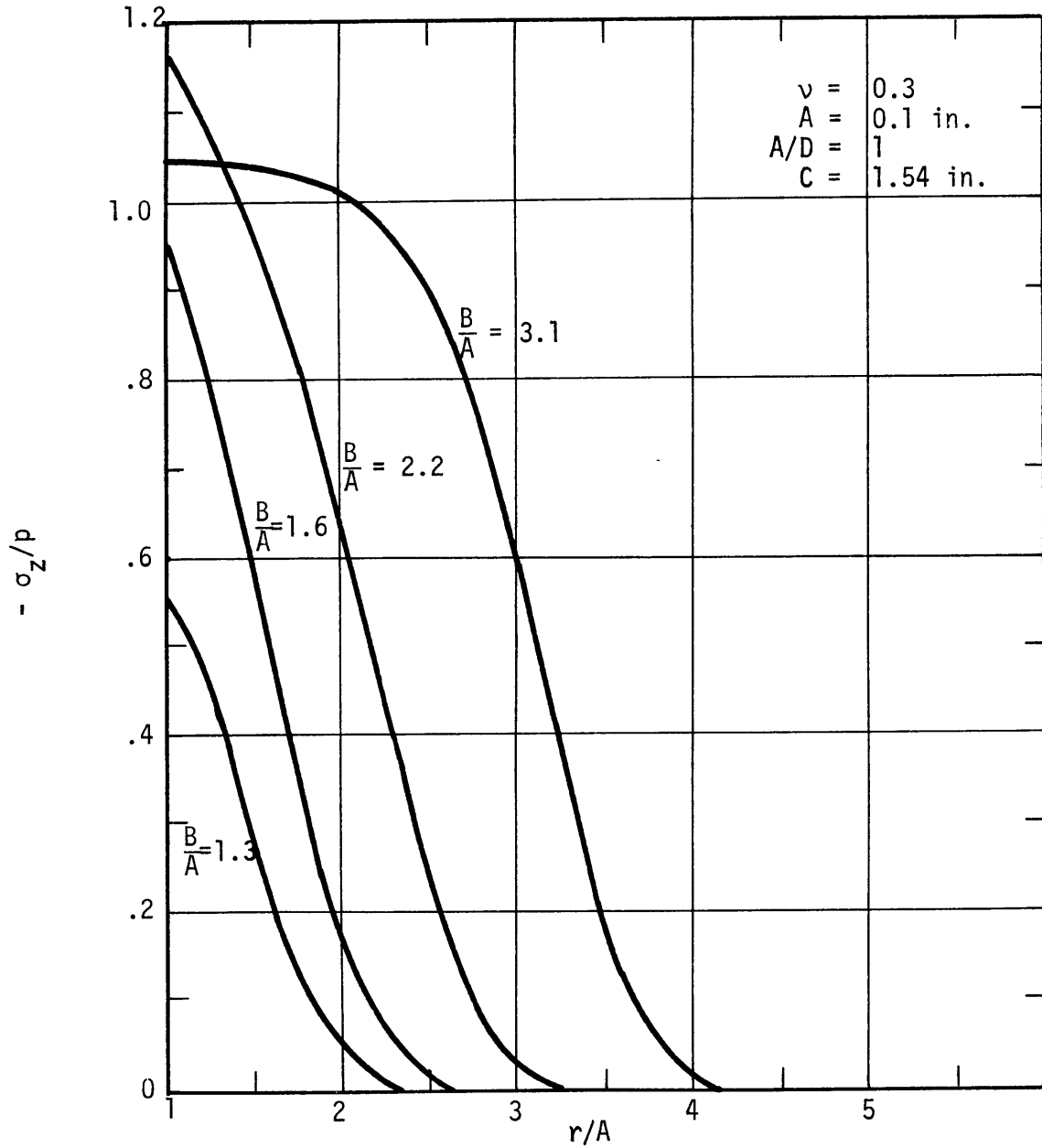


FIG. 12. SINGLE PLATE ANALYSIS-MIDPLANE σ_z STRESS DISTRIBUTION ($D = 0.1 \text{ in.}$)

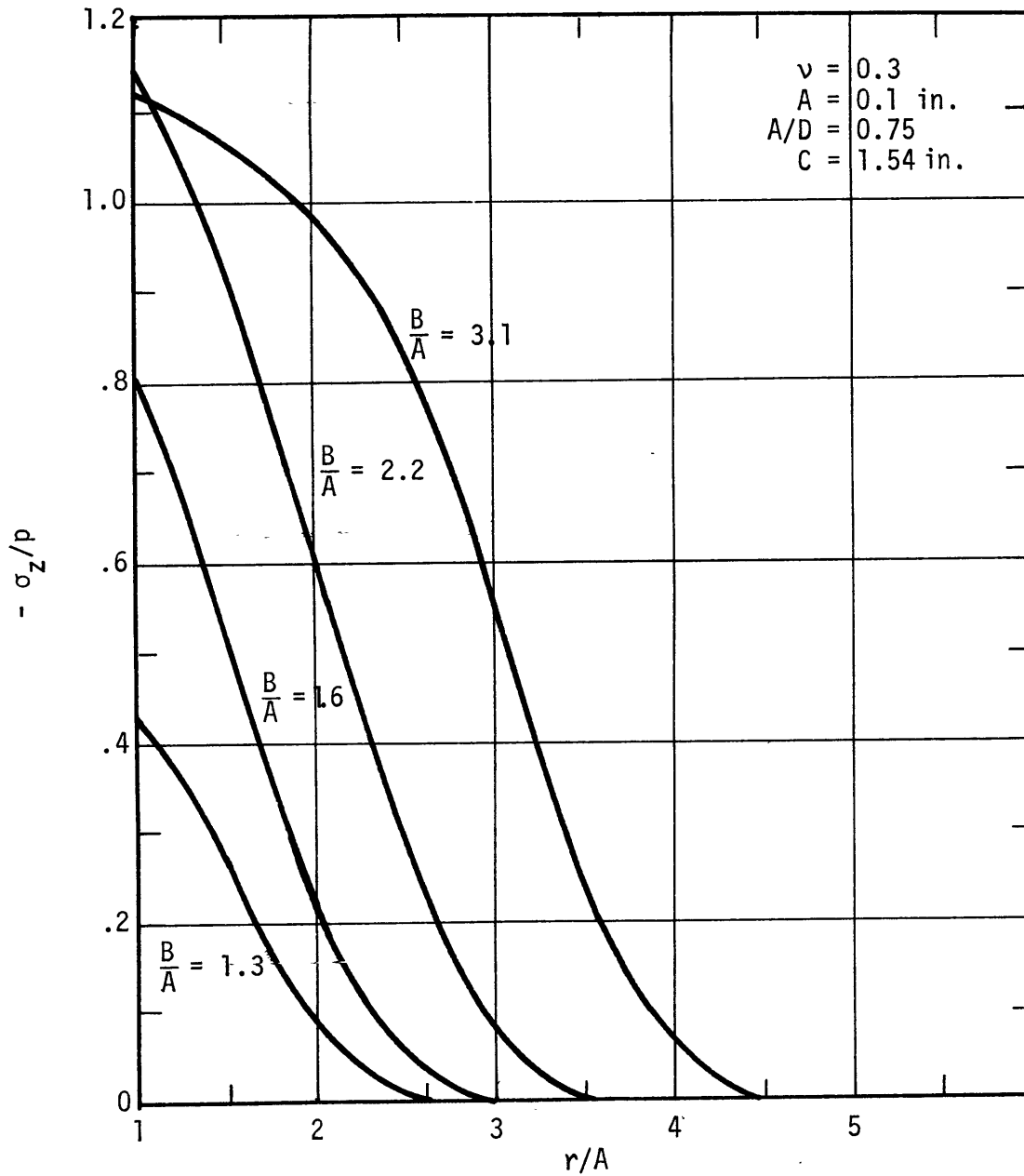


FIG. 13. SINGLE PLATE ANALYSIS-MIDPLANE σ_z STRESS DISTRIBUTION ($D = 0.133 \text{ in.}$)

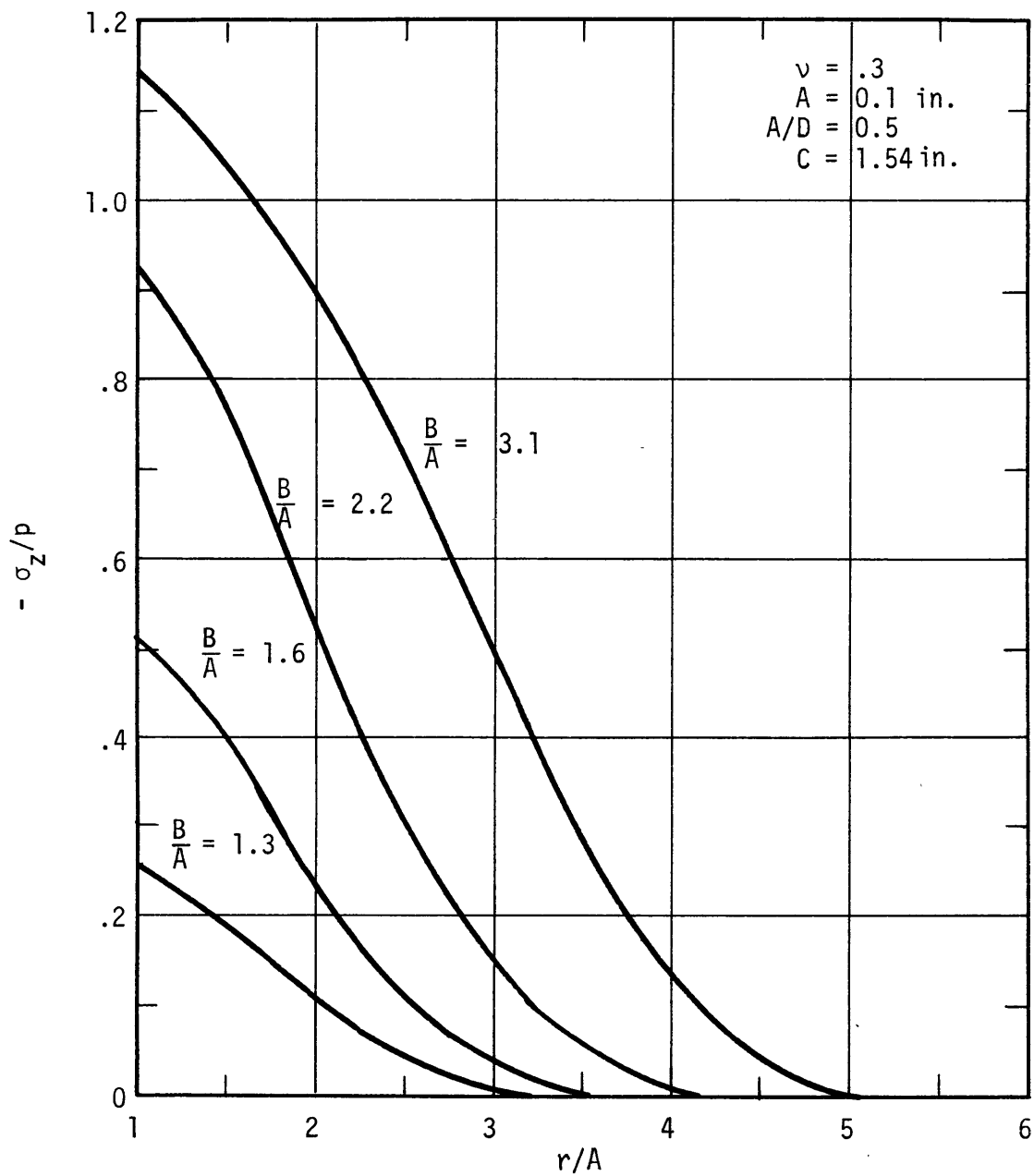


FIG. 14. SINGLE PLATE ANALYSIS-MIDPLANE σ_z STRESS DISTRIBUTION (D = 0.2 in.)

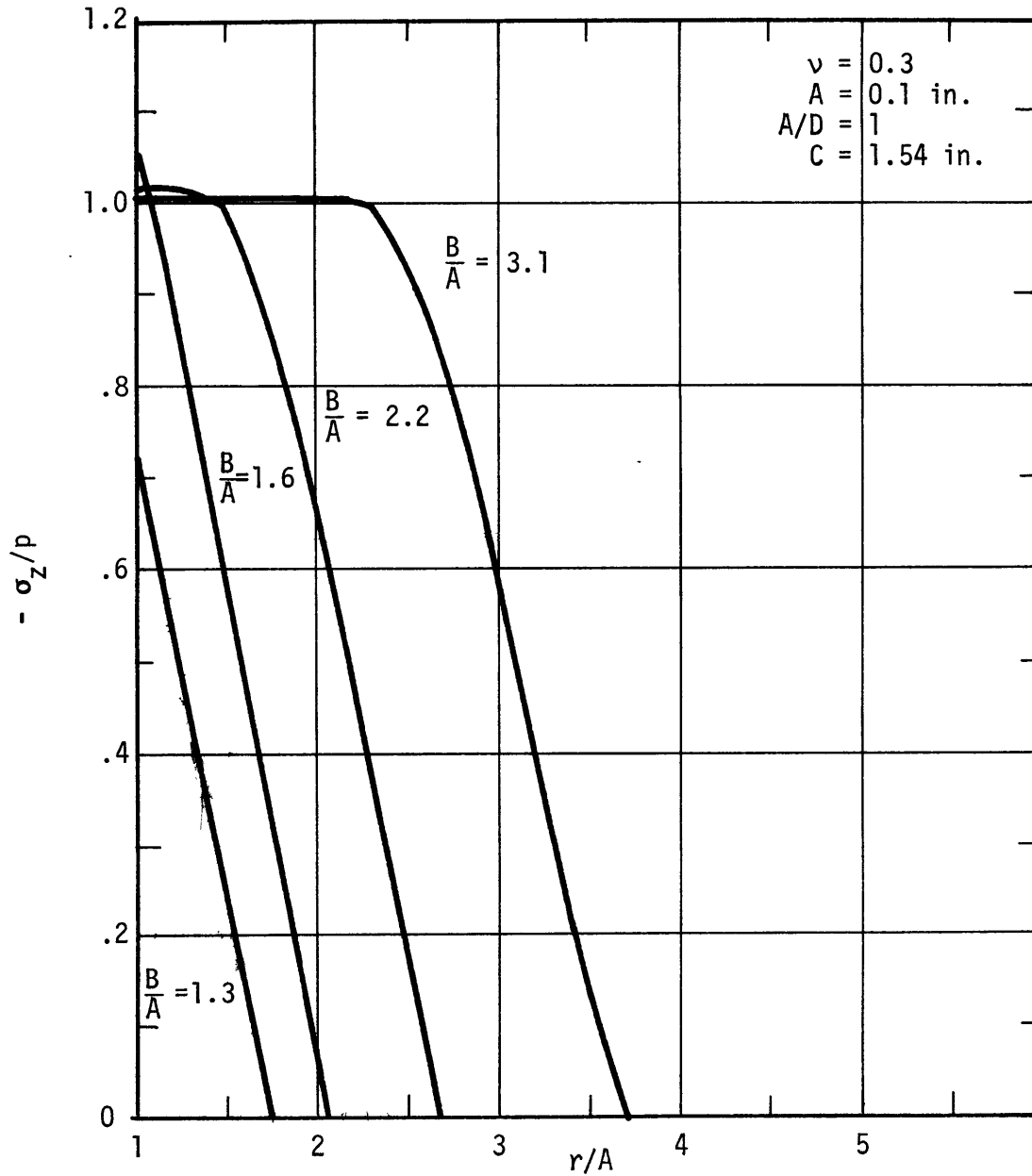


FIG. 15. INTERFACE PRESSURE DISTRIBUTION IN A BOLTED JOINT

(D = 0.1 in.)

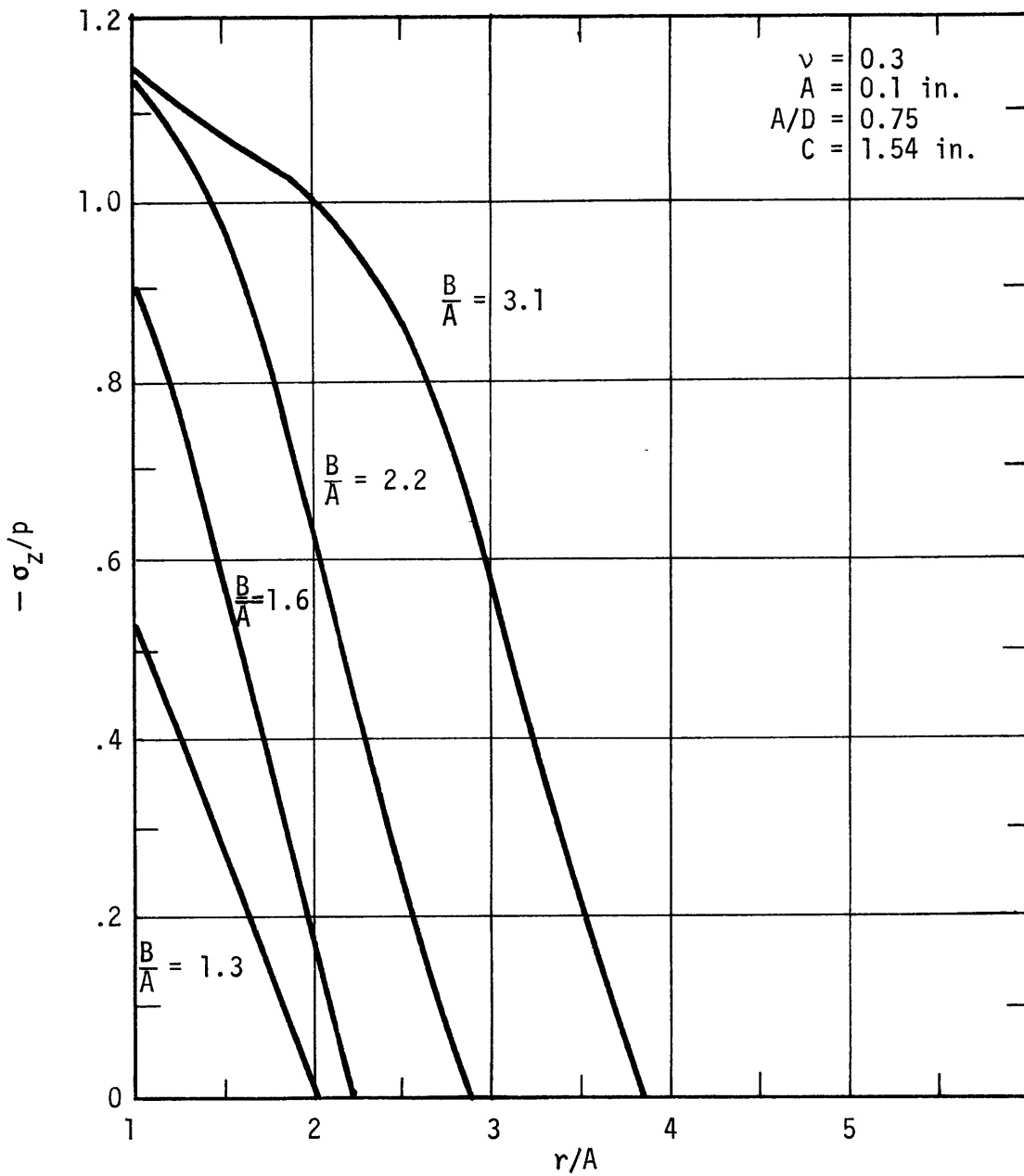


FIG. 16. INTERFACE PRESSURE DISTRIBUTION IN A BOLTED JOINT
($D = .133$ in.)

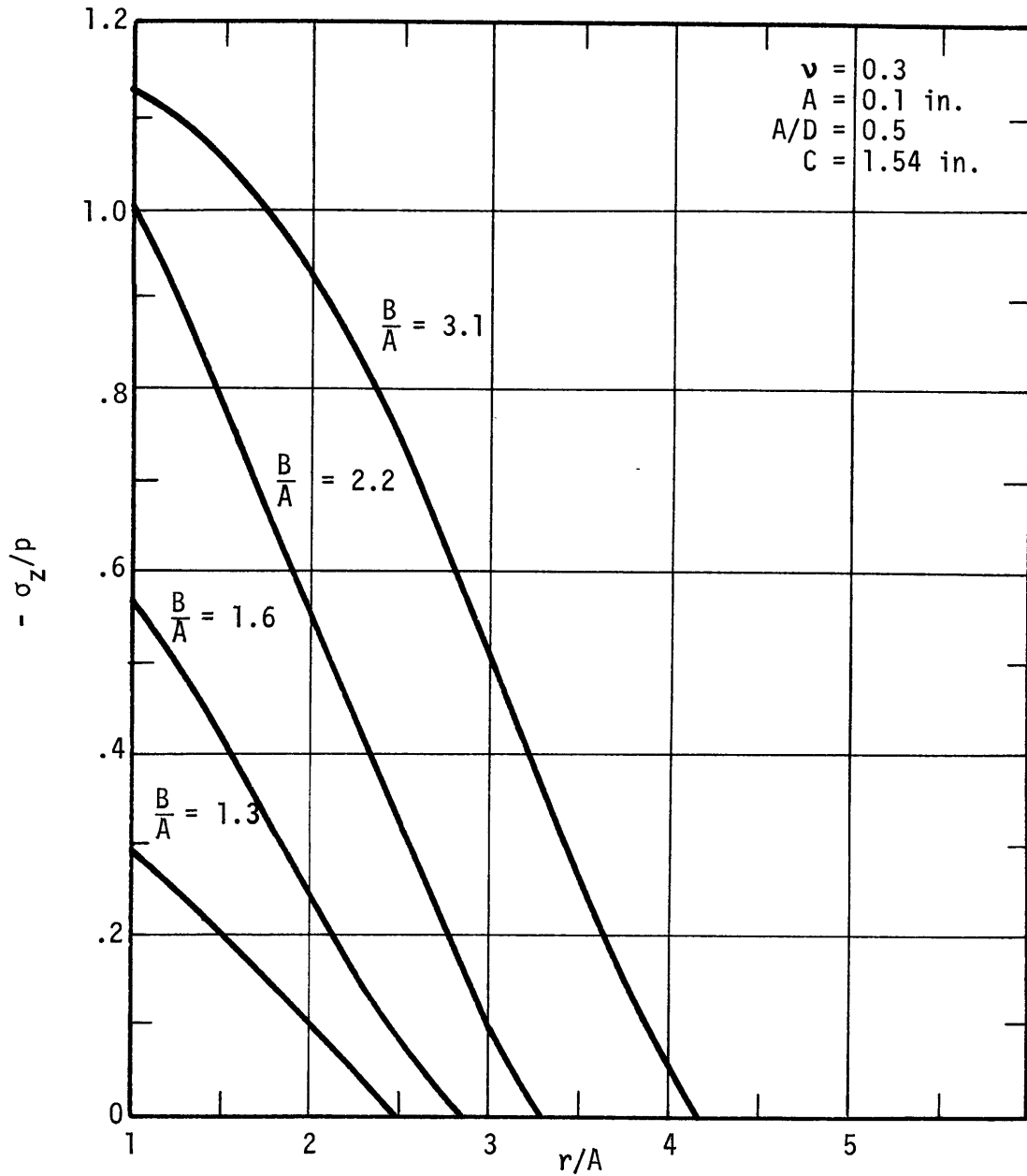


FIG. 17. INTERFACE PRESSURE DISTRIBUTION IN A BOLTED JOINT

($D = 0.2$ in.)

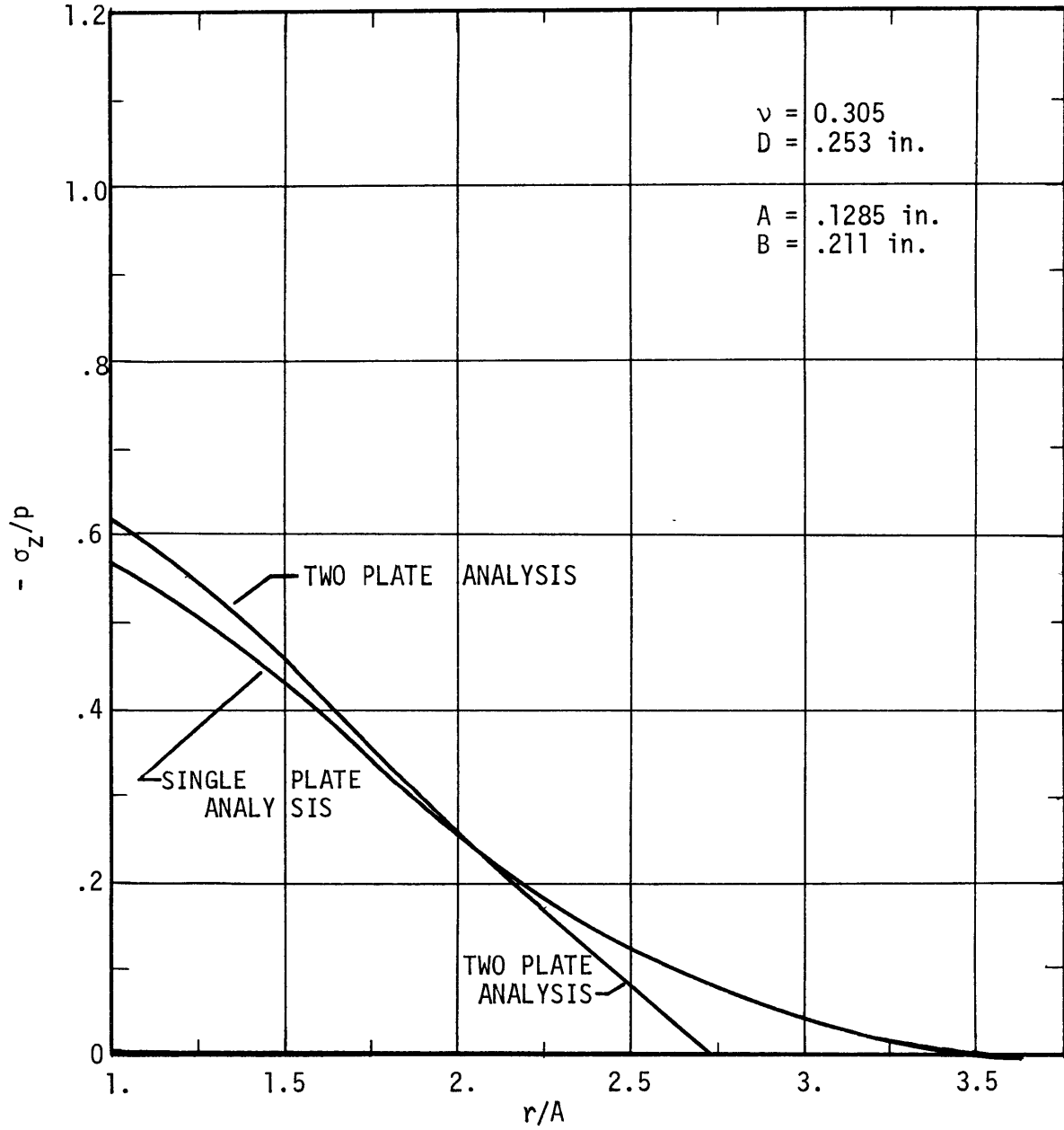


FIG. 18. FINITE ELEMENT ANALYSIS RESULTS FOR 1/4 INCH PLATE PAIR.

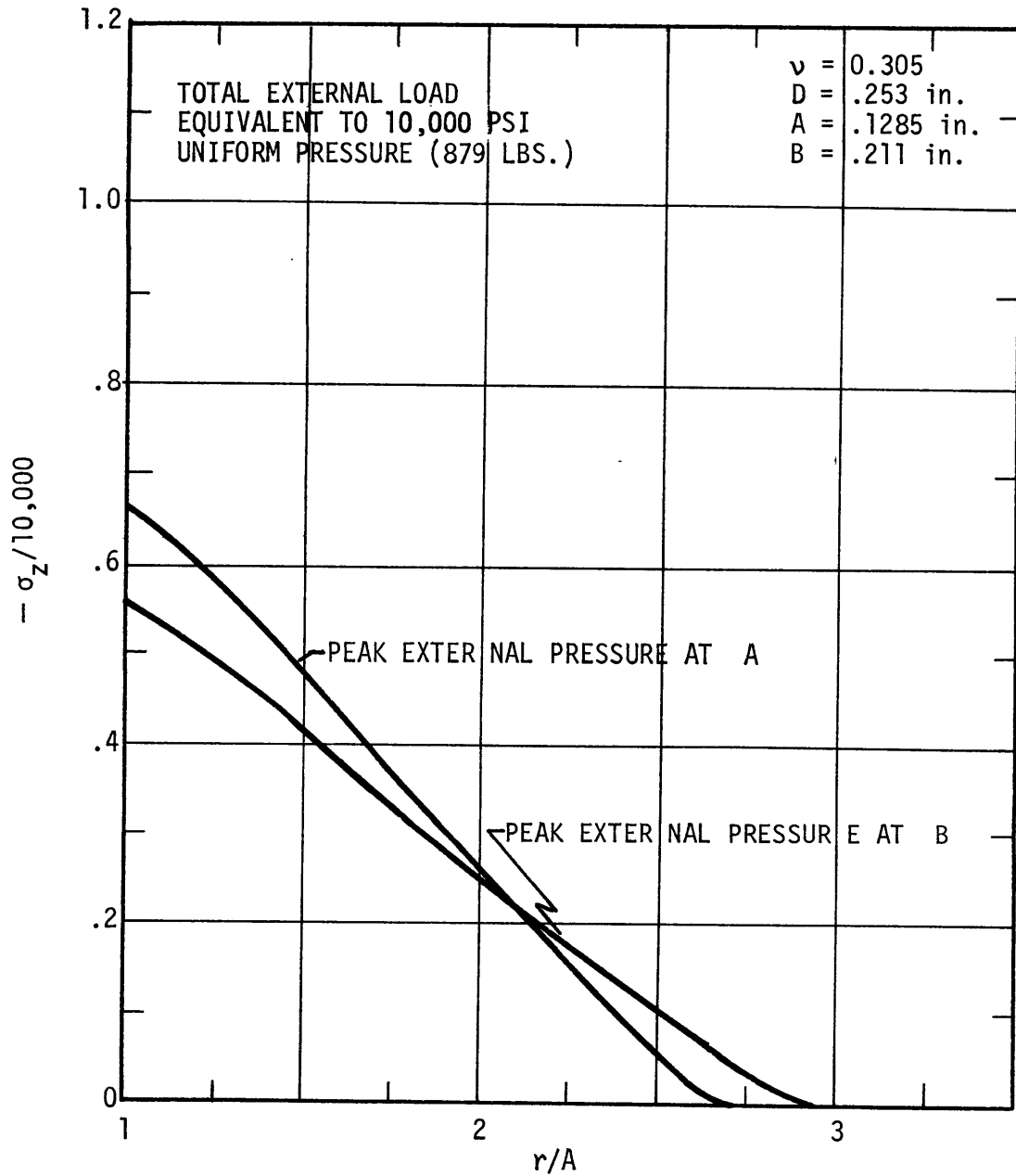


FIG. 19. PRESSURE IN JOINT, TRIANGULAR LOADING

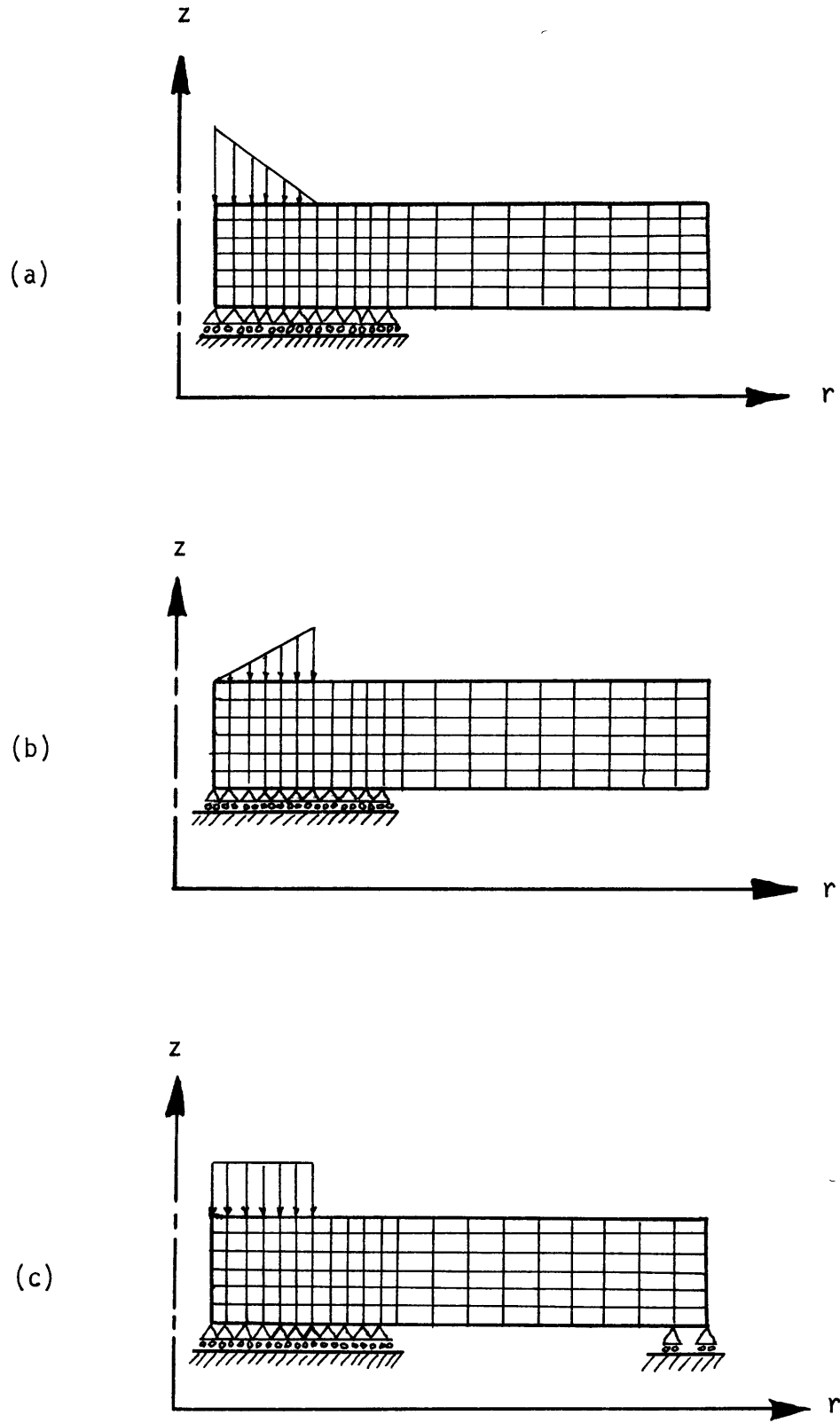


FIG. 20. VARIATIONS OF LOADING AND BOUNDARY CONDITIONS.

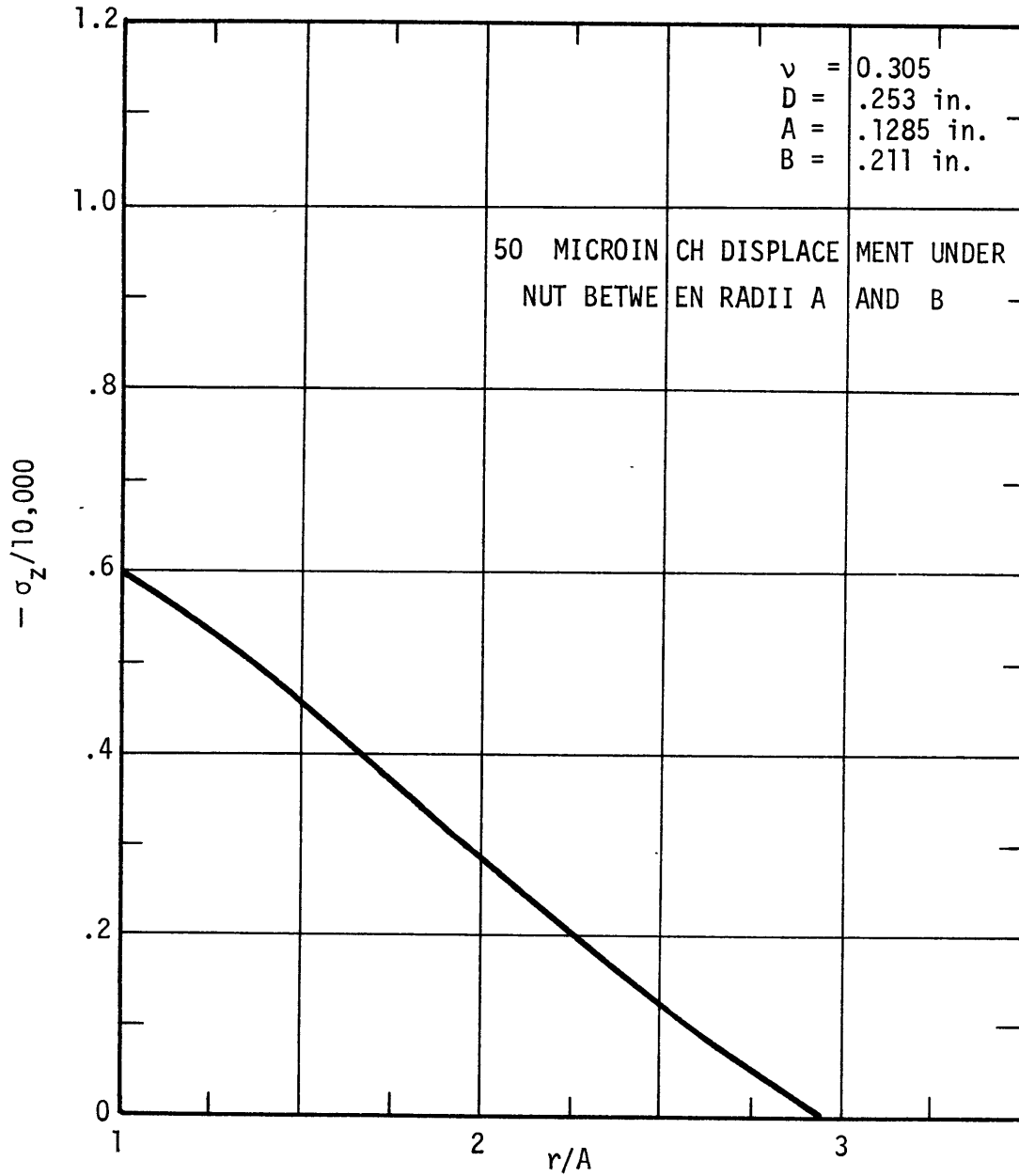


FIG. 21. PRESSURE IN JOINT, UNIFORM DISPLACEMENT UNDER NUT.

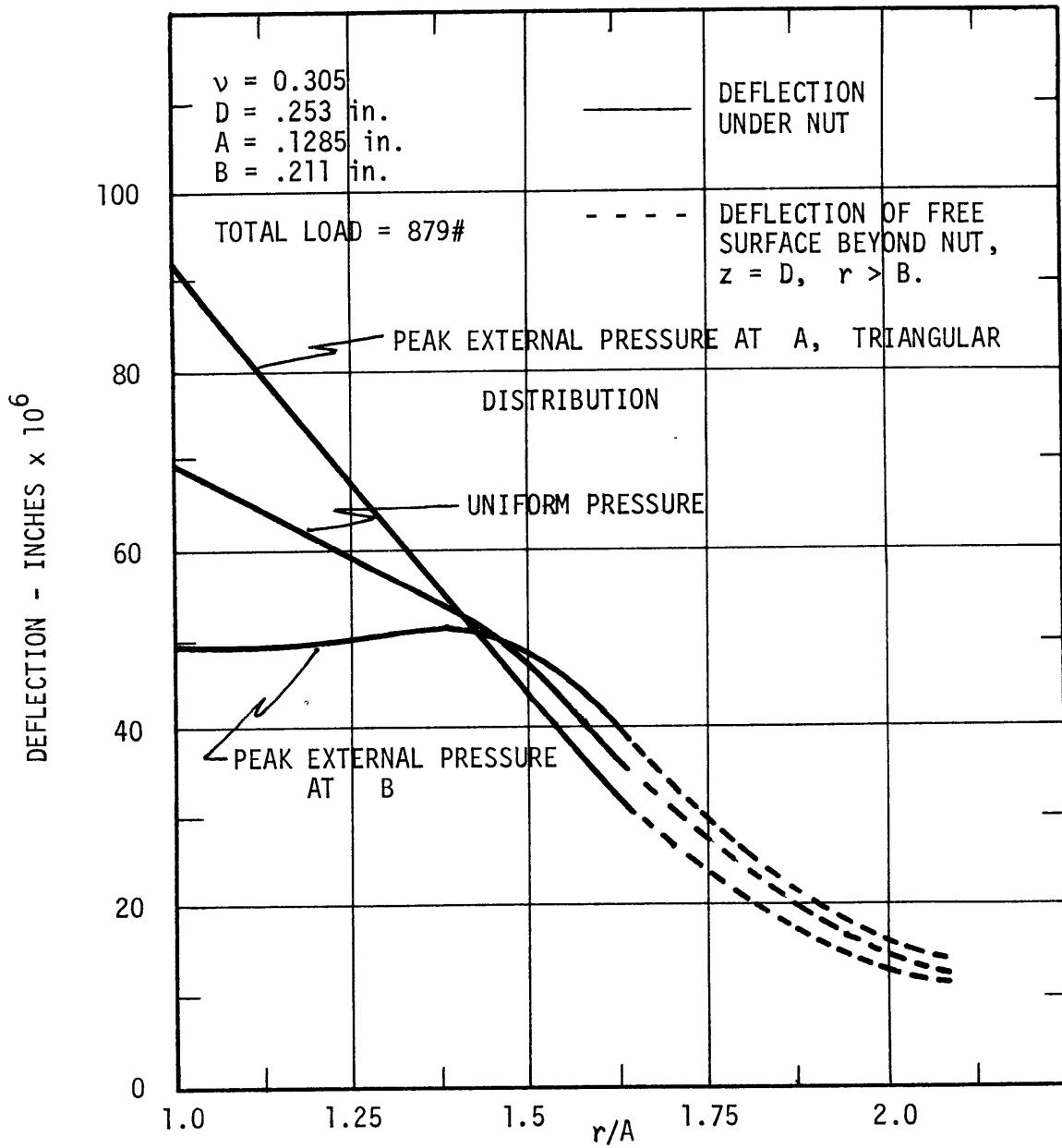


FIG. 22. DEFLECTION OF PLATE UNDER NUT.

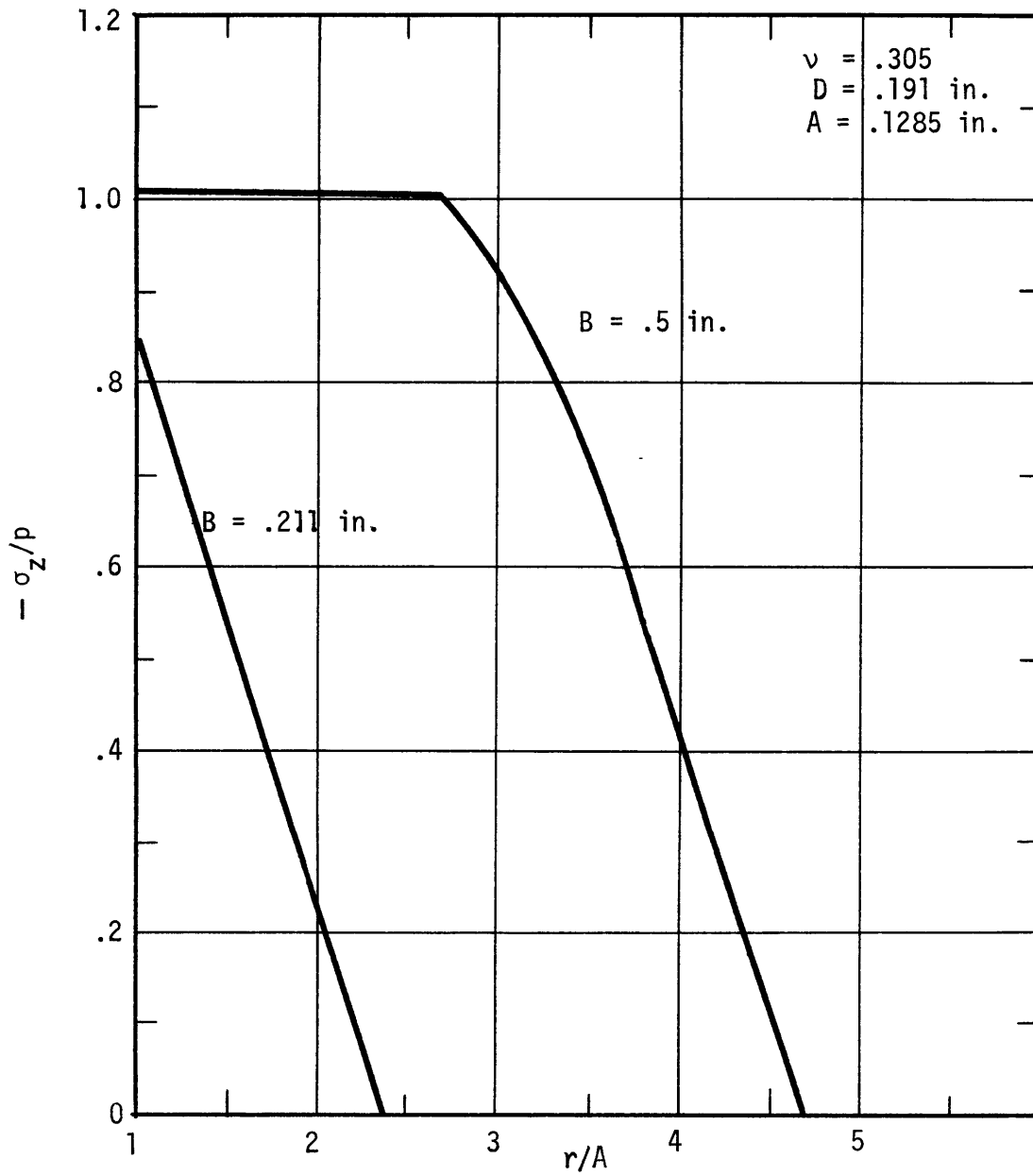


FIG. 23. FINITE ELEMENT ANALYSIS RESULTS FOR 3/16 INCH PLATE PAIR.

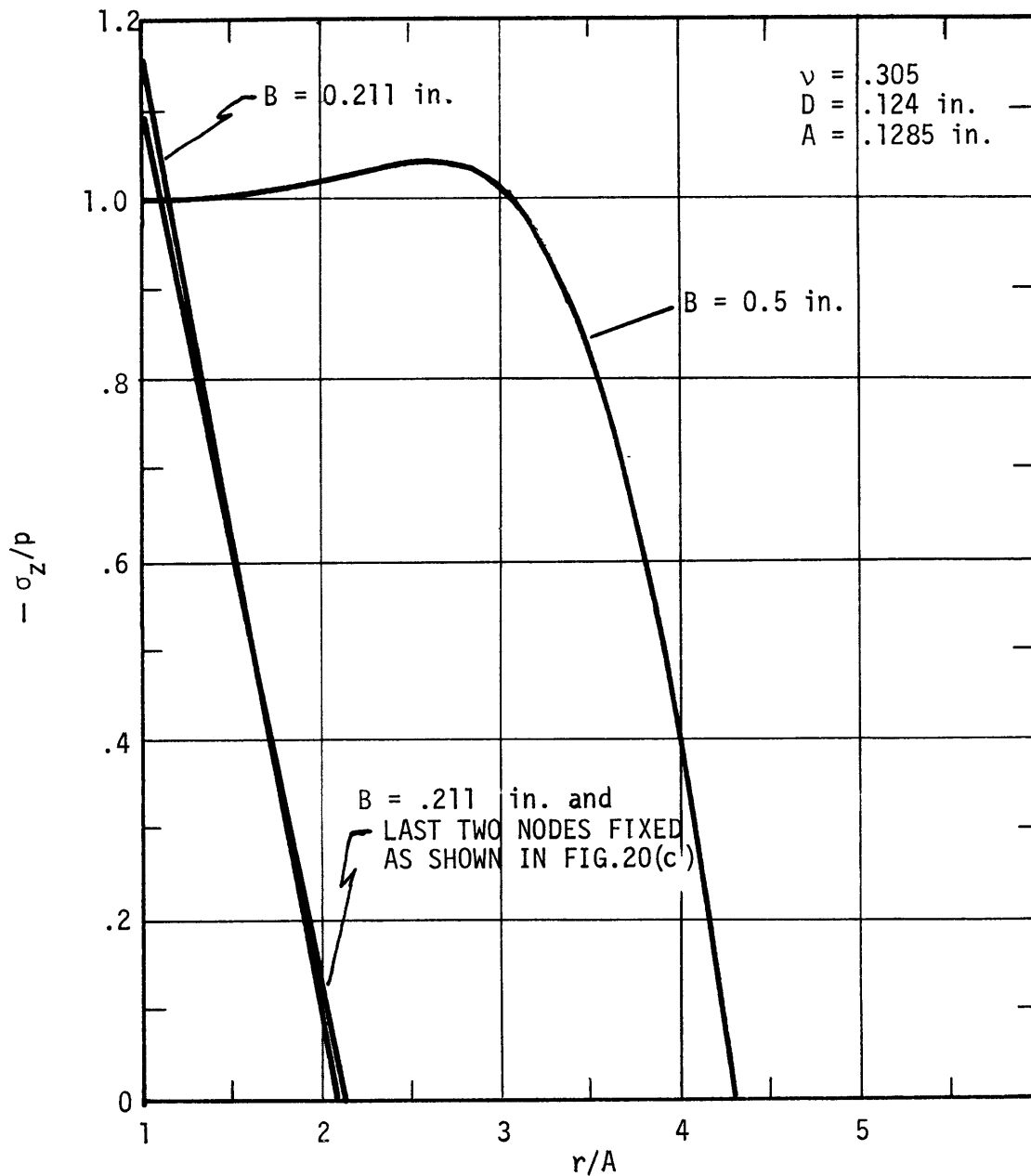


FIG. 24. FINITE ELEMENT ANALYSIS RESULTS FOR 1/8 INCH PLATE PAIR.

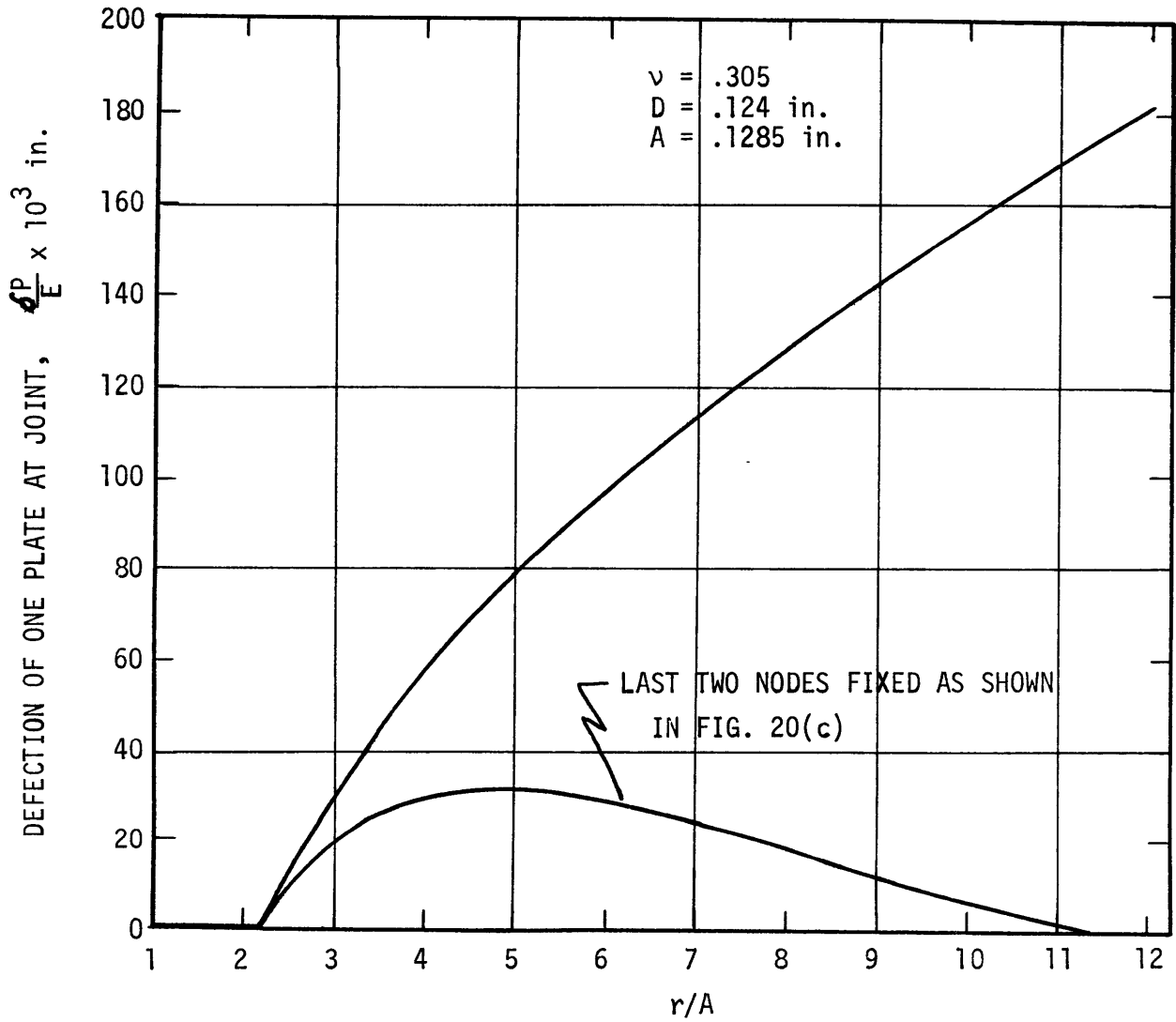


FIG. 25. GAP DEFORMATION FOR FREE AND FIXED EDGES — FINITE ELEMENT ANALYSIS, 1/8 INCH PLATE PAIR.

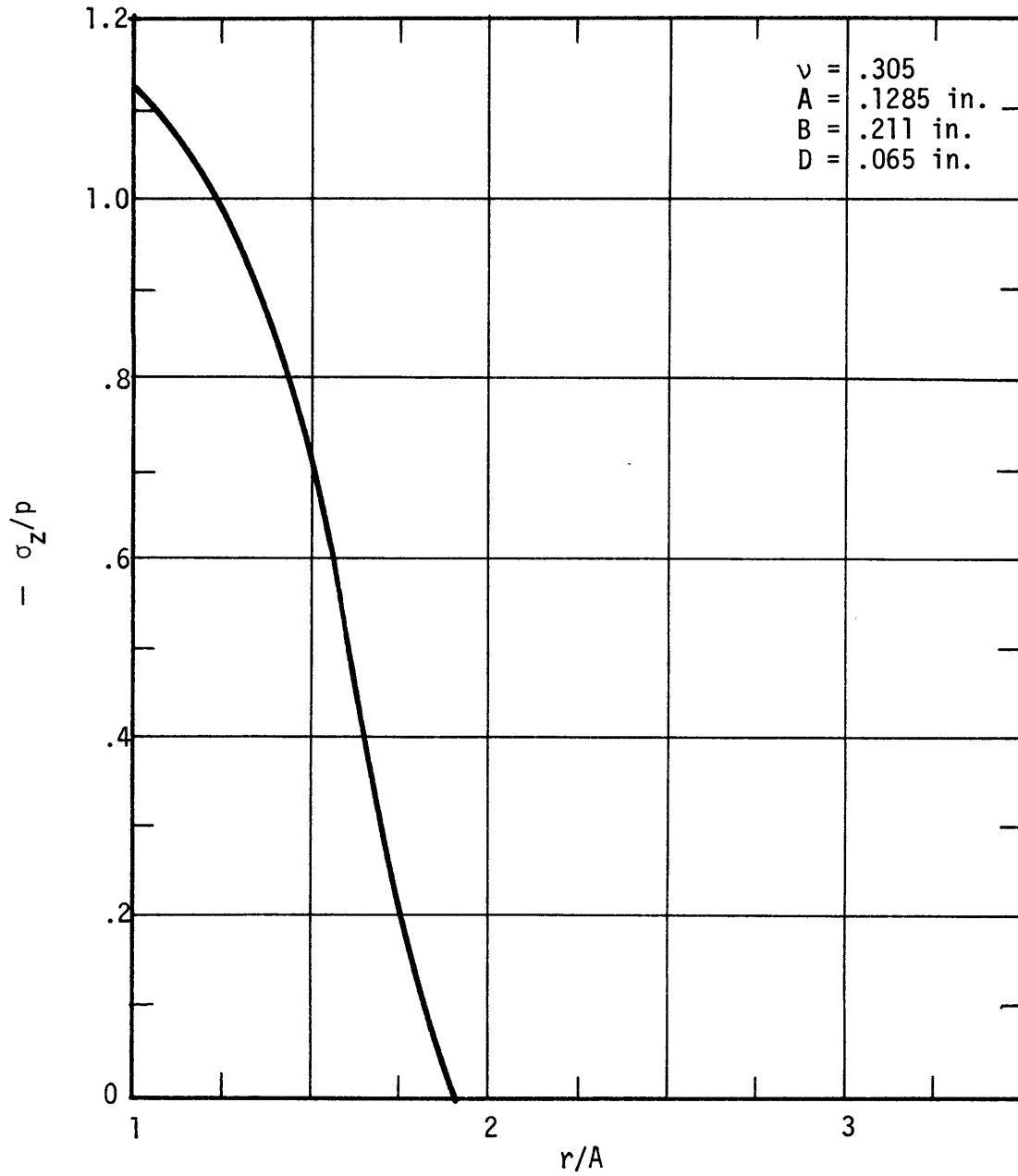


FIG. 26. FINITE ELEMENT ANALYSIS RESULT FOR 1/16 INCH PLATE PAIR.

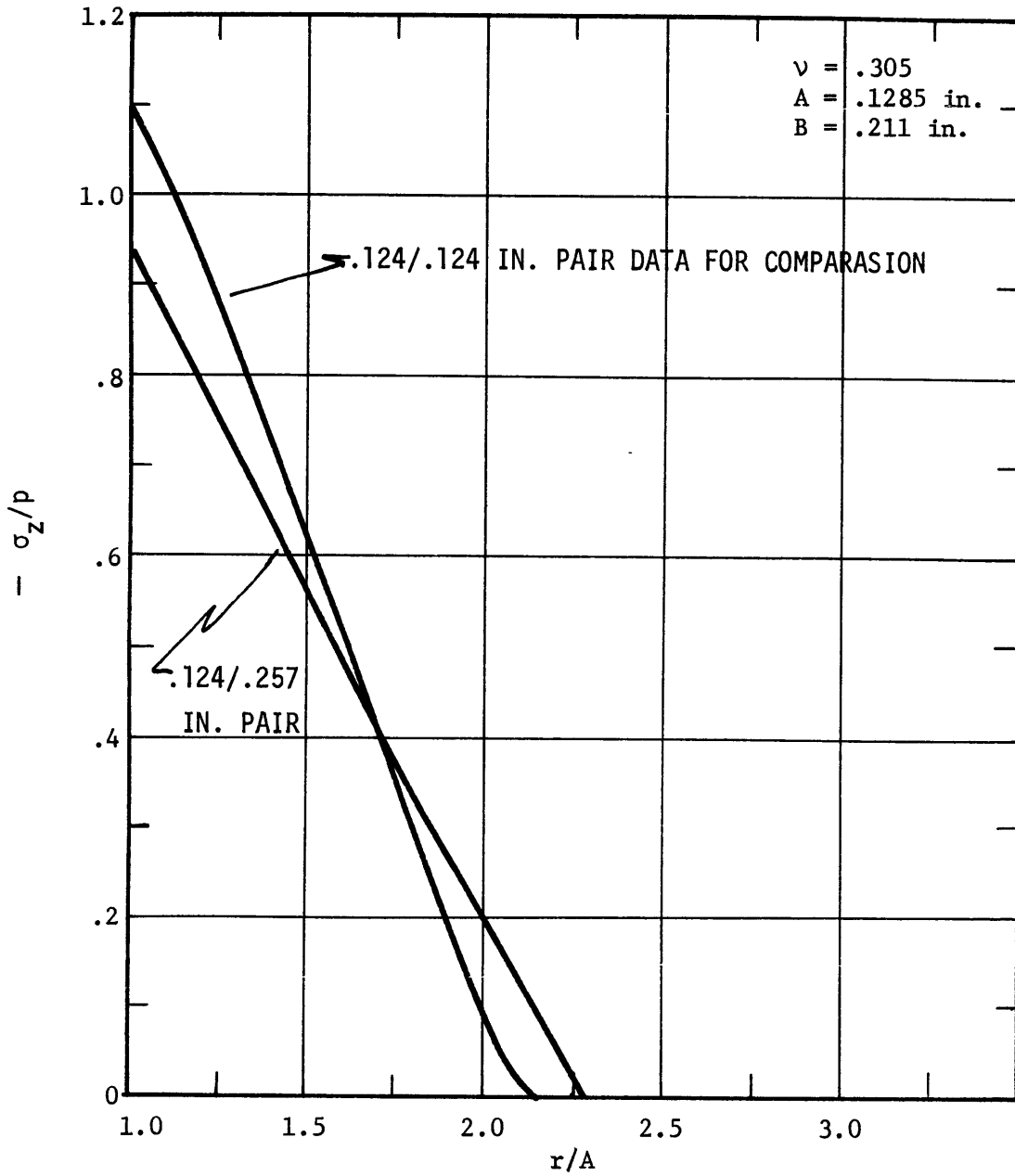


FIG. 27. FINITE ELEMENT ANALYSIS RESULTS FOR 1/8 INCH PLATE MATED WITH 1/4 INCH PLATE.

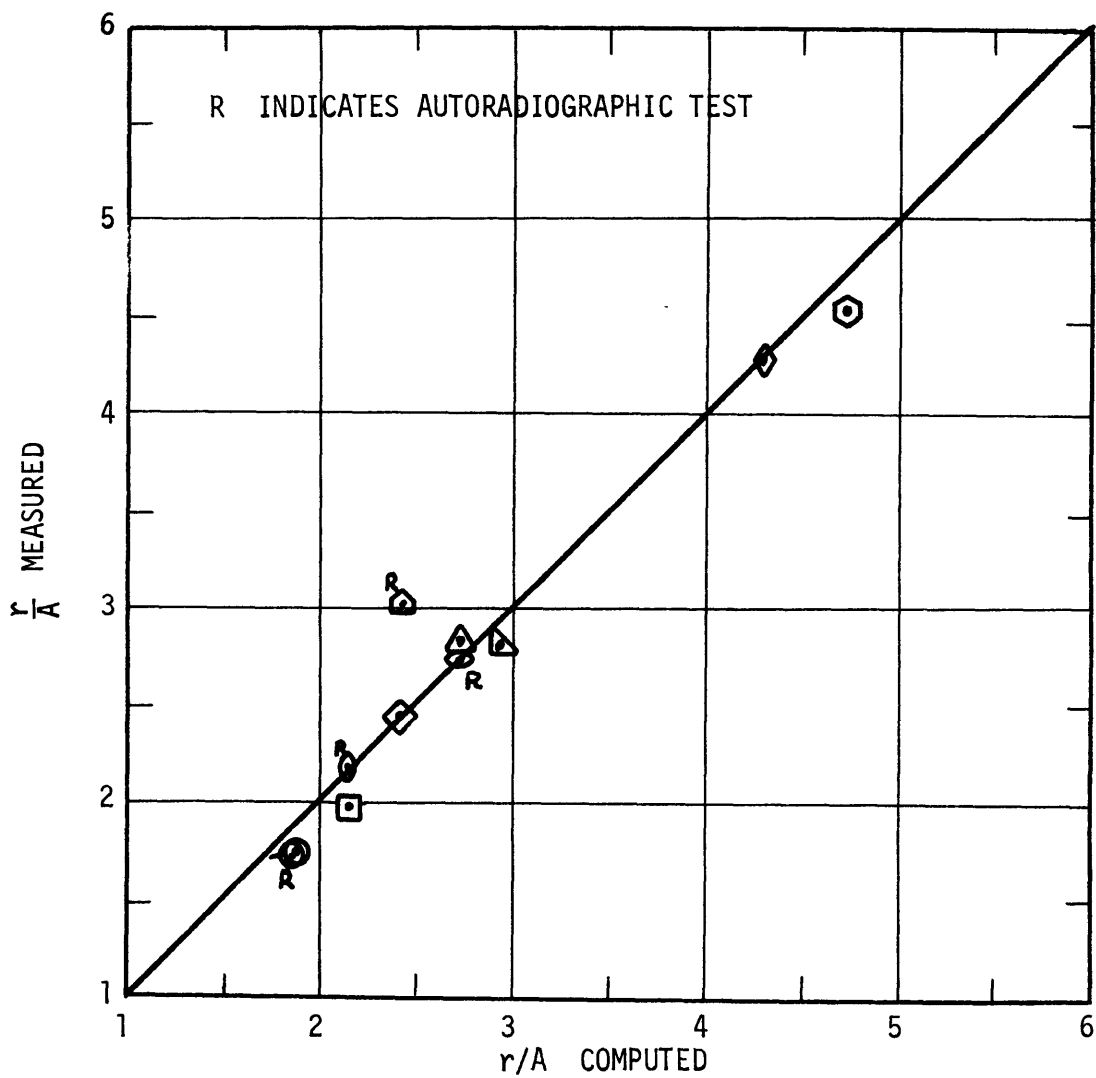


FIG. 28. COMPARISON BETWEEN TESTED AND MEASURED SEPARATION RADII.

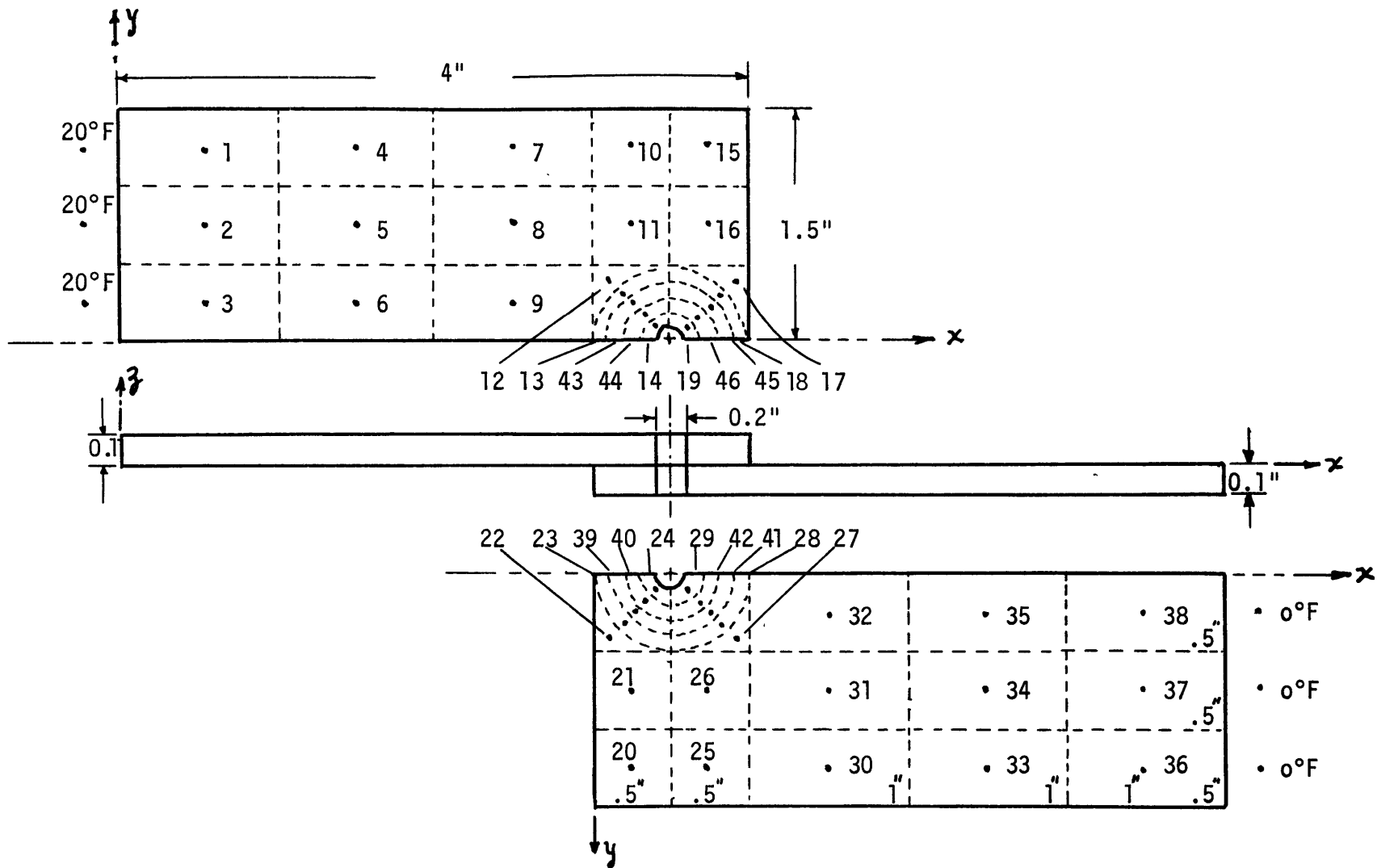


FIG. 29. LOCATION OF NODES — STEADY STATE HEAT TRANSFER ANALYSIS